Molecular Analysis of Cortical Malformation in Mammalian Cortex by Using Proteomics Approaches

by

Berfu Nur Yiğit

A Dissertation Submitted to the
Graduate School of Sciences and Engineering
in Partial Fulfillment of the Requirements for
the Degree of

Doctor of Philosophy

in

Molecular Biology and Genetics

KOÇ ÜNİVERSİTESİ

March, 2024

Molecular Analysis of Cortical Malformation in Mammalian Cortex by Using Proteomics Approaches

Koç University

Graduate School of Sciences and Engineering

This is to certify that I have examined this copy of a doctoral dissertation by

Berfu Nur Yiğit

and have found that it is complete and satisfactory in all respects, and that any and all revisions required by the final examining committee have been made.

Committee Members:

_____

Prof. Dr. Nurhan Özlü (Advisor, Koç University)

_____

Prof. Dr. Arzu Çelik (Boğaziçi University)

_____

Assoc. Prof. Umut Şahin (Boğaziçi University)

_____

Assist. Prof. Dr. Ayşe Koca Çaydaşı (Koç University)

_____

Assist. Prof. Dr. Serkan Kır (Koç University)

Date: March 26, 2024

ABSTRACT

The layered structure of the cerebral cortex is formed through a complicated sequence of highly controlled stages during corticogenesis. During this process, the perturbation of neuronal migration and cell division can result in a rare disorder called cortical heterotopia. Heterotopia patients can have recurrent epileptic seizures, developmental delays, and mild intellectual disabilities. Heterotopia has been challenging to study because human mutations associated with the disease often fail to form heterotopia in mouse models. Eml1 is a heterotopia-associated gene where the perturbations cause heterotopia formation in humans and mice. During my Ph.D., I focused on the investigation of the functional role of EML1 in heterotopia formation through comprehensive cellular and biochemical analysis, including imaging, BioID proximity labeling, proteomic profiling via label-free proteomics or dimethyl labeling, phosphoproteomics, and microtubule-pelleting assays.

In the first part of my thesis, I showed that heterotopia-associated mutant EML1 reduces the protein-microtubule binding affinity. BioID proximity labeling of wild-type and mutant EML1 revealed that EML1 interacts with many microtubule and cytoskeletal organization proteins, most of which are lost in mutant-expressing cells. Thus, the wild-type protein interactome is impacted by a heterotopia-causing mutation. This work identified several novel interactors, along with known interaction partners of EML1. Proteome profiling in cortices and primary neuronal cells in a conditional Eml1 knockout (cKO) mouse versus control showed dysregulations in microtubule organization and protein metabolic processes upon Eml1 depletion. These large-scale proteomic analyses are essential for studying the underlying mechanism in brain development and heterotopia formation.

In the second part of my thesis, I present my contributions to the published article, which focuses on the cell cycle-dependent regulation of an adhesion protein, protocadherin-7. In this project, as my side project, I unveiled the spatiotemporal regulation of the protein and its' palmitoylation-dependent regulation in cell division.

ÖZET

Serebral korteksin katmanlı yapısı, kortikogenez sırasında yüksek düzeyde kontrol edilen aşamaların karmaşık bir dizisi yoluyla oluşmaktadır. Bu süreç sırasında nöronal göç ve hücre bölünmesindeki bozulma, kortikal heterotopi adı verilen nadir bir bozukluğa yol açabilmektedir. Heterotopi hastalarında tekrarlayan epileptik nöbetler, gelişimsel gecikmeler ve hafif zihinsel engeller olabilmektedir. Heterotopi hastalığının araştırılması oldukça zordur çünkü hastalıkla ilişkili insan mutasyonları fare modellerinde sıklıkla heterotopya oluşturmada başarısız olmaktadır. *Eml1*, insanlarda ve farelerde düzensizliklerin heterotopya oluşumuna neden olan heterotopya ile ilişkili bir gendir. Doktora eğitimim sırasında, EML1'in heterotopi oluşumundaki işlevsel rolünün, görüntüleme, BioID yakınlık etiketlemesi, etiketsiz proteomik veya dimetil etiketleme yoluyla proteomik profilleme, fosfoproteomikler ve mikrotübül peletleme deneyleri ile gösterdim.

Tezimin ilk bölümünde heterotopya ilişkili mutant EML1'in protein-mikrotübül bağlanma afinitesini azalttığını gösterdim. Yabani tip ve mutant EML1'in BioID yakınlık etiketlemesi, EML1'in çoğu mutant eksprese eden hücrelerde kaybolan birçok mikrotübül ve hücre iskeleti organizasyon proteini ile etkileşime girdiğini ortaya çıkardı. Bu nedenle, vahşi tip protein interaktomu, heterotopiye neden olan bir mutasyondan etkilenmektedir. Bu çalışma, EML1'in bilinen etkileşim ortaklarının yanı sıra birkaç yeni etkileşimciyi tanımladı. Koşullu *Eml1* nakavt (cKO) faresinde kortekslerde ve birincil nöron hücrelerinde proteom profili, kontrole göre *Eml1* susturulmuş hücrelerde mikrotübül organizasyonunda ve protein metabolik süreçlerinde düzensizlikler gösterdi. Bu büyük ölçekli proteomik analizler, beyin gelişimi ve heterotopi oluşumunun altında yatan mekanizmayı incelemek için gereklidir.

Tezimin ikinci bölümünde, bir adezyon proteini olan protocadherin-7'nin hücre döngüsüne bağlı düzenlenmesini konu alan yayınlanmış makaleye katkılarımı sunuyorum. Bu projede yan projem olarak proteinin uzay-zamansal düzenlemesini ve hücre bölünmesindeki palmitoilasyona bağlı düzenlemeyi ortaya çıkardım.

ACKNOWLEDGEMENTS

First and foremost, I would like to express my sincere gratitude to my supervisor, Prof. Dr. Nurhan Özlü, for guiding me during my doctoral studies with her knowledge, enthusiasm, decency, and encouragement. I gained great knowledge and learned valuable experiences from her. It has been a great pleasure and privilege to work with her.

Besides, I would like to thank my thesis monitoring committee members, Prof. Dr. Arzu Çelik and Assist. Prof. Dr. Ayşe Koca Çaydaşı, for their precious contributions that helped shape my research. I would also like to thank the other members of my thesis committee, Assist. Prof. Dr. Serkan Kır and Assoc. Prof. Umut Şahin, for their comments and critical reading of my thesis.

I would like to also express my gratitude to M.Sc. PIs, Prof. Dr. Melih Acar, and Assist. Prof. Dr. Timuçin Avşar. You showed me the greatest and purest science, I am honored to be your student.

I would like to acknowledge the financial support of the Scientific and Technological Research Council of Turkey (TUBITAK) during my doctoral education and research. Additionally, I gratefully acknowledge the Proteomics Facility of Koç University and the Molecular Imaging Core Facility of Koç University Research Center for Translational Medicine (KUTTAM-CMIC) for their technical assistance.

I cannot express how deeply grateful I am to start this doctoral journey with Ceyda Seren Ceyhan. Besides teaching me thousands of scientific concepts, you showed me the very naive side of each person. You are one of the bravest people I know, and I hope you never change. As I initiate this doctorate graduation thing now, I urge you to hurry up and join me. We still have much to accomplish together, but from now on, as two doctors. I am looking

forward to our new adventures not only in academia but throughout life. I'm so glad you exist. I love you very berry much you are the greatest addition to my life and thank you for being my sister.

I started my PhD experiment with Cansu Akkaya. Cansu, I still can't believe how easily you were using the mouth pipette, as I still think it is the most cursed invention ever. Nonetheless, I am glad our paths crossed, and starting with someone as sweet and knowledgeable as you are a great blessing. Büşra Akarlar, your positive energy is not only pleasant for our lab but also for our LC-MS/MS. Without your expertise, it would not have been possible to finish all these proteomics experiments, thank you. Nazan, thank you for adding so many perspectives to me; I have learned a lot from every discussion we've had. Danny, thanks for your scientific discussions and always being cheerful, as well as for suggesting new computer games.

Additionally, I would like to extend my gratitude to all members of the NOZLU lab. Thank you individually for all your support and for providing an academic family for the past five years. Dilaray, I have no doubt you will achieve great result, best of luck on your EML1 doctoral journey.

My dearest friends Emincan Kaya and Batuhan Rendeci, it is hard to understand why things turned out this way. It was too early, and you both saddened me deeply. You only made me laugh a lot, thank you for coming into my life and always making me laugh. May the place you have gone be peaceful.

For my family, I extend my deepest gratitude: Nuran, Ali, Onur, Ümran, Aren and Yosun. To my dear mother, Nuran, you tried to provide everything to me, your support has been invaluable not only throughout my doctoral journey but throughout my entire life. You always wanted me to become a doctor, not a medical one, but look, we made it! I love you very much. To my dad, Ali, you are perhaps the most emotional man I have ever known, thank you for teaching me how to be a good person. To my brother, Onur, in one of the most beautiful moments of my childhood, there was you playing Half-Life or Tomb Raider in your room, and me watching you. My feelings in that room and next to you never changed; always safe and happy, the perks of being a little sister.. I'm so glad you exist. To my aunt, Ümran, thank you for always being by my side and having my back in addition to your constant support and presence. And to dear Aren, our little one, thank you so much for taking on the role of being the youngest in the family, as let's admit it, in each year that title was starting to feel a bit strange for me. Along with this title, it's important to mention that you've also stolen our hearts. Even though you're far away now, I'm thrilled and excited to accompany you as your aunt and friend through every moment of your life.

Finally, Yosun. Writing about you still incredibly challenging for me. I shared 17 years of my life with you, and witnessing your absence deeply saddened me. You were my best friend and at the same time my baby. When I started my academic journey, you were there, fascinated to destroy all my printed electrophoresis images. I wish you were still by my side; I would have printed a specific copy of this thesis just to see your fascination with paper and for your final art with it. Thank you for entering and becoming a big piece in my life with bringing only joy and love, my little paw. I will see you in another life where we are both cats.

*For living, loving, and laughing**...***

TABLE OF CONTENTS

LIST OF FIGURES

ABBREVIATIONS

AP - Apical Progenitors

aRG - Apical Radial Glia

BP - Basal Progenitors

bIP - Basal Intermediate Progenitors

bRG - Basal Radial Glia

BSA - Bovine Serum Albumin

cDNA - Complementary DNA

CKAP4 - Cytoskeleton-Associated Protein 4

CST - Cell Signaling Technology

cKO - Conditional Knockout

DCX - Doublecortin

DMSO - Dimethyl Sulfoxide

DNA - Deoxyribonucleic Acid

Dhx15 - DExH-box helicase 15

Ddx3x - DEAD-box helicase 3, X-linked

Ddx6 - DEAD-box helicase 6

Dnajc7 - DnaJ heat shock protein family (Hsp40) member C7

Dnmt1 - DNA methyltransferase 1

EDTA - Ethylenediaminetetraacetic Acid

EG - Epidermal Growth Factor

EGF - Epidermal Growth Factor

Eif2s3x - Eukaryotic translation initiation factor 2 subunit 3, X-linked

EMAP - Echinoderm Microtubule-Associated Protein

EML1 - Echinoderm Microtubule-Associated Protein-Like 1

EML4 - Echinoderm Microtubule-Associated Protein-Like 4

ER - Endoplasmic Reticulum

FGF - Fibroblast Growth Factor

GFP - Green Fluorescent Protein

GO - Gene Ontology

GFAP - Glial Fibrillary Acidic Protein

HEK - Human Embryonic Kidney

HeCo - Heterotopic Cortex

iPS - Induced Pluripotent Stem Cells

KIF1B - Kinesin Family Member 1B

LFQ - Label-Free Quantification

MAP - Microtubule-Associated Protein

MAPs - Microtubule-Associated Proteins

mTORC1 - Mammalian Target of Rapamycin Complex 1

MTOC - Microtubule Organizing Center

MT - Microtubules

Nat10 - N-acetyltransferase 10

NEC - Neuroepithelial Cells

NP - Neural Progenitor

NSC - Neural Stem Cells

NSL - Nonsense-Mediated mRNA Decay Enhancing Factor

PDL - Poly-D-lysine

PCDH7 - Protocadherin-7

PCDHs - Protocadherins

PCR - Polymerase Chain Reaction

PNVH - Periventricular Nodular Heterotopia

PTM - Post-Translational Modification

RIPA - Radioimmunoprecipitation Assay

RG - Radial Glial Cells

Rpl10a - Ribosomal protein L10a

Ruvb1 - RuvB-like AAA ATPase 1

SBH - Subcortical Band Heterotopia

SAP - Subapical Progenitors

SH - Subcortical Heterotopia

SDS - Sodium Dodecyl Sulfate

siRNA - Small Interfering RNA

TFA - Trifluoroacetic Acid

TEMEM55B - Transmembrane Protein 55B

TTC5 - Tubulin-specific Ribosome-Associating Factor 5

UniProt - Universal Protein Resource

VZ - Ventricular Zone

VSP41 - Vacuolar Sorting Protein 41

WT - Wild Type

Chapter 1

INTRODUCTION

The cerebral cortex is a highly complex part of the brain responsible for higher cognitive functions and undergoes a finely organized developmental process known as corticogenesis. During this process, a diverse set of neurons, originating from progenitor cells, is organized across the layers of the cerebral cortex through communication and coordination with microtubules (MT), actin, and intermediate filament networks (Lasser et al., 2018; Menon & Gupton, 2016; Pacheco & Gallo, 2016). The dynamic interactions between the cells ensure the proper cortical layer formation and function for cognitive processes (Romero et al., 2018).

Among the multiple molecular players involved in cortical development, microtubules, and microtubule-associated proteins (MAPs) are important regulators of neurogenesis, including cell proliferation, neuronal migration, and axonal guidance as brain development relies heavily on MT function. The defects in MT and MT-associated proteins can lead to cortical malformations which result in developmental delays, and intellectual and motor disabilities, often accompanied by epileptic seizures (Kielar et al., 2014; Noctor et al., 2001; Romero et al., 2018).

Echinoderm microtubule-associated protein-like 1 (EML1), from the EMAP protein family, is essential in cortical malformations with its mutations associated with severe phenotypes in both humans and mice (Kielar et al., 2014; Markus et al., 2021; Shaheen et al., 2017). Patients with *Eml1* mutations show a spectrum of abnormalities, including human ribbon-like subcortical heterotopia (SH), hydrocephalus, and corpus callosum pathology (Kielar et al., 2014; Oegema et al., 2019; Shaheen et al., 2017).

Heterotopic Cortex (HeCo) mouse model with spontaneous *Eml1* mutations, shows a disruption of the proper distribution of radial glial cells (RG), leading to their detachment from the ventricular zone and subsequent formation of heterotopia (Bizzotto et al., 2017; Kielar et al., 2014; Uzquiano et al., 2019). RG are the primary neuronal progenitors in the developing cortex, guiding neuronal migration and supporting neurogenesis through complex mechanisms with their distinct morphology and positioning within the developing cortex (Götz & Huttner, 2005; Noctor et al., 2001). HeCo RG exhibits an abnormal proliferation outside the ventricular zone (VZ), a phenotype associated with the formation of cortical heterotopia.

The investigation of the molecular mechanism underlying EML1-associated SH has revealed its effect on the destabilization of the primary cilium, which is a signalling hub containing various receptors and signalling molecules involved in developmental pathways regulating crucial processes during cortical development including cell proliferation, differentiation, and neuronal migration (Götz & Huttner, 2005). The EML1-dependent cilia impairment problems highlight the critical role of microtubule dynamics in the pathogenesis of SH (Uzquiano et al., 2019). However, microtubule-related perturbations underlying EML1-mediated cortical malformations have remained elusive. Understanding these connections is crucial for explaining the complexities of corticogenesis.

In this thesis, I investigate the dysregulations of *Eml1* depletion on cortical development with analysis of imaging and interactome network analysis of heterotopia-associated mutant EML1 protein and the proteome change of *Eml1* conditional knockout (cKO) mice with a forebrain-specific inactivation of *Eml1*. Through a combination of imaging, BioID, label-free proteomics, phosphoproteomics, dimethyl labelling, and

microtubule proteome, I aim to find the molecular mechanism underlying Eml1 mediated regulation of microtubule dynamics and its consequences for cortical development which will advance our understanding of neurodevelopmental-disorders-associated with MT dysfunction.

In the second part of the thesis, during my Ph.D. I was involved in a side project focused on the cell cycle-dependent regulation of the adhesion protein PCDH7. During cell division, the plasma membrane undergoes dramatic reshaping (Rieder & Khodjakov, 2003) and protocadherins (PCDHs) are the largest cell surface protein subgroup in the cadherin superfamily. In our laboratory's previous work, it was shown that PCDH7 enriches the mitotic membrane (Özlü et al., 2015). In this project, I first generated a stable cell line and then used live and fixed cell imaging to characterize PCDH7 localization during cell division.

By using first chemical inhibition of palmitoylation mechanisms and subsequent knockdown methods (both siRNA and shRNA), in combination with cell cycle synchronization, I showed that palmitoylation mechanisms control PCDH7 localization to the mitotic membrane and cleavage furrow specifically, via a specific palmitoyltransferase, ZDDHC5. This study revealed the spatiotemporal regulation of PCDH7 and its dependence on palmitoylation mechanisms during cell division and PCDH7 became one of the first examples of the role of palmitoylation in the cell cycle-dependent localization of a protein.

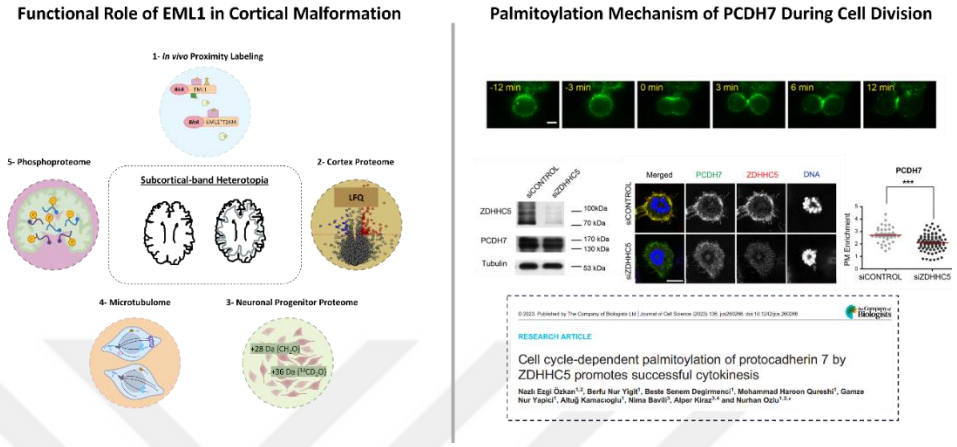

Figure 1. Overview of my thesis

Chapter 2

PROTEOMIC ANALYSIS OF EML1 DEPENDENT CORTICAL MALFORMATION

2.1 LITERATURE REVIEW

2.1.1 Mammalian cortex

The cerebral cortex is a highly complex part of the brain responsible for higher cognitive functions, including perception, decision-making, working memory, advanced forms of communication, and motor planning. As one of the most complex and most divergent regions of the brain, the cerebral cortex contains around 16 billion neurons which is more than %80 percent of the total brain mass (Azevedo et al., 2009). This complex structure is precisely controlled with the orchestrated events during development, including progenitor proliferation, neuronal migration, synaptogenesis, and establishment of neural networks. This process is also called corticogenesis with the different cell types contributing to the architecture of the cortex through communication and coordination with microtubules (MT), actin, and intermediate filament networks (Kirkcaldie & Dwyer, 2017; Lasser et al., 2018; Menon & Gupton, 2016; Pacheco & Gallo, 2016). Understanding the diversity and development of the cortical layers is a subject of significant interest in the neuroscience field which also covers the distribution of these processes resulting the critical development disorders such as cortical malformations and neuropsychiatric diseases.

The development of the cerebral cortex from neural stem cells (NSCs) and neural progenitors (NPs) to the complex cortical circuit networks of billions of neurons is a remarkable process shared across all mammalian species. While the "inside-out" development

of the cerebral cortex is similar for all mammals, certain aspects like timing and cortical folding of the brain's structure differ between species. Neuroepithelial cell (NECs) amplification takes around 1 day in mice and up to 2 weeks in primates. Similarly, neurogenesis takes 1 week in mice and almost 4 months in humans (Figure 2.1). This prolonged neurogenesis in humans is one of the essential keys to allowing increased numbers of neuronal epithelial cells (NECs) and radial glial cell (RGCs) divisions.

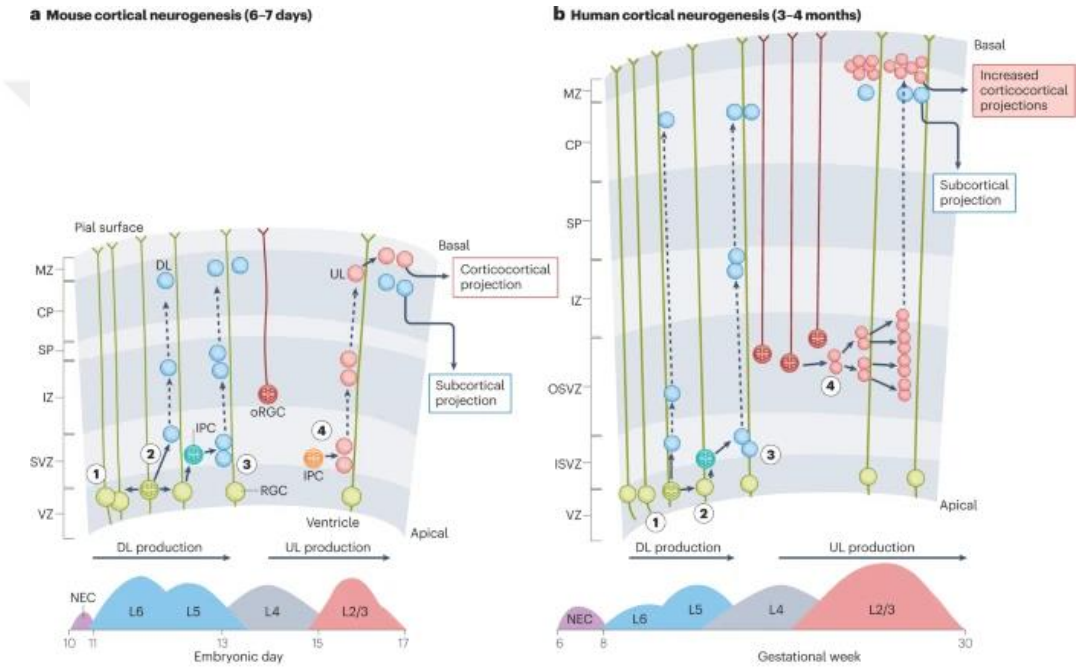

Figure 2. 1 Species specific characteristics of cortical development

(Adapted from (Vanderhaeghen & Polleux, 2023))

Rather than the timing differences, one of the other unique concepts in the cortical folding mammalian cortices can be classified into lissencephalic species characterized by smooth-surfaced cortices (e.g. small rodents and small primates) and gyrencephalic species exhibiting convoluted surfaced (e.g. most primates) (Kelava et al., 2013). The complexity of corticogenesis highlights the importance of unraveling the mechanisms responsible for

assembling this complex structure explaining how the diverse array of cortical cell types are formed and how they form complex patterns of connections within the cortex. Insights into these processes provide knowledge of not only normal brain development but also provide valuable information on underlying causes of various pathological conditions affecting the cerebral cortex.

2.1.2 Cellular diversity in the neocortex

The mammalian cerebral cortex has a unique diversity of cell types that are generated during development through a series of temporally regulated events and the formation of the layered cerebral cortex is depended on the proliferation, migration, and differentiation of these cells. During early corticogenesis, neuroepithelial cells (NECs) form the ventricular zone (VZ) and are responsible for the expansion of the neocortex (Figure 2. 2). The cerebral cortex is divided into two main regions the neocortex and the allocortex. The neocortex is the part of the cortex tgat has unique six distinct layering. There are three classes of neural progenitor cells (NPC): basal progenitors (BP), apical progenitors (AP) and subapical progenitors (SAP). Apical progenitors located in the ventricular zone (VZ) have three types: apical radial glia (aRG), apical intermediate progenitors (aIP), and neuroepithelial cells (NEC). Basal progenitors are also divided into two groups basal intermediate progenitors (bIP) and basal radial glia (bRG).

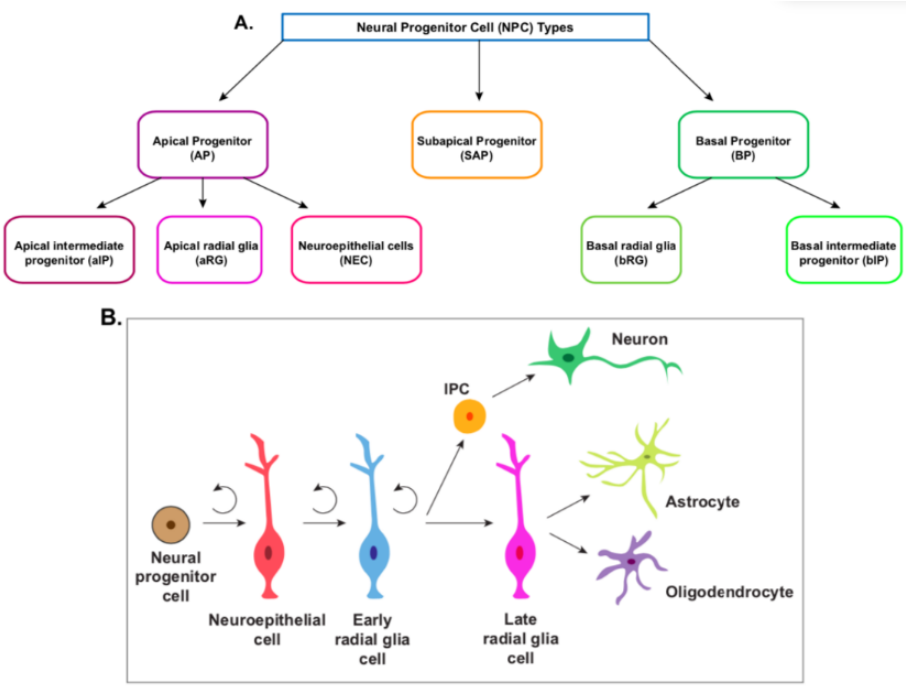

Figure 2. 2 Classification of neural progenitors and their neuronal differentiation fates

(Adapted from (Florio & Huttner, 2014)) **A.** Neuronal progenitor cell types. B. Neural progenitor cells as the stem cells of the nervous system and neuroepithelial cells are one of the earliest forms of neural progenitors radial glial cells. Early radial glial cells divide asymmetrically to form intermediate progenitor cells and another radial glial cell. Intermediate progenitors then undergo a limited number of divisions to form immature neurons and late glia cells which differentiate into non-neuronal lineage oligodendrocytes and astrocytes.

NECs are the neuronal stem cells (NSCs) which have ability to generate neurons and glia. Compared to neural progenitor (NP) cells, NECs differ in their multipotent division status, they are multipotent, whereas NP cells are monopotent with limited fate (Taverna et al., 2014). NECs are highly polarized epithelial cells and apical plasma membranes of NECs are connected to the cerebrospinal fluid and basal plasma reaches the basal lamina

(Figure 2.3). These distinct connections provide a highly rich and dynamic environment which is required for the regulation of neurogenesis (Götz & Huttner, 2005; Lehtinen et al., 2011; Stocker & Chenn, 2015). During the division NECs undergo interkinetic nuclear migration which is the ability of going cell division while cells migrating, and mitosis of these cells are limited in the ventricular zone.

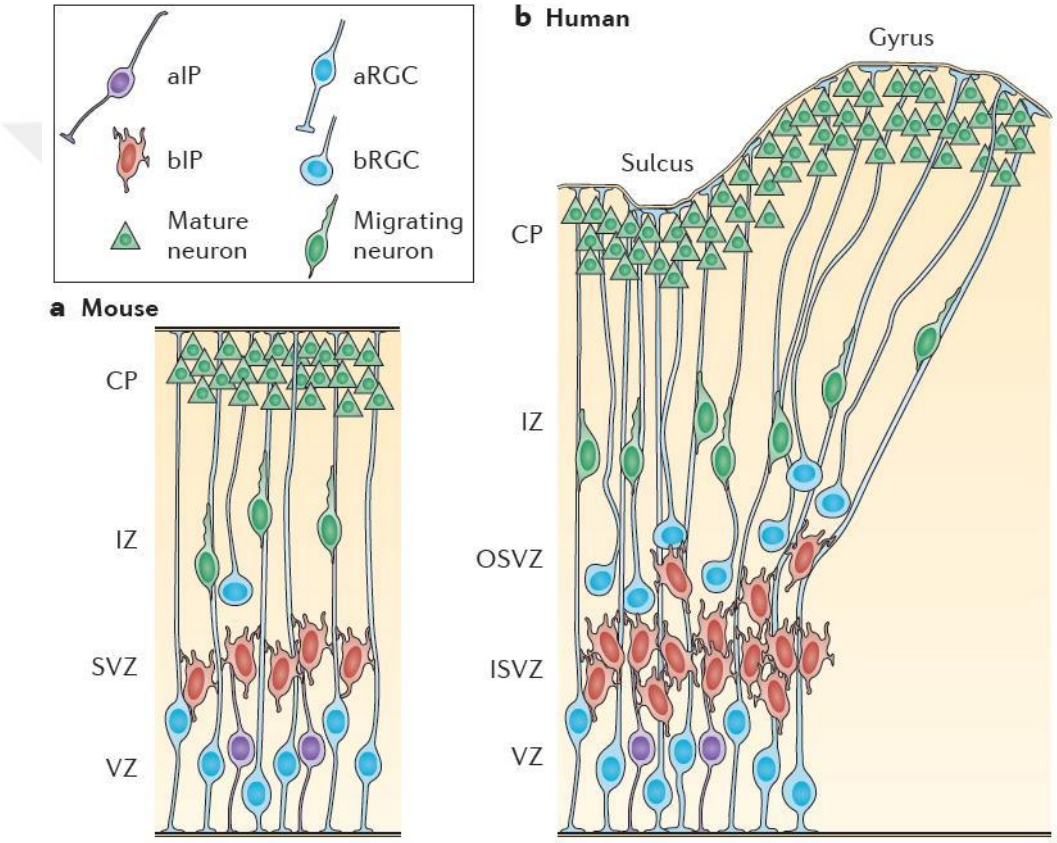

Figure 2. 3 Progenitor cells in the mouse and human developing neocortex (Adapted from (Sun&Henver,2014)

Neural stem cells and progenitor cells are divided into two subgroups according to their locations where they perform the mitotic activity. Apical radial glial cells (aRGCs) undergo cell division at the ventricular surface and basal radial glial cells (bRGCs) position in

the subventricular zone and inner subventricular zone. RGCs have the unique characteristics of glial cells expressing the glial markers such as GFAP, and GLAST and they serve as scaffolding for the migrating neurons in the neocortex (Campbell & Götz, 2002; Rakic, 2007). In the 'inside-out' manner RGCs can undergo asymmetric cell division and provide one RGC or one postmitotic neuron and one intermediate progenitor cell.

Intermediate progenitor (IP) cells can be also grouped into two populations basically according to again the positioning of these cells in the layers of the cortex: apical IP cells and basal IP cells. Whereas basal IP cells, delaminate from the ventricular zone and migrate into the subventricular zone, the apical IP cells reside in the ventricular zone and have a short attachment to the surface (Hevner & Haydar, 2012; Kowalczyk et al., 2009). Although the full mechanism of the division and transition of the progenitor cells is not understood, it is known that several transcriptional regulators including T-box brain protein 2, insulinoma-associated protein 1, and TMF-regulated nuclear protein 1 seem to be involved and the control of the neocortex size depends on the balance of the proliferation and differentiation of these progenitor cells (Sun & Hevner, 2014). Disruption of any of these systems result in brain malformation.

2.1.3 Inside-out cerebral cortex development and neuronal migration

During neurogenesis, radial glial progenitors divide at the ventricular zone surface and provide direct or indirect generation of neurons by supplying intermediate progenitors, short precursors, and outer subventricular zone radial glial progenitors (Fietz et al., 2010; Hansen et al., 2010; Haubensak et al., 2004; Hevner, 2006). Newborn cortical neurons then migrate along the radial glial fibers which provide the layering of the neocortex

(Figure 2.4.). The scaffold of radial glial fibers extends vertically between the ventricular zone and the pial surface of the cortex which provides 'railway' tracks for the guidance of the neurons during the radial migration (Rakic, 1988). This trajectory of these fibers defines the migration route and final position of the new neurons in the cortex. It is well-known that this migration occurs in an 'inside-out' manner which is, that early-born neurons migrate to the deep layers whereas late-born neurons migrate past early-born neurons to produce superficial layers (Greig et al., 2013). The cell-to-cell interaction is tightly regulated during the migration and disruption leads to severe defects in neuronal positing and cortical layer formation (Anton et al., 1997).

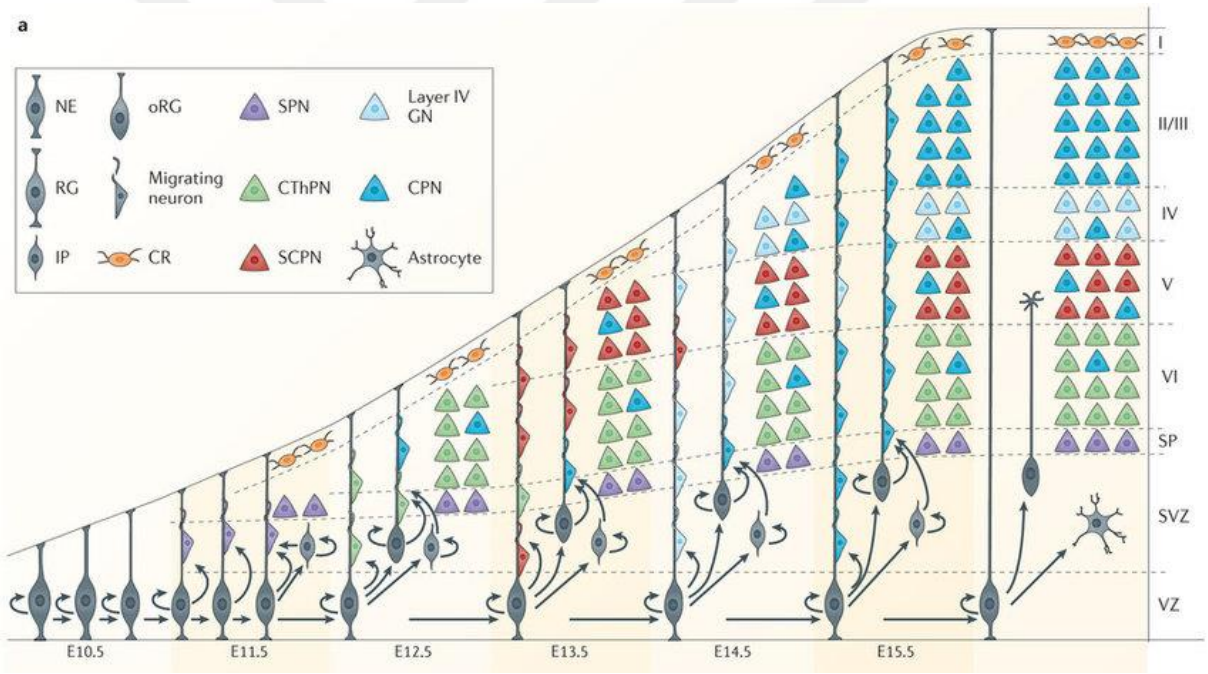

Figure 2. 4 Formation of inside-out neocortex

(Adapted from (Greig et al., 2013))

After the neurons complete their radial migration on the fibers, they detach and begin the terminal differentiation stage. This process includes increasing cell soma size and neuropill

volume, growth, and branching of the dendrites and axons for synaptic connections and affects the final size of the neocortex. These soma sizes and dendritic and axonal extents are different across mammals and correlate with brain size and cortical expansion (Reillo et al., 2011) .

2.1.4 Neural progenitor cell division: symmetric and asymmetric divisions

Neuronal progenitor cell division is a very crucial decision between the asymmetric and symmetric divisions for the cells to normal formation and functioning of the nervous system. The processes include decisions between the asymmetric and symmetric divisions which both contribute uniquely to the complexity of diverse cell types (Figure 2.5.). Asymmetric cell division in neurogenesis has been extremely studied specifically in model organisms such as Drosophila and Caenorhabditis elegans, to understand the fate determination of the neuronal progenitor cells (Arata et al., 2010; Knoblich, 2008). It is known that the fate of cells in asymmetric division comes either through extrinsic signals from the microenvironment or intrinsic polarization within the cells which results in distinct phenotypes in two daughter cells and the cell polarity during the division plays a crucial role in the decision of the symmetric or asymmetric division which influences the fate of daughters (Knoblich, 2008).

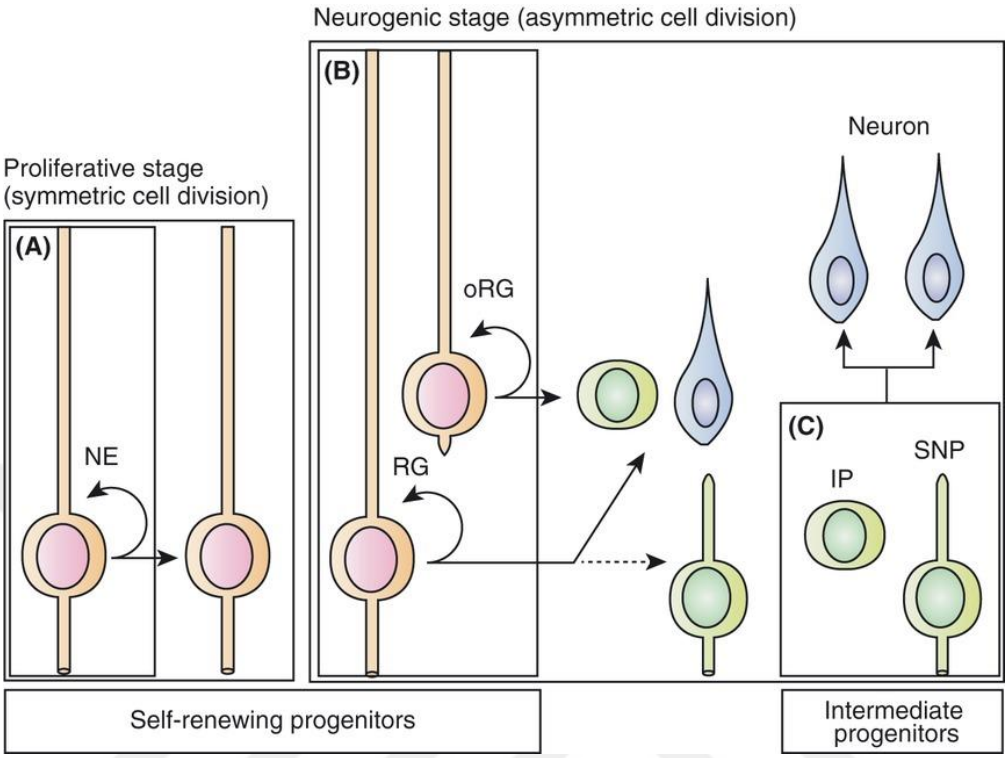

Figure 2. 5 Symmetric and asymmetric divisions in neuronal progenitor cells

(Adapted from (Matsuzaki & Shitamukai, 2015))

For the asymmetric cell division in mammalian neural progenitors, there are two proposed models of dynamics: Chenn, McConnel, and Huttner models. Chenn & McConnel's models propose the transition from the symmetric division plane in the proliferation stage to the asymmetric vertical plane in the neurogenic stage (Chenn & McConnell, 1995). The other hypothesis suggested by Huttner and his colleagues points out that tilt in the division plane of radial glial cells enables asymmetric positioning of the cellular components (Huttner & Brand, 1997) . The orientation of the cleavage plane and the mitotic spindle have great importance in the determination of the division type. In the symmetric division, the vertical division plane

provides equal distribution of the cellular components in neural epithelial cells between the twp daughter cells. On the other hand, asymmetric division has an oblique cleavage plane which provides unique fates and characteristics for the two daughter cells (Haydar et al., 2003; Kosodo et al., 2004; Kosodo et al., 2008). With the progress in neurogenesis, the asymmetric division becomes a more dominant choice of division. The primary cilium and centrosomes are also key players in the cell division fate determination. The primary cilium acts as a sponsor antenna taking extracellular signals that are critical for cell division and differentiation and centrosomes regulate the spindle orientation to establish the orientation of the division plane (Corbit et al., 2005; Eggenschwiler & Anderson, 2007; Mora-Bermúdez et al., 2014).

2.1.5 Cortical malformations and heterotopia

The cerebral cortex is formed by a finely organized developmental process known as corticogenesis. During this process, diverse neuron types, originating from progenitor cells, are organized across the layers of the cerebral cortex through communication and coordination with microtubules, actin, and intermediate filament networks. The dynamic interactions between the cells ensure the proper cortical layer formation and function for cognitive processes (Romero et al., 2018; Stouffer et al., 2016). The disruption of these processes can result in cortical malformations which is a rare disorder with occurring %1 of the population. Approximately, %14 of epilepsy patients has neuronal migration disorder. and the abnormality can be detected through their clinical expressions such as intellectual and motor disabilities, from mild to severe, drug-resistant epilepsy, and developmental delay. Although cortical malformations can be categorized into three based on the affected brain size, cortical folding, and abnormal neuronal positioning, it is a spectrum rather than an isolated single phenotype.

Periventricular and subcortical band heterotopia, result from the cortical neuronal migration abnormalities and misplacement of the neurons in the layers of the neocortex (Figure2.6). While the heterotopia phenotype is generally linked to migration defects, cell division, cell polarity and behavior of radial glial cells can also contribute to heterotopia formation (Beattie et al., 2017; Bizzotto et al., 2017). The most common heterotopia is periventricular heterotopia which results from the nodule formation along the wall of the ventricles. The other and rarely encountered one is subcortical band heterotopia caused by band-like clusters located underneath the gray tissue of the cerebral cortex. Abnormal nodule and cluster formations in the cerebral cortex can have many causes such as abnormal positioning of precursor cells, cell cycle characteristic changes, neuronal migration abnormalities, and abnormal signals coming from the environment to the cells.

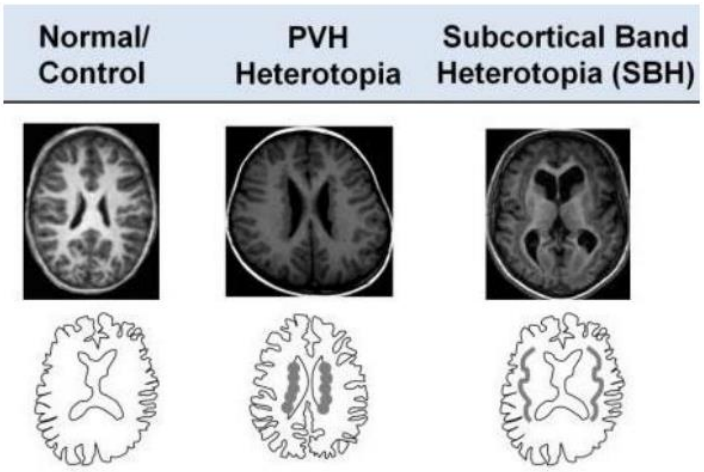

Figure 2. 6 MRI images and illustrations of brain malformations (Adapted from (Romero et al., 2018))

Genetic mutations affecting the microtubule cytoskeleton such as *PAFAH1B1*, *TUBA1A, LIS1, TUBA1A, DCS,* and kinesins *KIF5C* and *KIF2A* have been linked to subcortical band heterotopia (Di Donato et al., 2018; Poirier et al., 2013). Genetic screening in a large cohort of lissencephaly patients revealed the majority of patients having DCX

mutations with a few linked to *PAFAH1B1* mutations and these two genes collectively explain 80% of patients (Vriend & Oegema, 2021). Human heterotopia patients can have de novo mutations or homozygous mutations with family histories of genes like *EML1, ACTG1*, *CRADD*, and *KATNB1* (Di Donato et al., 2018; Kielar et al., 2014) (Figure 2.7). Some of the genes such as *CCDC85C, RHOA, AFADIN, α-E-CATENIN* can result in similar and severe phenotypes in the mouse when they are suppressed or downregulated during corticogenesis (Cappello et al., 2012; Mori et al., 2012). The pathogenesis of subcortical heterotopia remains a poorly understood and challenging research topic due to the rare occurrence in mouse models and mutations associated with the disease failing to give the phenotype or result in lethality in mouse models.

Among the heterotopia-associated genes, Echinoderm microtubule-associated protein-like 1 (*EML1*), from the EMAP protein family, has appeared as an important in cortical malformations with its mutations associated with severe phenotypes in both humans and mice (Kielar et al., 2014; Markus et al., 2021; Shaheen et al., 2017). Patients with *EML1* mutations show a spectrum of abnormalities, including human ribbon-like subcortical heterotopia (SH), hydrocephalus, and corpus callosum pathology (Kielar et al., 2014; Oegema et al., 2019).

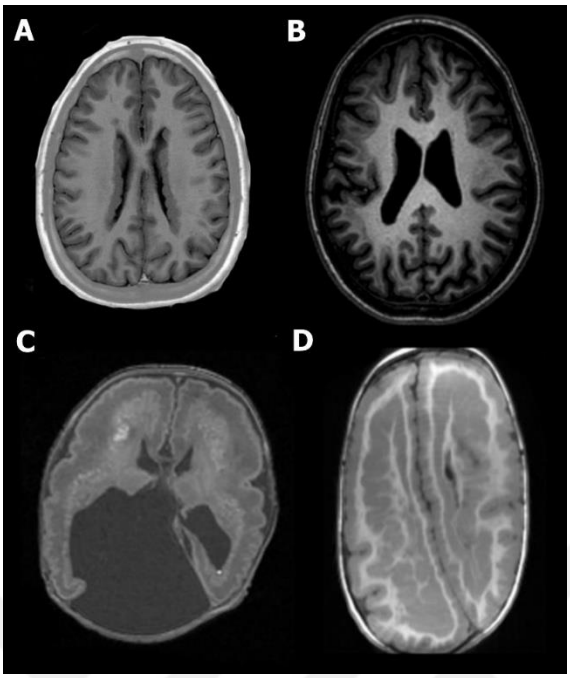

Figure 2. 7 MRI images of human heterotopia patients

A-T1-weighted axial image of bilateral continuous PNVH in woman with FLNA mutation. B-T1-weighted axial image of SBH in a woman with DCX mutation. C, D- EML1-associated ribbon-like heterotopia in infancy (C) and at 3 years of age (D). (Adapted from (Vriend & Oegema, 2021)).

2.1.6 EMAP proteins

Microtubules are one of the cytoskeleton structures in eukaryotic cells with a dynamic network by the tubulin heterodimers to perform several crucial cellular processes such as cell division, intracellular structural organization, and transportation of intracellular RNAs, proteins, and organelles, as well as flagellar and ciliary motility. This critical cytoskeleton component and its regulations through polymerization and depolymerization are tightly regulated by microtubule-associated proteins (MAPs). The microtubules and microtubule-associated proteins (MAPs) are some of the main regulators of neurogenesis,

including cell proliferation, neuronal migration, and axonal guidance as brain development relies heavily on microtubule function. The defects in microtubules and MAPs can lead to cortical malformations (Hirokawa et al., 2009; Kaverina & Straube, 2011).

2.1.7 Structure of EMAP proteins

The Echinoderm Microtubule-Associated Protein (EMAP) family (EML proteins) is a novel class of MAPs that primarily decorate the microtubule network and function in mitotic spindle formation (Richards et al., 2014; Suprenant et al., 1993). Mammals have six EML proteins, based on their protein structures they can be classified into two subgroups EML1-2-3-4 and EML5-6 (Figure 2.8).

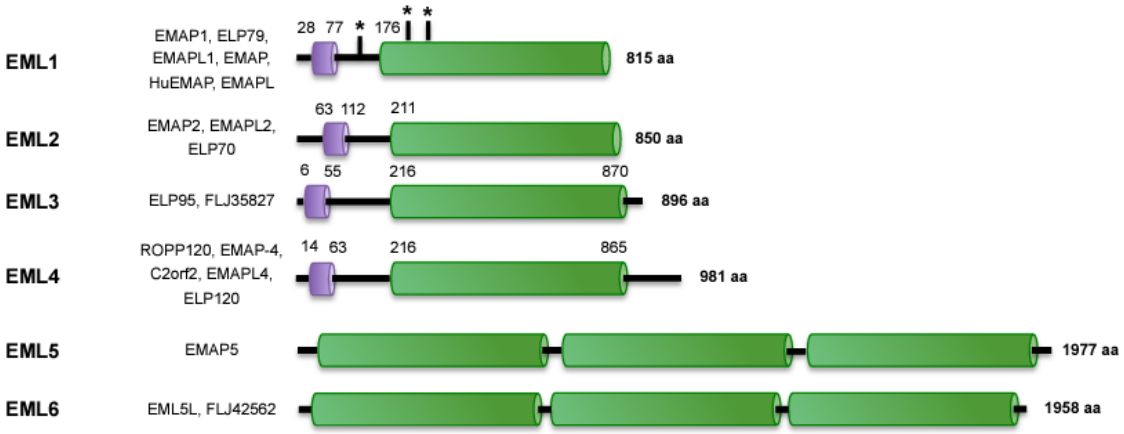

Figure 2. 8 Structural domains of the EMAP proteins (Adapted from (Fry et al., 2016))

EML1-2-3-4 proteins having a molecular weight ranging from 70kDa to 120kDa contain a coiled-coil domain and hydrophobic HELP motif at the N-terminal, and the C-terminal domain has approximately 650 residues of multiple tryptophan-aspartic acid (WD) repeats. Whereas EML5-6 has a molecular weight larger than 200kDa and three hydrophobic HELP motifs and WD repeats (Sabir et al., 2017). EML1 and EML4 are highly expressed

during the early stages of mouse embryo development and expressions get lower in late embryos and adult tissues in the nervous system (Houtman et al., 2007) . Likewise, EML5 is also mainly expressed in the adult nervous system (O'Connor et al., 2004).

Although the EMAP family suggests they have important functions, so far little is known about them and their binding to the microtubules. For the EMAP family, the HELP motif within the N-terminal is one of the crucial sides for the microtubule binding. It is shown that the isolated TAPE domain of EML1 and the N-terminal of EML4 tight association with soluble α/β-tubulin heterodimers (Richards et al., 2014; Sabir et al., 2017). Further studies revealed that binding to the microtubules requires also the trimerization domain (Figure 2.9.) (Richards et al., 2015). The trimerization domain is composed of the specific amino acid motif (Ala-Leu-Ala-Asp, ALAD motif) and it is essential to maintain the coiled-coil structure. This domain strongly associates with the microtubules and deletion of the trimerization domain from the structure, reducing the interaction of protein-microtubule binding but the trimerization domain alone is not sufficient for the MT binding (Richards et al., 2015). These findings also suggest that not only one domain, but the involvement of a complete N-terminal region is responsible for the microtubule binding possible because the basic nature of the N-terminal side of proteins also helps microtubule binding. For EML5-6, they have a unique structural organization that lacks coiled-coil structure at the N terminal but they have three repeats of the TAPE domain, It is known that EML6 protein can co-localized with the meiotic spindles oocytes in mouse ovaries to maintain the spindle integrity and chromosome segregation (Yin et al., 2020).

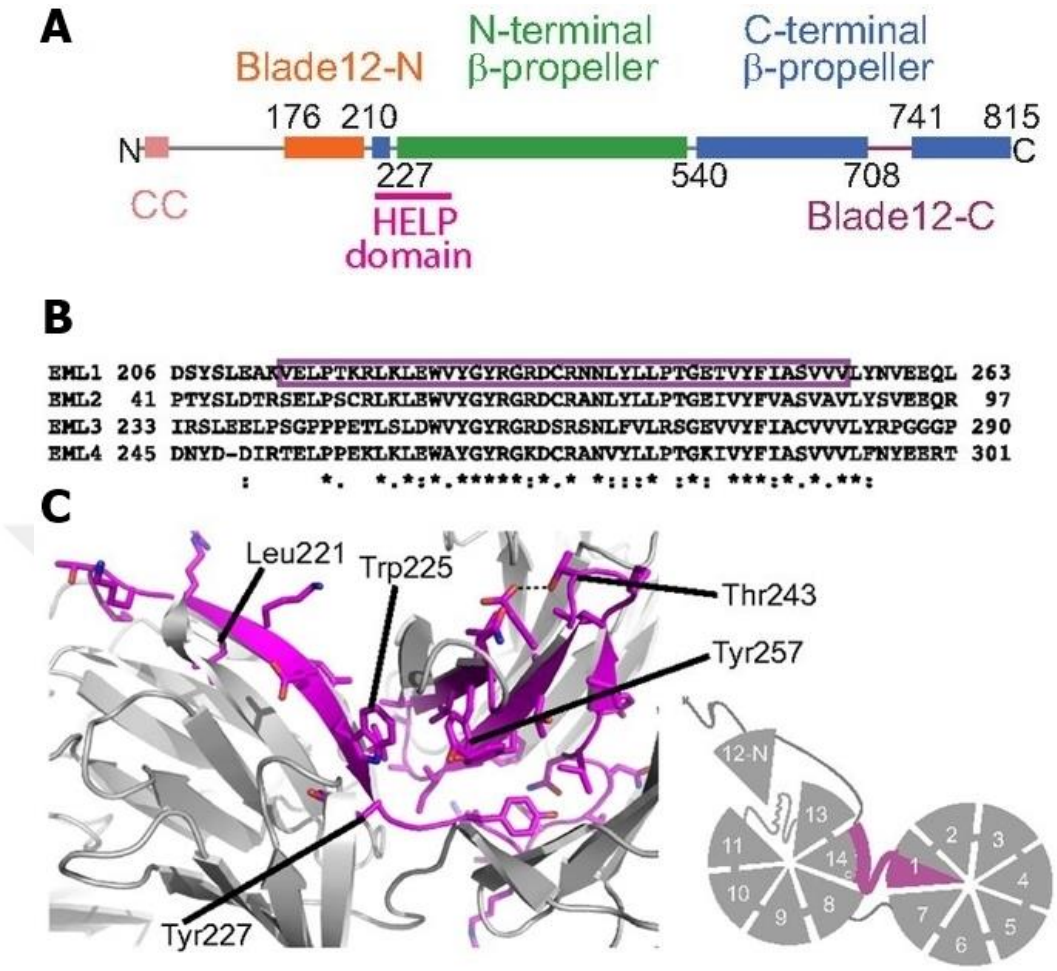

Figure 2. 9 EML1 motif organization and structural model

A- EML1 motif organization, B- Position of the HELP motif in EML1-2-3-4, C-Position of HELP motif in the structural model of EML1 (Adapted from (Richards et al., 2014)).

2.1.8 Eml1 and Eml1-associated heterotopia formation

Echinoderm microtubule-associated protein like 1 (EML1), from EMAP protein family, is microtubule binding protein highly expressed in dividing neuronal progenitor cells,

and its perturbations associated with severe phenotypes in both humans and mice. Heterotopia has been a challenging disease to study because the human mutations associated with the disease failed to give the phenotype or result in lethality in mouse models. However, there is spontaneously arisen one mouse model that is widely used in heterotopia, called HeCo (Heterotopic Cortex) mice showing bilateral SBH. The transcriptome and whole-genome single nucleotide polymorphism analysis showed that HeCo mice have a mutation in EML1 (Kielar et al., 2014). This discovery showed that the first-time perturbation of the human heterotopia-associated gene, EML1 also causes heterotopia formation in the mice. Determining the role of EML1 in neuronal cells is crucial in elucidating the molecular causes of heterotopia and rare neurological disorders.

In the adult HeCo mice, heterotopic abnormal neuronal cell accumulation is in the rostro-medial region of the cortex, and it is found that there are early-born neurons and late-born neurons clustered in this heterotopic region. The abnormal neuronal layering and accumulation first suggest that the heterotopia accumulation is caused by the perturbation of the radial glial cell migration tracks during the corticogenesis. However, it is found that HeCo cells have normal migration capacities, which shows not the migration but that other systems are dysregulated during the corticogenesis (Kielar et al., 2014). For this reason, the identification of the *EML1* gene mutations in HeCo mice provided great insight into the disturbed molecular mechanisms involved. The early retrotransposon insertion into intron 22 of the *EML1* gene led to abnormal transcripts and truncated Eml1 proteins which inhibited the normal functioning of cortical progenitors in HeCo mice. Investigation of the progenitor cell proliferation defects in HeCo mice revealed that there are disruptions in mitotic spindle orientation which is also affecting the fate determination of sister cells (Kielar et al., 2014). This finding suggests that rather than the migration defects, the neuronal progenitor cell division might be one of the answers to perturbations in these cells. Furthermore, there are

eight gene mutations have been identified as a heterotopia formation in human patients: Arg138*, Thr243Ala, Trp225Arg, Arg523*, Val254Met, Gly439Asp, and Gly478Val (Kielar et al., 2014; Markus et al., 2021; Oegema et al., 2019; Shaheen et al., 2017).

Although the mechanism of EML1-microtubule binding and its effect on the microtubule dynamics is not well defined, it is known that the HELP motif in EML1 protein provides the binding of the protein to the tubulins (Richards et al., 2014). Human heterotopia-associated mutation in the HELP motif of EML1 protein, Thr243Ala mutation significantly reduces the protein-microtubule binding (Figure 2.10.). This abnormal interaction may interfere with the normal organization of the microtubules and function of the mitotic spindles leading to the misaligned cell division and resulting in the abnormal cell population in the neocortex.

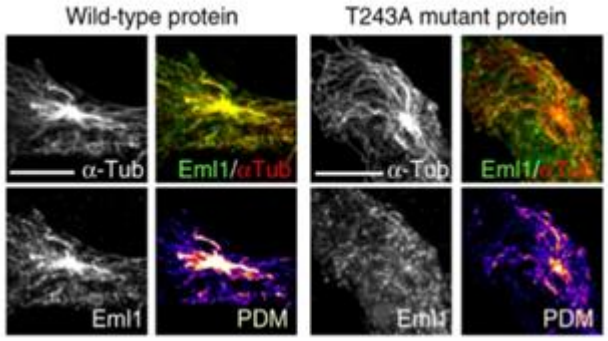

Figure 2. 10 EML1 wild-type and T243A mutant protein - microtubules bindings in Vero cells (Adapted from (Kielar et al., 2014))

For the disrupted microtubule dynamics in these cells, HeCo neuronal progenitor cells have perturbed microtubule dynamics with specifically slower microtubule plus-end growth rates compared to the wildtype cells (Bizzotto et al., 2017). Further analysis also shows that

the shape and size of the cell bodies in HeCo cells are quite different from the normal cells particularly these cells have increased horizontal area (Figure2.11.). Although the total number of cells in the ventricular zone is not different between the HeCo and WT cortices, the increased horizontal area in the heterotopic mice, may alter the proper layer formation in the neocortex.

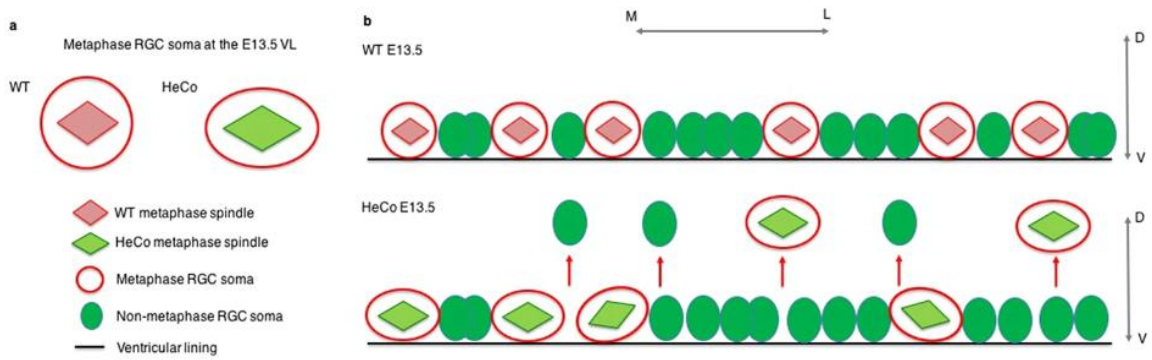

Figure 2. 11 Schematic representation of spindle length and cell size for HeCo cells

(Adapted from (Bizzotto et al., 2017))

Moreover, investigation into the molecular mechanism underlying EML1-associated heterotopia has revealed its effect on the destabilization of the primary cilium, which is a signaling hub containing various receptors and signaling molecules involved in developmental pathways regulating crucial processes during cortical development including cell proliferation, differentiation, and neuronal migration. In the HeCo cortices at embryonic day E12.5 and E13.5, there is a reduction of gamma-tubulin and Arl13b indicating that centrosome and primary cilia defects. With new studies, HeCo progenitors, fibroblasts of heterotopia patients, and cortical progenitors produced from iPSC; It has been shown that there are defects in primary cilia structure (the microtubule-based organelle that is critical for regulating progenitor behavior) and Golgi functions (Uzquiano et al., 2019). Progenitor cells receive environmental signals by connecting to the ventricular surface with primary cilia structures. However, although these structures are shorter and less numerous in HeCo progenitor cells

an increase in the number of vesicles within the cell was also observed. Due to these defects, it has been suggested that progenitor cells in HeCo mice are abnormally positioned within the cortex (Figure 2.12).

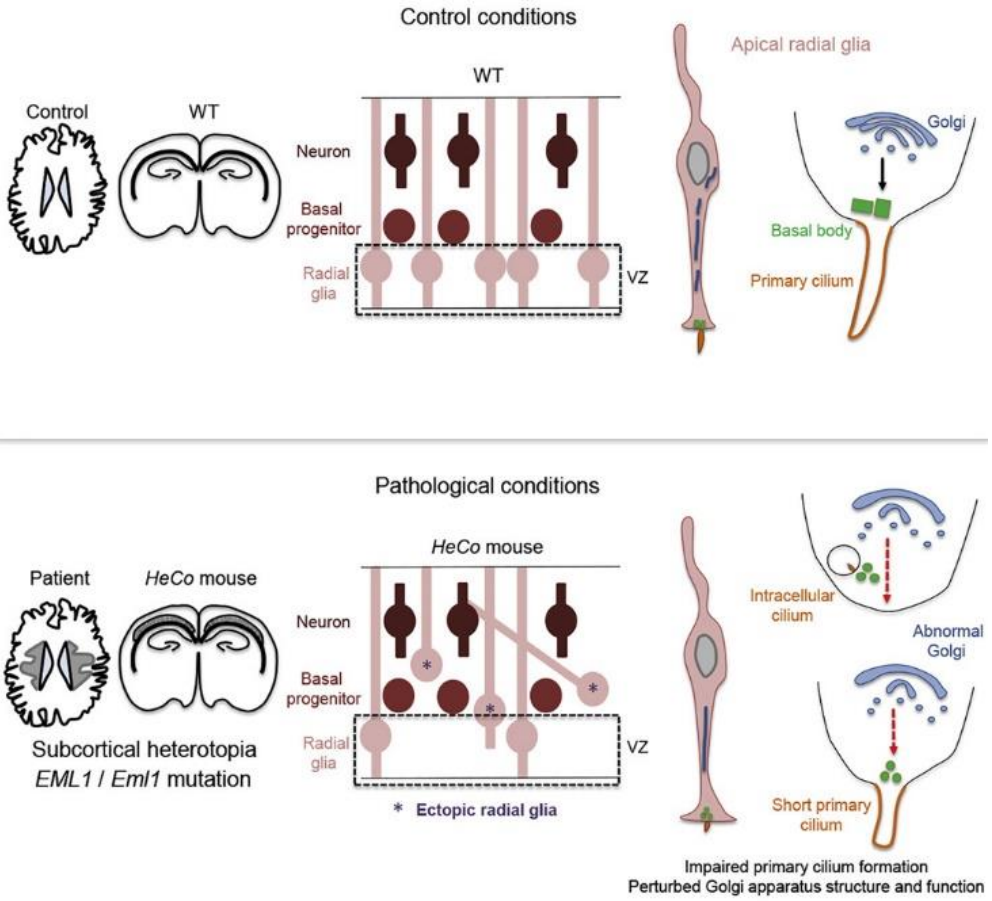

Figure 2. 12 Dysregulation of radial glial progenitor cells in control and HeCO cortices

While the distribution of the cell population is preserved in the normal cortex, the distribution and location of B- HeCo radial glial cells in the cortex with primary cilia deformation changes. (Adapted from(Uzquiano et al., 2019))

Studies in HeCo mice and EML1 mutated human patients have provided great insights into the pathogenesis of subcortical band heterotopia and its association with abnormalities in

primary cilia structures and cellular organelles. EML1 is essential for normal neuronal progenitor proliferation and brain development. The known eight distinct gene mutations linked to heterotopia in human patients highlight the genetic heterogeneity of the disorder and require more analysis to understand the disorder. Additionally, while the precise role of EML1 in microtubule dynamics remains incompletely understood, studies showed that the HELP motif mediates the microtubule interactions and mutations in this domain disrupt this interaction and potentially lead to abnormalities in the microtubules and primary cilia defects with the combination of Golgi abnormalities. While perturbations of *Eml1* in neuronal progenitor cells have been associated with defects in cilia and progenitor cell detachment from the ventricular zone, our understanding of *Eml1* regulation at the protein level remains limited. In this thesis, I show how EML1 depletion rewires proteins in the cortices, neuronal progenitor primary cells, and MTs-MAPs during cerebral cortex development. Multiple comprehensive proteomic analyses revealed that EML1 depletion causes severe disruptions in microtubule cytoskeleton organization and MAPs-microtubule binding, and our findings provide valuable insights into microtubule regulation in cortical malformations.

2.2 MATERIAL AND METHODS

2.2.1. EML1 and EML1Thr243Ala localizations during the cell cycle

2.2.1.1 Cloning of EML1 and EML1Thr243Al into pLenti-CMV-puro backbone

Normal EML1 and mutant EML1Thr243Ala cDNAs were cloned into the pLenti-CMV-puro vector (addgene #17448) using Gibson cloning technique (Gibson et al., 2009). The primer pair used was as follows: forward 5' GAA GAC ACC GAC TCT AGA GCA CCA TGG AGG ACG GCT TCT C 3' and reverse 5' CTC ACC ATG GTG GCG ACC GGT GTA ATG ACT CGC CAC TGC ATG AT 3' (The mutation point is in the middle of the EML1; thus, the same primer pair was used for both normal EML1 and mutant EML1Thr243Ala).

For polymerase chain reaction (PCR) mixture, 0.5 µL Q5 High Fidelity DNA Polymerase (New England Biolabs-M0491), 10 µL 5X Q5 Reaction Buffer, 1 µL 10 mM dNTPs, 2.5 µL 10 µM cloning primer pair, 1.5 ng DNA, 1 µL DMSO, and 34.5 µL nuclease-free water were used. The PCR reaction conditions were initial denaturation at 98°C for 30 seconds, followed by 35 cycles of denaturation at 98°C for 10 seconds, annealing at 59°C for 30 seconds, extension at 72°C for 30 seconds, and final extension at 72°C for 2 minutes.

The background vector pLenti-CMV-puro (addgene #17448) was prepared for cloning by digestion with BamHI-HF (New England Biolabs, 3136) enzyme. For digestion, 2.5 µg of vector was incubated with 1 µL BamHI-HF at 37°C overnight.

PCR-amplified EML1 and mutant EML1Thr243Ala DNAs and digested pLenti-CMV-puro vector were confirmed by loading onto a 1% agarose gel. Successfully amplified DNA

sequences and digested vectors were purified and then ligated with each other using the Gibson Assembly mixture. For this reaction, a ratio of 1:2 of vector to DNA sequence with 25 ng vector and 18 ng insert, mixed with 3.75 µL Gibson Assembly mixture, was incubated at 50°C for 30 minutes. The ligated vector and DNA sequence were then amplified using chemically competent E. coli Stbl3 bacterial cells. In the transformation, 1 µL of the Gibson mixture was incubated with 50 µL of bacteria on ice for 30 minutes, followed by a 1-minute heat shock at 42°C and 2 minutes of incubation on ice, then 1 mL LB broth was added to the bacteria and incubated at 37°C for 60 minutes at 300 rpm. Colonies grown on ampicillin LB agar were verified the next day by colony PCR.

For colony PCR, colonies were picked with 200 µL tips and transferred to a second plate, then PCR tubes were streaked onto the second plate. These tubes were amplified using the same primers used for cloning with 10 µL EmeraldAmp Max HS PCR Master and visualized on a 1% agarose gel. Successful colonies for normal EML1 and mutant EML1Thr243Ala were selected and confirmed by primary double enzyme digestion. For this, the DNAs of selected colonies were digested with 0.2 µL EcoRI (which cuts within EML1) and 0.2 µL BamHI (which cuts within the vector). The vectors confirmed by this digestion, were also sent for Sanger sequencing.

2.2.1.2 Generation of stable cell lines expressing EML1:GFP and EML1Thr243Ala:GFP

In this thesis six different stable cell lines have been generated using lentiviral transduction with pLenti-CMV-GFP, pLenti-CMV-EML1-GFP, and pLenti-CMV-EML1Thr243Ala-GFP viruses in N2A and HeLa cells (Figure 2.13). For viral transduction, lentiviruses were packaged in HEK293T cells using packaging vector (psPAX2, Addgene#12260) and envelope vector (pCMV-VSV-G, Addgene #8454) and transfected with PEI transfection. The viruses were collected at 48- and 72-hours post-transfection and filtered.

These prepared viruses were then added to N2A and HeLa cells in the presence of 2 micrograms/ml protamine sulfate (Sigma-Aldrich, P4505), followed by the establishment of stable cell lines with puromycin antibiotic selection.

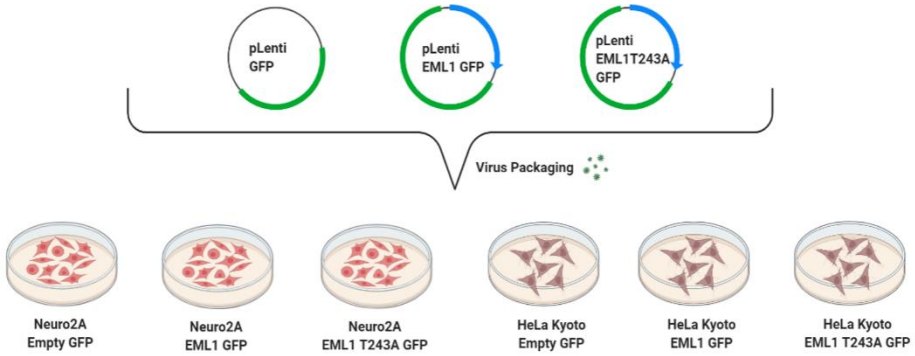

Figure 2. 13 Generation of N2A and HeLa cell lines expressing EML1:GFP and EML1Thr243Ala:GFP

(Created with BioRender.com)

These established cell lines were first confirmed using the western blot technique. For this, samples were lysed in RIPA buffer and run in 10% SDS-PAGE gels. After a 3-hour wet-transfer at 70V, the blots were blocked with 4% non-fat dry milk in TBS containing 0.1% Tween-20 and incubated with primary antibodies diluted in 4% BSA in TBS containing 0.1% Tween-20 (anti-tubulin, Cell Signaling Technology, 3873, GFP, Roche, 11814460001, EML1 Genetex, GTX100252, Histone CST 9715S). Signals were visualized using HRP-conjugated secondary antibodies (Cell Signaling Technology, 7074S and 70765) and detected with ECL (Pierce, 32106; Bio-Rad, 1705061).

2.2.1.3 Imaging of EML1:GFP and EML1Thr243Ala:GFP during the cell cycle

After the generation of stable cell lines, cells were synchronized at the interphase, metaphase, and cytokinesis stages. For this purpose, HeLa cells were blocked with 2mM

thymidine for 20 hours, followed by incubation with 25 ng/ml Nocodazole for 4-5 hours for mitotic synchronization. Since N2A cells did not reach the nice synchronization levels with thymidine, in this cell, serum supplementation was removed for 20 hours, followed by incubation with 25 ng/ml Nocodazole for 4 hours. After Nocodazole treatment, both cell groups were incubated in normal medium for 1 hour to allow these cells to enter cytokinesis.

For immunofluorescence (IF) staining, cells were fixed with methanol for 5 minutes at -20°C and then with 4% paraformaldehyde for 5 minutes at room temperature. Then they blocked with 5% BSA and primary antibodies (GFP Invitrogen, A11120, Tubulin CST 2128S) were incubated overnight in 3% BSA. Images were taken at 63x magnification using a Leica DMi8/SP8 TCS-DLS confocal microscope.

2.2.2 Defining interactomes of EML1 and EML1Thr243Ala in neuronal cells using BioID approach

2.2.2.1 Cloning of EML1 and EML1Thr243Ala cDNAs into BioID Vectors

EML1 and EML1Thr243Ala proteins were cloned into BirA C-terminal (pcDNA3.1 mycBioID, Addgene #35700) and BirA N-terminal (pcDNA3.1 MCS-BirA(R118G)-HA, Addgene #36047) vectors using the Gibson cloning technique (Gibson et al., 2009). The primer pairs: BirA N-terminal, forward primer: 5’ CTG TGC TGG ATA TCT GCA GAA TTC ATG GAG GAC GGC TTC TCC 3’, reverse primer: TGA TCA GCG GTT TAA ACT TAA ACT TAA GCT TCT AAA TGA CTC GCC ACT GC; and for EML1 BirA C-terminal, forward primer: 5’ TAC GTC TCC GGA TTC GGA TTC GAA TTC ATG GAG GAC GGC TTC TCC AG 3’, reverse primer: CGG TGT TGT CCT TGG ATC CGT GAA TGA CTC GCC ACT GCA TG. PCR recipe was 0.5 µL Q5 High-Fidelity DNA Polymerase, 10 µL 5X Q5 Reaction Buffer, 1 µL 10 mM dNTPs, 2.5 µL 10 µM cloning primer pairs, 1.5 ng DNA, 1

µL DMSO, and 34.5 µL nuclease-free water. PCR reaction conditions: initial denaturation at 98°C for 30 seconds, followed by 35 cycles of denaturation at 98°C for 10 seconds, annealing at 60°C for 30 seconds, extension at 72°C for 30 seconds, and a final extension at 72°C for 2 minutes.

BirA N-terminal and BirA C-terminal were prepared for Gibson assembly by EcoRI and HindIII double digestion. For digestion, 2.5 µg vector was incubated with 1 µL EcoRI-HF and 1 µL HindIII-HF at 37°C overnight. The sizes of PCR amplified DNAs and digested backbones enzymes were confirmed by loading onto a 1% agarose gel. After the confirmations, vectors and PCR products were purified using clean-up kit.

For the Gibson assembly reaction mix, a vector-to-insert ratio of 1:2, along with 25 ng vector, 18 ng insert, and 3.75 µL Gibson mix were incubated at 50°C for 30 minutes and then 1µL of products were used to transform chemically competent E. coli DH5α bacterial cells. Positive colonies first confirmed using colony PCR using 10 µL EmeraldAmp Max HS PCR Master Mix and the same cloning primer mixes and bands were visualized on a 1% agarose gel and positive colonies were selected for DNA sequencing using the Sanger method.

2.2.2.2 Biotinylation capacities of EML1 and EML1Thr243Ala BioID vectors in neuronal cells

The biotinylating capacities of vectors were confirmed using immunofluorescence (IF) and western blot in N2A cells. For IF N2A cells were seeded on the coverslips in 12-well cell culture plates. Then, cells were transfected with four different vectors (BirA N-terminal EML1 wild-type, BirA N-terminal EML1 mutant, BirA C-terminal EML1 wild-type, BirA C-terminal EML1 mutant) and cells were treated with 50 mM D-biotin (Life Technologies,

#B1595) at 24 hours post-transfection. Cells grown in the relevant biotin-containing medium for 24 hours were then collected, fixed with 4% PFA, and stained with Myc (Mouse, Santa Cruz, sc-40), HA-tag (Mouse, abcam, ab16918), and biotin (Rabbit, not commercial, gift of Dr. Timothy J Mitchison, Harvard Medical School)) antibodies. For WB, one group of N2A cells was cultured in normal medium, while another group was cultured in 50 mM biotin-containing medium. Untreated cells (NT) served as controls. After 24 hours of culture in the respective media, cells were collected, lysed, and lysates were combined with 2X Laemmli solution.

2.2.2.3 Analysis of proximity biotinylation maps of EML1 and EML1Thr243Ala in neuronal cells

N2A cells were transiently transfected with PEI and 40 µg BioID constructs and after 24 hours, cells were incubated overnight in the presence of 0.05 mM D-biotin (Life Technologies, #B1595), followed by cell lysis in the lysis buffer (150 mM NaCl, 0.5% SDS, 2% NP40, 1mM EDTA, 10mM IAA, 10 mM Tris pH 7.6 and Protease Inhibitor Cocktail) (Figure 2. 14). The lysates were centrifuged at 14,000g for 10 min at 4°C, and the protein concentrations were measured using a bicinchoninic acid (BCA) assay (Thermo Fisher Scientific). Equal amounts of protein lysates in different conditions were incubated with streptavidin beads overnight at 4°C. The bound proteins were washed with several wash buffers respectively for 10 min, wash buffer 1 (2%SDS), wash buffer 2 (1% Triton X-100, 2% sodium deoxycholate, 1mM EDTA, 50 mM NaCl, 50 mM HEPES pH 7.5), wash buffer 3 (1% Triton X-100, 0.5% NP-40, 0.5% sodium deoxycholate, 1mM EDTA, 50 mM NaCl, 10 mM Tris pH 8.1) and wash buffer 4 (50 mM NaCl, 50 mM Tris pH 7.4).

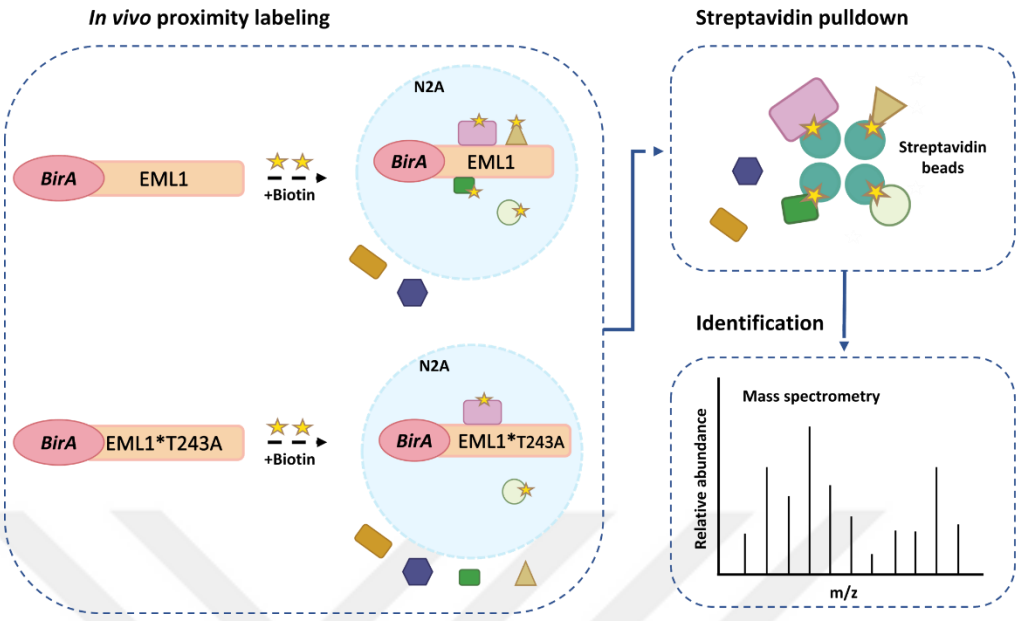

Figure 2. 14 Bio-ID proximity interactome of EML1 and EML1Thr243Ala

To identify biotinylated proteins mass spectrometry on bead digestion was performed. Briefly, proteins on the beads were reduced with 100 mM DTT in 50 mM ammonium bicarbonate buffer at 56°C for 45 min and alkylated with 100 mM iodoacetamide at RT in the dark for 30 min. MS grade trypsin (Pierce) was added to the beads for overnight digestion at 37°C. The resulting peptides were purified using C18 StageTips. Finally, the eluted peptides were analyzed by Thermo Fisher Scientific Q-Exactive LC-MS/MS mass spectrometer. This experiment was performed three independent times.

The raw data were processed using Proteome Discoverer 2.3 (Thermo Fisher Scientific) and searched against the UniProt *mus musculus* database (accessed August 2022) with Sequest HT search engine with tryptic digest specificity, allowing maximum two missed cleavage, precursor mass tolerance 15 ppm, and fragment mass tolerance 0.05 Da (Liu et al., 2020). SAINTexpress analysis was performed using three biological replicates (Teo et al., 2014). Biotinylated proteins of negative control, transfected without DNA, were analyzed to

define non-specific interactions. Saint probability score ≥ 0.6 was used to define the proximal interactors of EML1 and EML1Thr243Ala. The final protein lists were analyzed using the STRING v11.5 database (Szklarczyk et al., 2021) and the g:Profiler annotation server (Raudvere et al., 2019). Selected protein interactions were visualized using Cytoscape 3.9.1 (Shannon et al., 2003).

*2.2.*3 Deep proteomic and phosphoproteomic analysis of *Eml1* cKO heterotopic mouse models cortical tissues

2.2.3.1 Cortical tissue collection

The tissues were collected and sent to Koç University from Fiona Francis laboratory, in Paris, France. Animal research was carried out conforming to national and international directives (directive CE 2010/63 / EU, French national APAFIS n ° 23424) with protocols followed and approved by the local ethical committee (Charles Darwin, Paris, France). For the cortical tissue collection, pregnant females were sacrificed by cervical dislocation, and embryos at E15.5 were collected.

2.2.3.2 Proteomic analysis of cortical tissues of *Eml1* cKO mouse model

For the whole proteome analysis, all biological replicates of E15.5 wildtype and *Eml1* cKO embryonic brain cortices were lysed in 8 M urea, 1 mM sodium orthovanadate, complete EDTA-free protease inhibitor mixture, phosSTOP phosphatase inhibitor mixture and 1% n-octylglucoside in 50 mM pH 8.0 ammonium bicarbonate. Then, reduction of disulfide bonds with 10mM dithiothreitol for 1 h at 56 °C and cysteine alkylation with 20 mM iodoacetamide (IAA) for 45 min in the dark at room temperature. Proteins were digested trypsin (at a ratio of 1:40 trypsin:protein) at 37 °C overnight, resulting in peptide being desalted on SepPak C18. Samples purified from salts using C18 Sep-Pak columns were divided into 200 µg for total

proteomic analysis and 700 µg for phosphoproteomic analysis to enable both types of analyses from the same tissues (Figure 2. 15).

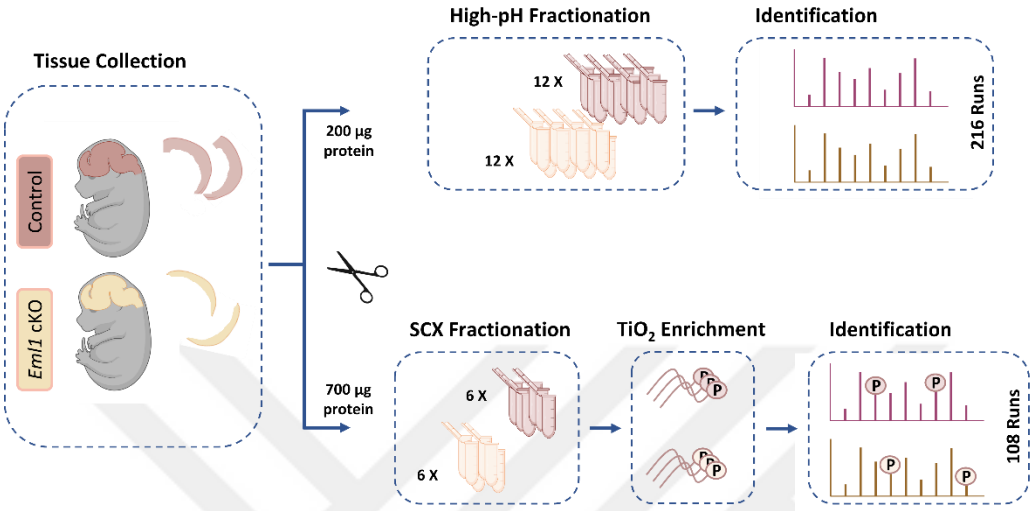

Figure 2. 15 Experimental workflow for the deep proteome and phosphoproteome analysis of E15.5 Eml1 cKO cortices (Created with BioRender.com)

Followingly, 200 µg samples were fractionated into 12 fractions using the high-pH fractionation technique. For this purpose, peptides were first reconstituted in a 50µL loading buffer (15mM ammonium hydroxide, 2% acetonitrile (ACN), pH:10) and loaded onto C18 Seppak. Bound peptides fractionated using ammonium hydroxide buffer with increasing percentage of acetonitrile from 6% to 90%. Then fractionated samples analyzed with three technical replicates in Thermo Scientific Q-Exactive LC-MS/MS mass spectrometer with a 90-minute gradient flow. Proteomic analysis of Eml1 cKO consists of three biological replicates of wildtype and *Eml1* cKO mouse cortices. The protein and peptide identification with label-free quantification (LFQ) was performed in the MaxQuant software (Cox & Mann, 2008). The search was subjected against the UniProt *mus musculus* database (accessed August 2022) with fixed modification carbamidomethyl (C) and variable modifications included acetylation (protein N-Term) and oxidation (M). Trypsin/P was selected as the proteolytic enzyme with 2 maximum missed cleavages. The match between runs function was enabled

for the search. Identified protein list filtered with at least two values from three replicates of WT or cKO to further quantification. Normalization is performed within the experimental groups and student t-test is performed in Perseus software (Tyanova et al., 2016). Dysregulated proteins were analyzed in g:Profiler and visualized using GraphPad Prism software and phyton scripts (Raudvere et al., 2019).

2.2.3.3 Phosphoproteomic profile of cortical tissues of *Eml1* cKO mouse model

700 µg from three replicates of WT and cKO used for phosphoproteomic analysis. The 700 µg samples were first fractionated using strong cation exchange (SCX). For this purpose, dried samples were reconstituted in a loading buffer (7mM KH2PO4, 30% ACN, pH 2.6) and loaded into the SCX resin-packed cartridges. The bound peptides were then eluted stepwise addition of elution buffers with increasing KCl from 30mM to 50mM concentrations resulting in 6 fractions from a sample. After this step, samples were again desalted using C18 SepPak columns to prepare the samples for phosphoenrichment. The phospho enrichment step was performed on C8 disks using 500µg of titanium dioxide beads, (5µm, Sachtleben), using GELoader tips (20µL GELoader, Eppendorf). The dried peptides from SCX were first reconstituted in a loading buffer and then loaded onto the positively charged columns at very low g force (50-100g). Then, bound phosphopeptides were washed with 0.1% trifluoroacetic acid (TFA) in 50% ACN and then eluted with 10% ammonia solution into a new tube containing 10% formic acid (FA). The eluted peptides were further and analyzed in a Thermo Scientific Q-Exactive LC-MS/MS mass spectrometer with a 120-minute gradient flow.

The protein and peptide identification with label-free quantification (LFQ) was performed in the MaxQuant software (Cox & Mann, 2008). free quantification (LFQ) was performed in the MaxQuant software (Cox & Mann, 2008). The search was subjected against the UniProt *mus musculus* database (accessed August 2022) with fixed modification carbamidomethyl (C) and variable modifications included phosphorylation (S, T, Y,)

acetylation (protein N-Term) and oxidation (M). The match between runs function was enabled for the search. Identified phosphorylation sites are filtered with at least two values from three replicates of WT or cKO to further quantification. Phosphopeptide normalization is with their counterparts of proteome values and student t-test is performed in Perseus software (Tyanova et al., 2016). Dysregulated phosphorylation sites.

2.2.4 Proteomic analysis of neuronal progenitor primary cell culture with quantitative proteomic approach

2.2.4.1 Collection of mouse neuronal progenitor primary cells

The samples were collected and sent to Koç University from Francis laboratory, Paris, France. For the collection of these cell populations, basically, first the culture plates were coated with Poly-D-lysine (PDL, P6407, Sigma Aldrich) overnight at cell culture incubator. The following day, PDL was removed, and the plates were coated with fibronectin (Poly-D-lysine (PDL, P6407, Sigma Aldrich). E14.5 prenant mice were sacrified and the uterus was placed in ice-cold basal medium, the cortex from both hemispheres was dissected and kept at 4 °C in basal medium. The medium was removed and substituted by pre-warmed sterile complete medium (basal medium complemented with 1 x B27 without vitamin A (12589-010, Gibco), 20 ng/ml of EGF (E9644, Sigma Aldrich) and 20 ng/ml of FGF (F0291, Sigma Aldrich). The tissue was dissociated, and each sample was centrifuged (3 min, 1000 rcf) and substituted by fresh pre-warmed complete medium followed by re-suspension of the cells with pre-warmed complete medium this provide highly enriched population of Pax6+ cells (Sun et al., 2011).

2.2.4.2 Proteomic profiling of *Eml1* cKO mouse neuronal progenitor primary cell culture

Proteins from the mouse neuronal progenitor primary cells were isolated in 8M urea, 50 mM ammonium bicarbonate lysis solution, followed by reduction, alkylation, and trypsin digestion steps, and then purified from salts on C18 StageTips (Figure 2.16). The primary amines of the peptides were labeled with stable dimethyl isotopes (Boersema et al., 2009) (Figure15). For this purpose, control cells were labeled as 'light' (+28 Da) and *Eml1* gene silenced cells were labeled as 'heavy' ('+36 Da'). In the light label: 0.6 M cyanoborohydride solution (NaBH3CN) and 4% formaldehyde solution (CH2O) were mixed and in the heavy label: 0.6 M cyanoborodeuteride solution (NaBD3CN) and 13CD2- formaldehyde solution (13CD2O) were mixed in 50mM sodium phosphate buffer (pH 7.5). After labeling, the samples were mixed in equal amounts based on one-to-one light:heavy intensities and fractionated into 12 fractions using the high-pH fractionation method. Primary cell samples were analyzed with two biological replicates. Each biological sample was further analyzed with three technical replicates. The fractionated samples were analyzed using a Thermo Scientific Q-Exactive LC-MS/MS mass spectrometer with a 90-minute gradient flow.

Protein contents in raw data were analyzed using MaxQuant software with selection of dimethNter0, dimethLys0, dimethNter8, and dimethLys8 as variable modifications quantitative data analysis modifications together with oxidation (M) and acetyl (protein-N-term) with fixed modification carbamidomethyl (C). Trypsin/P was selected as the proteolytic enzyme with 2 maximum missed cleavages. The match between runs function was enabled for the search. Identified protein list filtered with two values from replicates of WT or cKO to further quantification. Normalization is performed within the experimental groups and student t-test is performed in Perseus software (Tyanova et al., 2016). Dysregulated proteins were analyzed in g:Profiler and visualized using GraphPad Prism software and Cytoscape 3.9.1 and phyton scripts (Raudvere et al., 2019; Shannon et al., 2003).

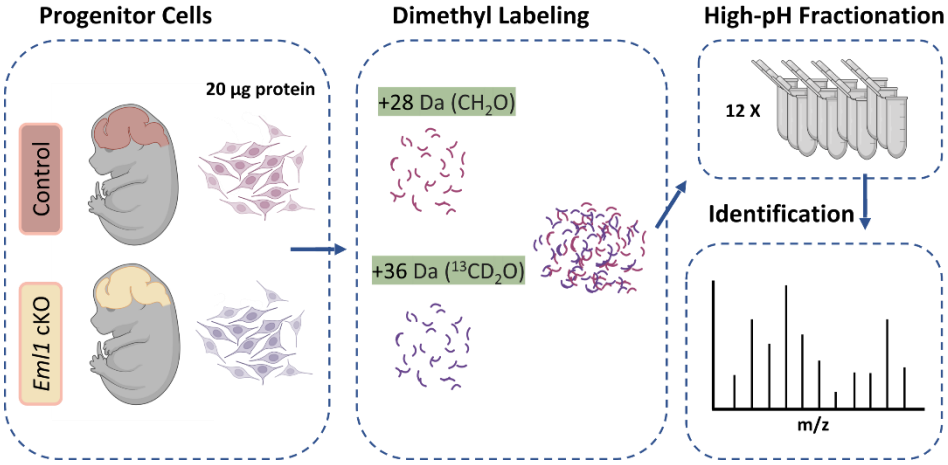

Figure 2. 16 *Eml1 cKO* neuronal progenitor primary cells proteomic profiling using dimethyl labeling (Created with BioRender.com)

2.2.5 MAPs proteome of *Eml1* cKO mouse neuronal progenitor primary cell culture

Microtubule-associated protein and microtubule proteome experiments were also performed with the Francis laboratory collected mouse neuronal progenitor primary cells. These provided cells were dissolved in a buffer containing protease and phosphatase inhibitors for microtubule pelleting (100 mM K-Pipes pH 6.8, 2mM EGTA, 1mM MgCl2, 0.5% NP-40, 1mM DTT) and then were centrifuged at 100,000xg for 30 minutes at 4°C to pellet the microtubules, followed by incubation at room temperature for 20 minutes with 25uM Taxol and 0.5mM GTP to stabilize the microtubules. The microtubules stabilized with Taxol were pelleted at 100,000rpm for 30 minutes at 25°C with a cushion of 40% glycerol in BRB80 buffer containing 1 mM DTT, 25 uM Taxol, 1 mM GTP, and protease inhibitor. The pellet was resuspended in CM buffer (100mM K-Pipes pH 7, 2mM EGTA, 1mM MgCl2) containing 20 uM cytochalasin D and 20 uM latrunculin B, followed by centrifugation at 100,000 rpm for 30 minutes at 25°C with a second 40% glycerol cushion. The final pellet containing

microtubules and microtubule-associated proteins was resuspended in a buffer solution and loaded onto an SDS-PAGE gel (Figure 2. 17). The SDS-PAGE gel was divided into 6 sections with on-gel fractionation. Proteins within these small gel sections were cut with trypsin into peptides and individually analyzed by LC-MS/MS after purification from salts. The protein database searches, and identification are performed by using the Proteome Discoverer2 software with the Sequest search engine with at least 2 unique peptides for each protein.

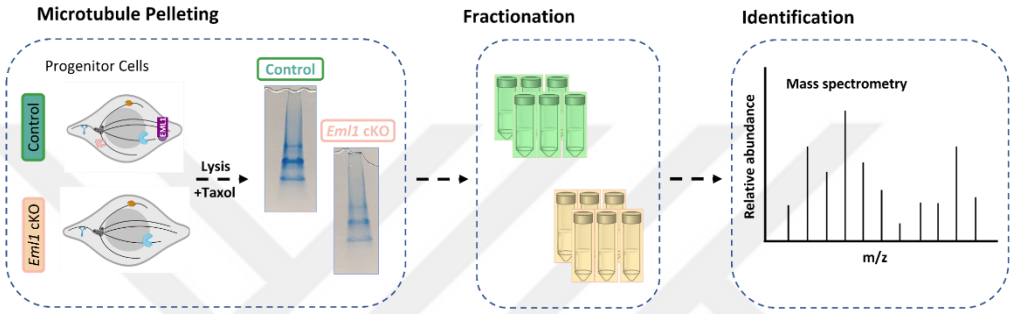

Figure 2. 17 MAPs proteome of *Eml1* cKO mouse neuronal progenitor primary cell culture (Created with BioRender.com)

2.3 RESULTS

2.3.1 EML1Thr243Ala Mutation Reduces Microtubule-Binding Affinity

Echinoderm microtubule-associated protein-like 1 (EML1), from the EMAP protein family, is associated with cortical malformations with its mutations associated with severe phenotypes in humans and mice. Among the identified EML1 mutations associated with heterotopia formation, the Thr243Ala missense mutation is linked to the formation of severe heterotopia. Thr243 position is located within the HELP motif and acts as a critical site within a bridge linking β-propeller structures in the EML1 protein and evolutionary conservation across EML1, EML4, and EML2.

First, EML1 and EML1Thr243Ala cDNAs is cloned into pLenti-GFP backbone to understand the characteristics of normal and mutant EML1 proteins since commercial antibodies for EML1 are not working well. For this purpose, I performed cloning of normal and mutant EML1 cDNAs (2445bp) into the pLenti-CMV-puro vector using the Gibson technique (Figure 2.18). Amplification of the vectors was successfully achieved using long Gibson primers, followed by ligation of the amplified DNAs into the digested pLenti-GFP vector by the Gibson master mix. Subsequently, a two-step confirmation process was performed to validate the colonies before sequencing analysis.

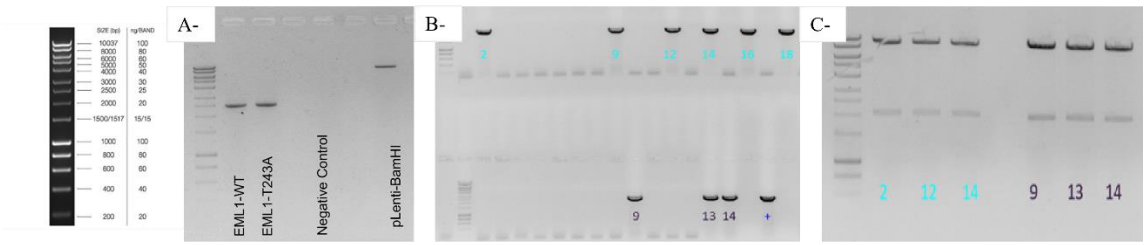

Figure 2. 18 Cloning of EML1 and EML1Thr243Ala cDNAs into the pLenti-GFP backbone

A- PCR amplification of normal and mutant cDNAs and digestion of the vector; B- Colony PCR (blue labels represent normal, purple labels represent mutant vectors); C) Secondary confirmation of selected colonies through enzyme digestion (blue labels represent normal, purple labels represent mutant vectors).

After the successful cloning of the vectors, six stable cell lines were generated in N2A and HeLa Kyoto cell lines. For this, viruses were initially packaged in HEK293t cells, and harvested viruses were then given to the target cell lines. Given that the generated virus vectors have the target protein fused to the GFP, fluorescence signals were monitored following transduction, and a western blot experiment was performed to understand the expression levels in both cell lines (Figure 2. 19).

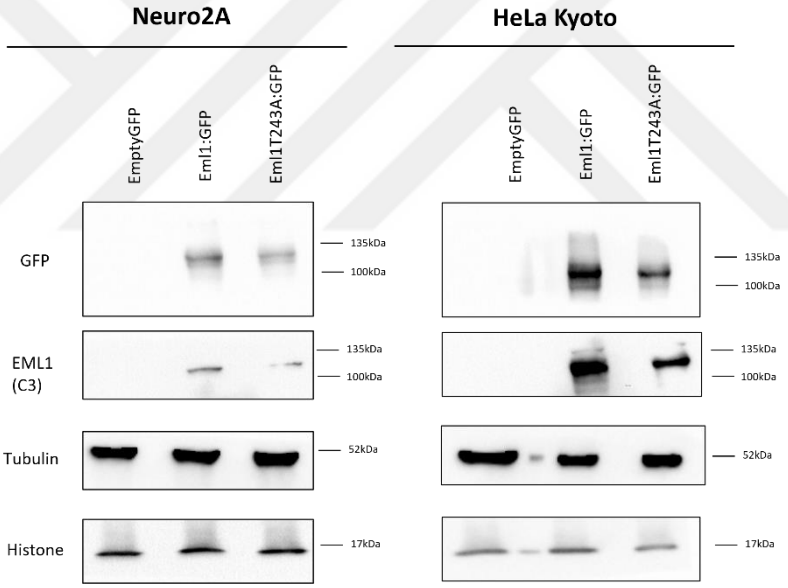

Figure 2. 19 EML1 and EML1Thr243Ala expressions in N2A and HeLa stable cell lines

For the immunostaining experiment, many optimizations were performed to visualize best for the EML1 protein. The optimal conditions found a combination of methanol (-20°C)

treatment for 5 minutes followed by fixation with 5% paraformaldehyde at room temperature for an additional 5 minutes for this microtubule-binding protein and images taken from a Leica DMi8/SP8 TCS-DLS confocal microscope at a magnification of 63x (Figure 2. 20 and Figure 2. 21). According to these results, the normal EML1 enriches at different locations during cell division. It is on the microtubules during interphase, enriches on spindle microtubules during metaphase, and localizes at the midzone during cytokinesis. However, for the mutant protein, these enrichments along microtubules notably decreased across all phases of the cell cycle.

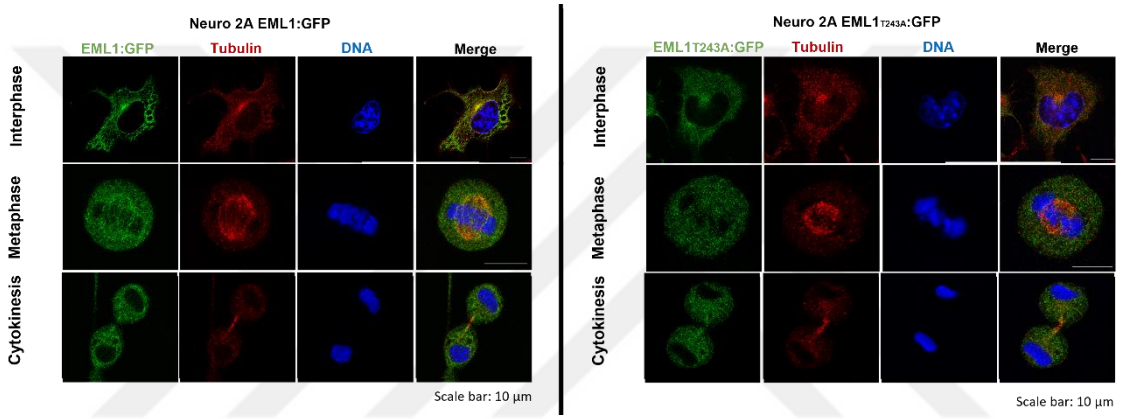

Figure 2. 20 Cell cycle-dependent localizations of EML1 and EML1Thr243Ala proteins in N2A cells

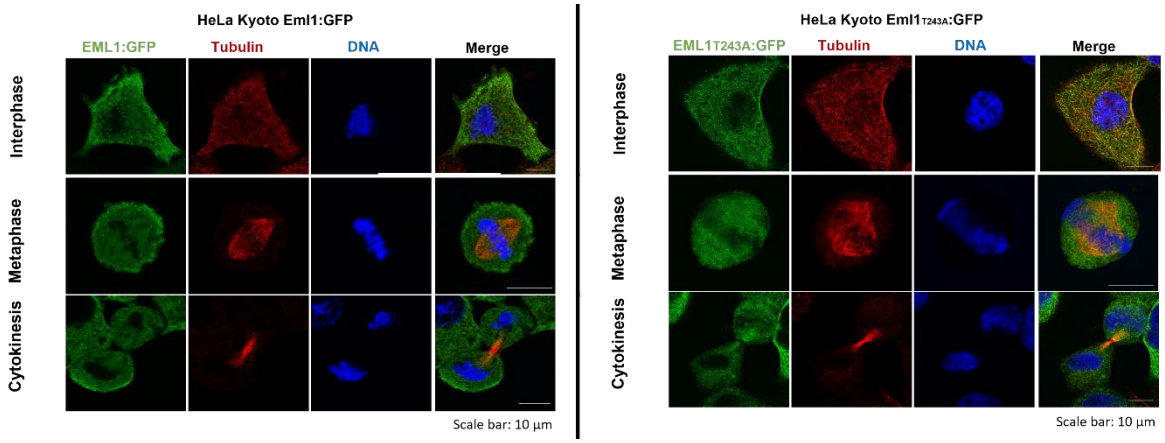

Figure 2. 21 Cell cycle-dependent localizations of EML1 and EML1Thr243Ala proteins in HeLa cells

EML1 is associated with heterotopia formation, thus experiments were initially aimed only at the N2A cell line. However, the addition of HeLa Kyoto cell lines in this overexpression localization experiment revealed differences in the localization of the normal protein in these two cells too. N2A (Neuro-2a) cells are generated from mouse neuroblastoma, HeLa cells originate from human cervical cancer, which resulting differences in cellular characteristics. These variances include distinct tissue origins and cellular functionalities, such as neuronal cells' reliance on highly dynamic microtubules for providing a structural backbone for axons and dendrites. Such variances can significantly influence the expression and localization patterns of EML1 protein, as evidenced by the observation of more cytosolic localization in HeLa Kyoto cells compared to N2A cell lines.

2.3.2 EML1Thr243Ala mutation causes fewer interactions and leads to severe disruptions of EML1-asociated cellular functions

To identify potential disruptions with the mutant protein I mapped the interactomes of normal and mutant proteins in the N2A cell line using the BioID approach. BioID method uses an abortive *E.coli* biotin ligase (BirA) fused to target protein to biotinylate its close proximity interactors. For this first, BirA was fused to the N-terminus and C-terminus of both EML1 and EML1*T243A proteins using the Gibson cloning and from the colony PCR results, the 5th colony for BirA N terminal EML1 wild-type, the 22nd colony for BirA N terminal EML1 mutant, the 57th colony for BirA C terminal EML1 wild-type, and the 76th colony for BirA C terminal EML1 mutant were selected and sent for Sanger sequencing (Figure 2. 22).

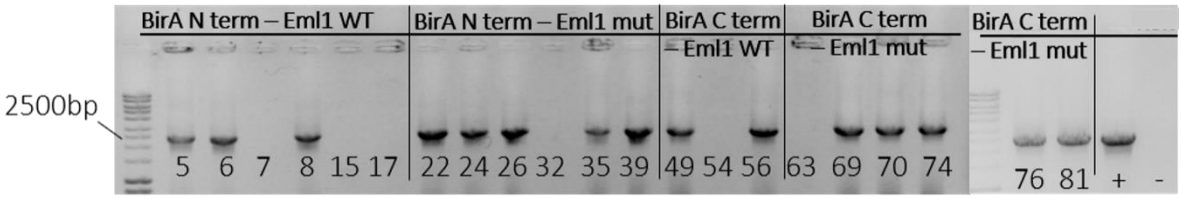

Figure 2. 22 Colony PCR of BioID vectors

In Sanger sequencing, forward and reverse primers were used to read the entire sequence of normal and mutant protein sequences. The accuracy of the cloned EML1 wild-type and EML1 mutant DNA sequences, as well as the mutation point, was confirmed by this sequencing (Figure 2. 23).

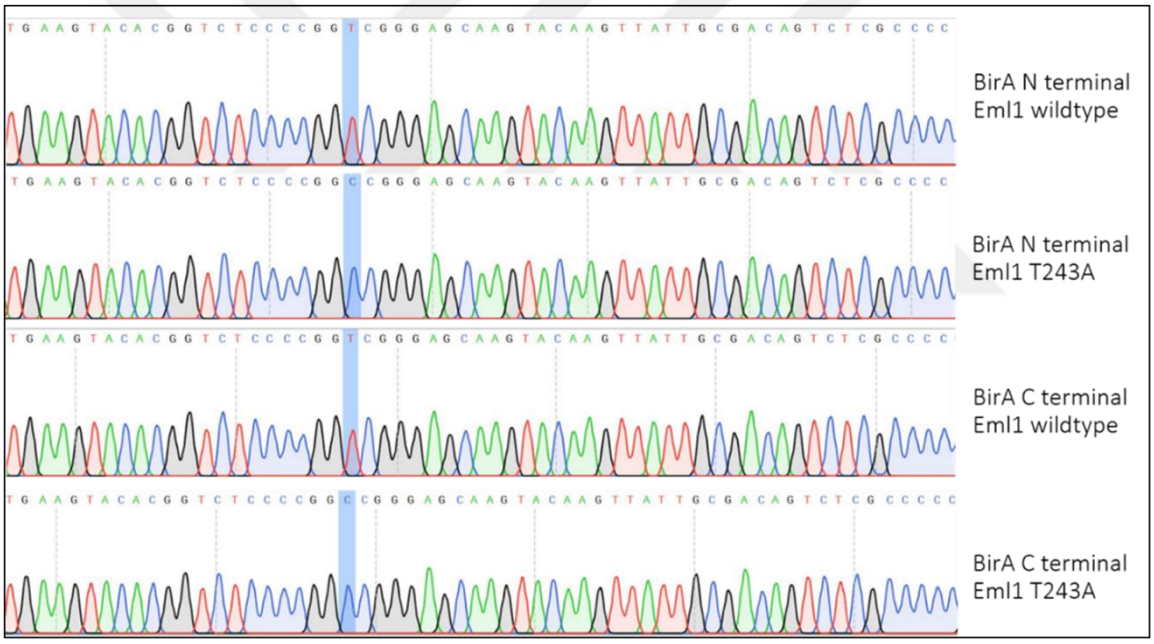

Figure 2. 23 The sanger sequence readings of the selected colonies *(the blue-highlighted position is the mutation site in the sequence)*

After the cloning of the vectors, the biotinylation capacities of the cloned vectors were analyzed with western blot experiments (Figure 2. 24). For this purpose, one group of cultured N2A cells was grown in a medium, while another group was grown in a medium supplemented with 50mM biotin. Untreated cells (NT) served as controls. Untreated cells (NT) served as controls. As a result, while only endogenously biotinylated proteins observed in cells without biotin supplementation, both EML1 wild-type and mutant vectors successfully biotinylated their surroundings only in the presence of biotin added to the medium, and their biotinylation pattern is different from the backbone vector.

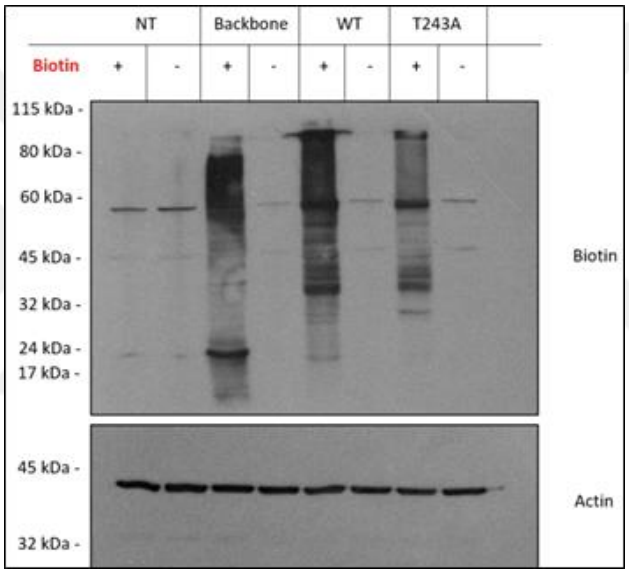

Figure 2. 24 Biotinylation patterns of BioID vectors

To identify the proximity interactome of both the normal and mutant proteins, vectors were transiently transfected into N2A cells. Following a 24-hour post-transfection period, biotinylated proteins were isolated using streptavidin agarose beads. Following the extensive washing steps, proteins on beads were tryptic digested, and peptides were analyzed by LC-MS/MS. Proteins captured in non-transfected N2A cell growth in biotin supplement media were used as a control. The significant interactors of EML1 and EML1Thr243Ala were

determined using the SAINT (Significance Analysis of INTeractome) label-free quantification tool. SAINT analysis calculates a SAINT probability (SP) score and folds changes over control lists for each prey protein. SP ≥0.6 score was used for filtering the significant interactions, resulting 49 and 30 proximal interactor proteins for N-terminal interactors of EML1 and EML1Thr243Ala respectively (Figure 2. 25).

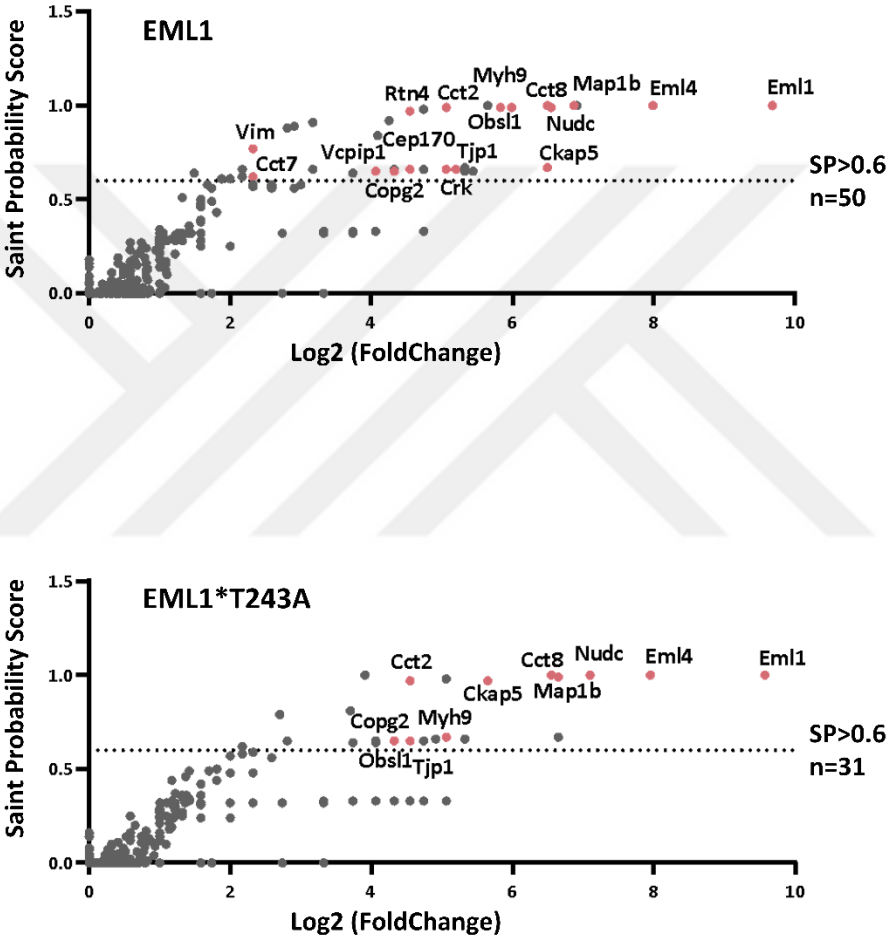

Figure 2. 25 Scoring of hits from N-terminal EML1 and EML1Thr243Ala BioID analysis, *each hit is represented on the scatter plots display its Saint Probability (SP) score versus its fold change in the spectral count over the control (microtubule related proteins are labeled in the graph).*

Both pulldown efficiency of the EML1 and EML1Thr243Ala proteins were detected in a same amount based on their SAINT scoring (SP=1 in both conditions) and EML1Thr243Ala interactome comprised significantly fewer proteins than the wild-type one (Figure 2. 26). Besides the unique interactions (26 for EML1 and 4 for EML1Thr243Ala) majority of 26 common interactions SP scores higher for EML1 in comparison to EML1Thr243Ala (Figure 2. 27).

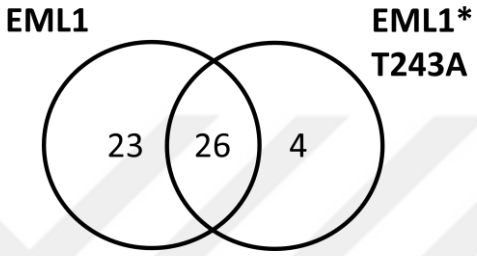

Figure 2. 26 Venn diagram showing overlapping of N-terminal EML1 and EML1Thr243Ala interactors with an SP ≥ 0.6.

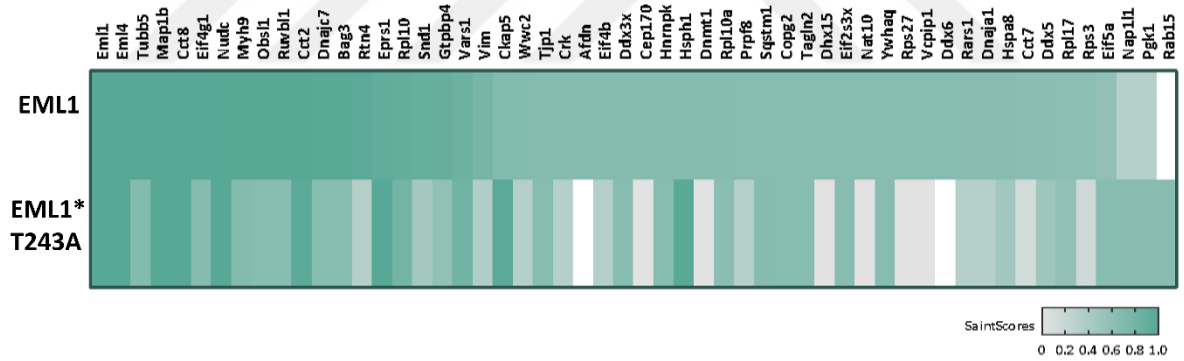

Figure 2. 27 Heat map showing the SP scores of N-terminal EML1 and EML1Thr243Ala proximal interactors

To further understand EML1 interactome and the perturbations caused by the heterotopia-associated mutation, I performed gene ontology (GO) analysis of the proximity interactome of both EML1 and EML1Thr243Ala (Figure 2. 28). Analysis based on biological processes revealed the enrichment of terms such as organelle organization, translation, peptide biosynthetic process, peptide metabolic process, spindle and cytoskeleton organization, and

cell cycles are highly enriched for the normal protein and get significantly affected for the mutant protein. Upon cross-referencing the BioID hits of EML1 with previous studies, it was revealed that 13 BioID hits (Dnmt1, Cep170, Dhx15, Ddx3x, Nat10, Ddx6, Eml4, Ruvb1, Eif2s3x, Rpl10a, Tjp1, Dnajc7, and Rpl10) had been previously reported (Bizzotto et al., 2017). Further investigation into the BioID hits of EML1 focused on cellular components associated with the microtubule (MT) cytoskeleton, spindle, and organelles (Figure 2. 29).

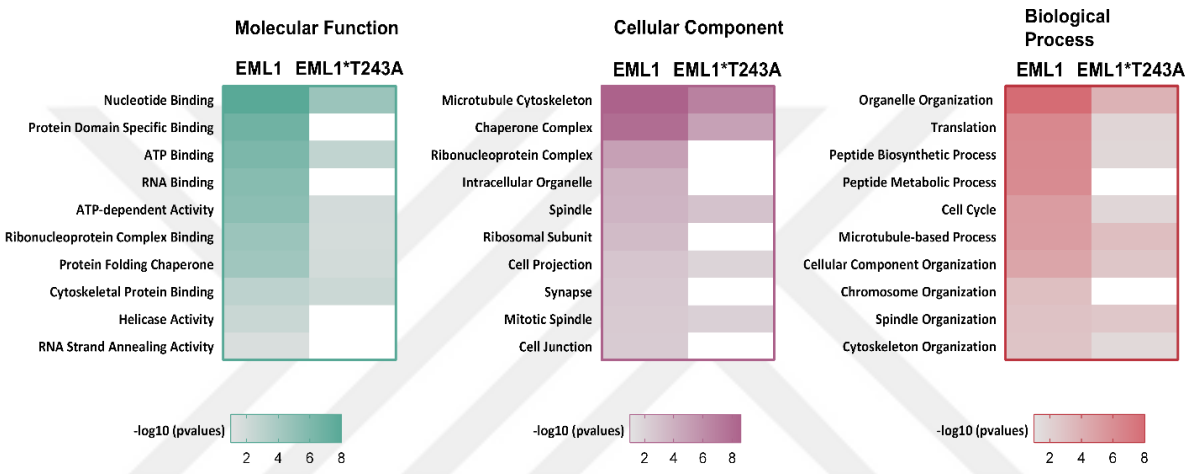

Figure 2. 28 Gene ontology (GO) annotation grouped into molecular function, cellular component, and biological process of EML1 and EML1Thr243Ala proximal interactors

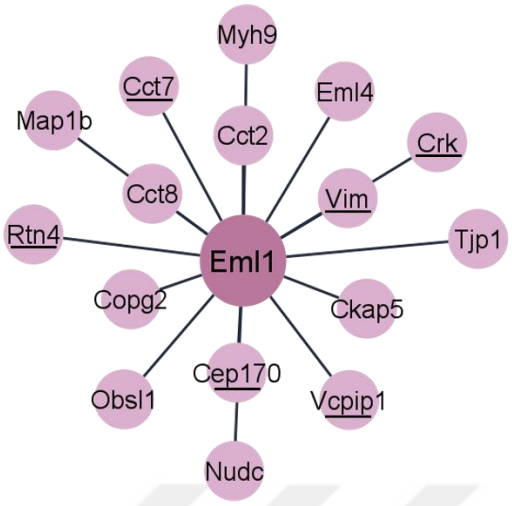

Figure 2. 29 Proximal interactors of N-terminal EML1 related to microtubule cytoskeleton, spindle, and organelle cellular components *(Underlined proteins lose interaction significance in EML1Thr243Ala SP<0.6)*

Then the same analysis for the C-terminal interaction partners of EML1 and EML1Thr243Ala proteins in N2A was performed. The significant interactors of C-terminal EML1 and EML1*T243A were determined using the again SAINT label-free quantification tool and SP ≥0.6 score was used for filtering the significant interactions (Figure 2. 30). Although the EML1 protein is a middle-sized protein (72kDa) there is a clear differentiation in the interaction partners between the C-terminal and N-terminal sites. Notably, the presence of the HELP motif and trimerization domain at the N-terminal region may contribute to this differentiation in the interactomes. Interestingly, approximately half of the interactors (29 interactors) were found to be common to both domains, while 20 interactors were specifically enriched in the N-terminal pulldown and 28 interactors for the C-terminal site (Figure 2. 31 and Figure 2. 32).

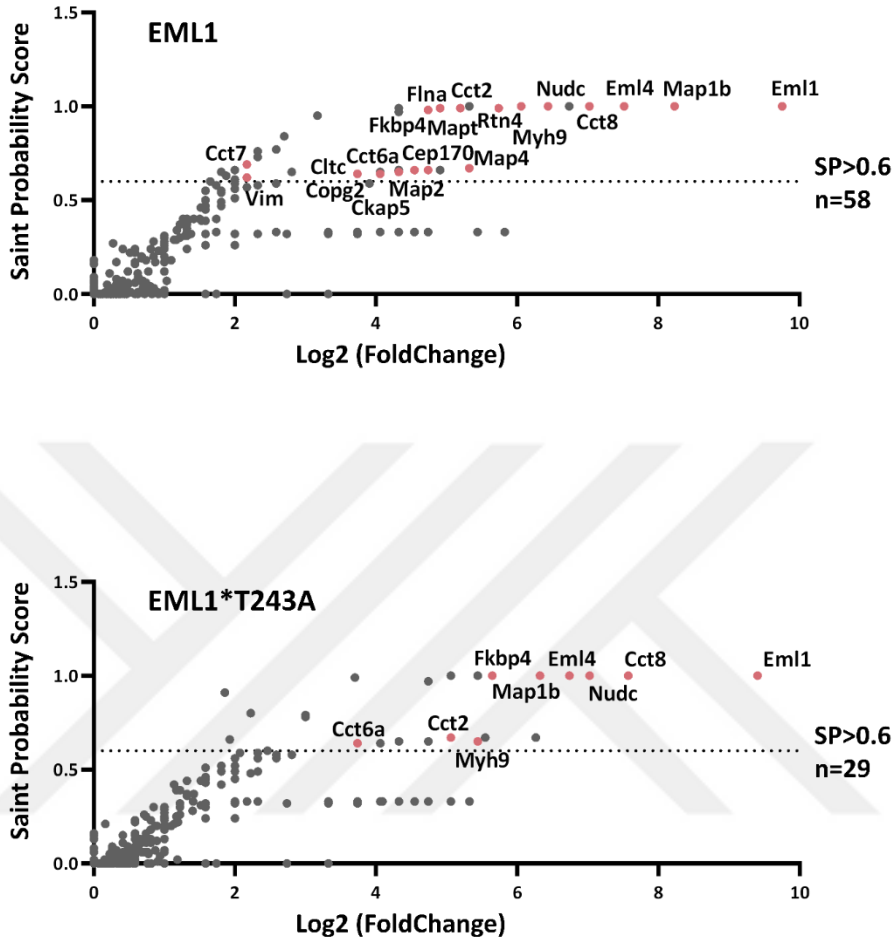

Figure 2. 30 Scoring of hits from C-terminal EML1 and EML1Thr243Ala BioID ,each hit is represented on the scatter plots display its Saint Probability (SP) score versus its fold change in the spectral count over the control (microtubule related proteins are labeled in the graph).

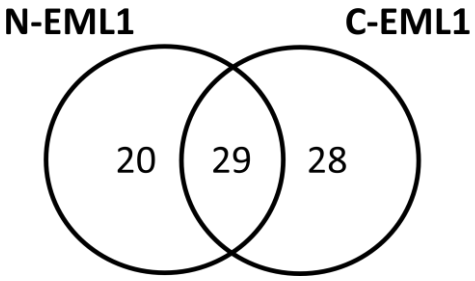

Figure 2. 31 Venn diagram showing overlapping of N-terminal EML1 and C-terminal EML1 interactors *with an SP ≥ 0.6.*

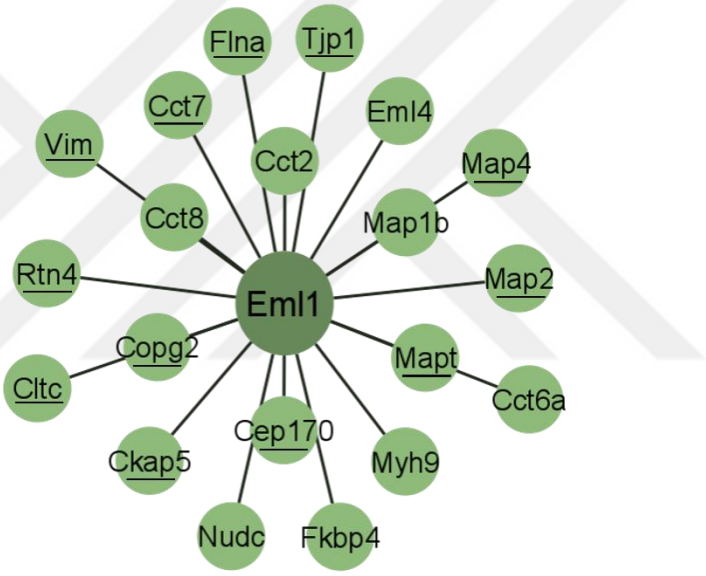

Figure 2. 32 Proximal interactors of C-terminal EML1 related to microtubule cytoskeleton, spindle, and organelle cellular components (Underlined proteins lose interaction significance in EML1Thr243Ala SP<0.6)

Notably, one of the specific interacting partners of EML1 (common in N and C terminals) was Cep170 protein, this protein plays a crucial role in centrosome maturation, and it is specifically identified in the EML1 WT interactome. In the heterotopic mutant interactomes, this interaction is lost, which is further validated in *Eml1* cKO progenitor cells (Donia, 2024). In this validation performed by Francis Lab, they checked the intensity of Cep170 at the centrosomes situated at the ventricular surface in embryonic brains at E12.5 and

E15.5, comparing between wild-type and conditional knockout (cKO) Eml1 embryos and they found a very significant decrease in Cep170 intensity in in Eml1 cKO embryos at both stages, even after normalization to γ-tubulin levels.

This finding also raised a question regarding the stability of the centrosome integrities in the N2A cell lines in normal conditions and as well as the BioID transfected conditions. To further investigate this the immunofluorescent experiment shows the centrosomes using gamma-tubulin staining (Figure 2. 33 and Figure 2. 34). According to the results, the finding of the Cep170 protein was not dependent on the cell line defects but rather a true catch from the BioID pulldown, since the centrosome integrities are normal in every condition, and no obvious change about this organelle.

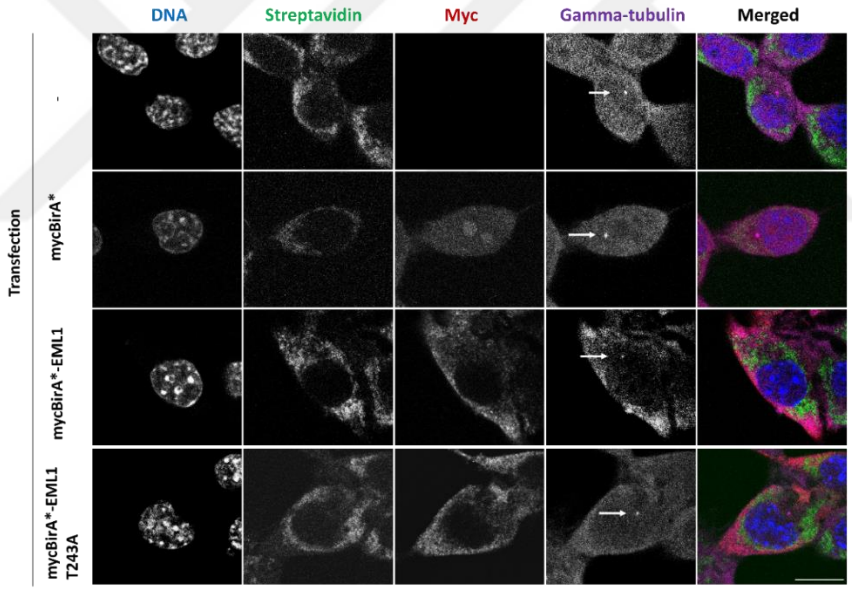

Figure 2. 33 Immunoflurescence staining of interphase N2A cells transfected with BioID vectors, DNA (blue), streptavidin (green), myc (red) and gamma tubulin (purple) Scale bar:10 um.

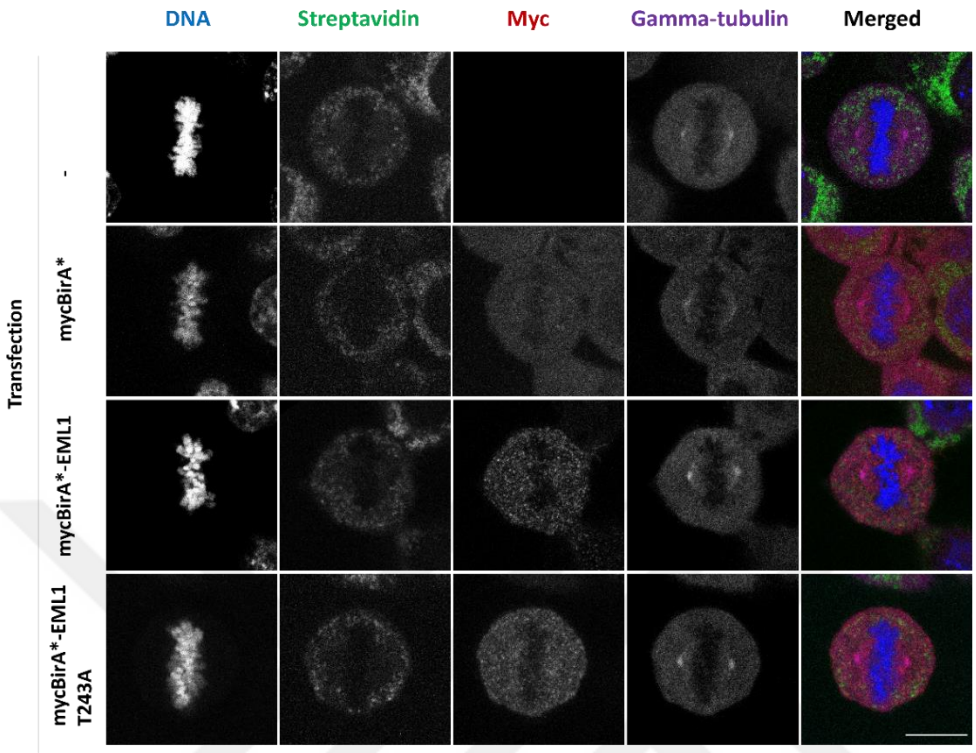

Figure 2. 34 Immunoflurescence staining of mitotic N2A cells transfected with BioID vectors, DNA (blue), streptavidin (green), myc (red) and gamma tubulin (purple) Scale bar:10 um

With using the BioID approach, I successfully identified interaction partners of both wild-type Eml1 and the heterotopia-associated mutant Eml1Thr243Ala protein in a neuronal cell line. Analysis of these interaction partners revealed that the mutant form of EML1 loses many interactions, and also results in disrupting several cellular processes. Furthermore, the validation of decreased Cep170 expression in the cortices of Eml1 cKO provides additional insights into the disruptions associated with heterotopia with centrosome dynamics. Together this finding shows the critical role of Eml1 in maintaining cellular functions including the centrosome integrity and showing hits of another underlying heterotopia pathogenesis.

2.3.3 Proteomic and phosphoproteomic profiling of *Eml1* cKO cortices revealed changes in the abundance of multiple synaptic proteins and limited phosphorylation dysregulations

I initially aimed to examine the proteomic and phosphoproteomic characteristics of the cortices in a forebrain-specific Eml1 cKO mouse model. EML1 perturbations cause cortical malformations in the early brain development. To systematically characterize the affected cellular pathways, I examined the proteomic characteristics of E15.5 cortices of *the Eml1* cKO mouse model. These mice generated by crossing homozygote *Eml1*-Flox mice with mice heterozygous for *Emx1*-Cre, resulting in forebrain-specific *Eml1* cKO animals, and 100% of these *Eml1* cKO mice exhibit subcortical heterotopia (SH) (Zaidi et al. 2024). I focused our analysis on E15.5 embryonic cortices, a critical time point where the effects of *Eml1* depletion on cortical morphology, radial glia detachment, and primary cilia perturbation are observed (Zaidi et al. 2024). To understand the mechanisms underlying the SH formation in this mouse model, I performed label-free quantitative proteomic analysis of *the Eml1* cKO mouse model at E15.5 across three independent biological replicates.

During the initial proteome profiling of the 200 µg cortices using high-pH fractionation to increase protein identification, I successfully identified a total of 8213 proteins, of which 6894 unique proteins were quantified after filtering. The logarithmic (log2) distributions of the quantified proteins showed consistent patterns across the three replicates of cKO and WT samples (Figure 2.35).

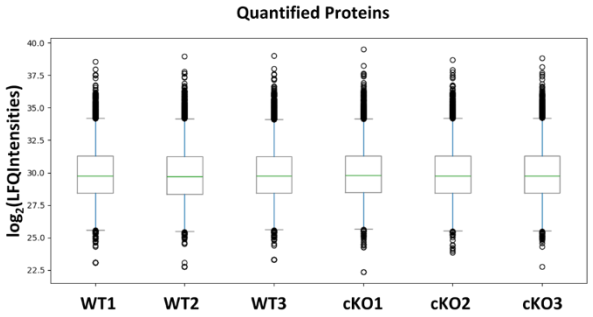

Figure 2. 35 Boxplot indicating the log2 LFQ Intensities of the three replicates of WT and cKO cortices Values outside this range are plotted as dots and represent outliers. Median values are indicated in the boxplot through the horizontal lines in the center of the distributions.

Additionally, I observed high quantitative accuracy between the three biological samples, with Pearson correlations exceeding 0.95 (Figure 2.36). The most abundant proteins detected were associated with LFQ intensities of the cortices enriched for key physiological processes relevant to diverse biological functions specifically, the top 100 enriched proteins were involved in ‘translation’, ‘regulation of mRNA metabolic processes’, ‘regulation of cellular component organization’, ‘glucose catabolic processes’, and ‘pyridine nucleotide metabolic processes’.

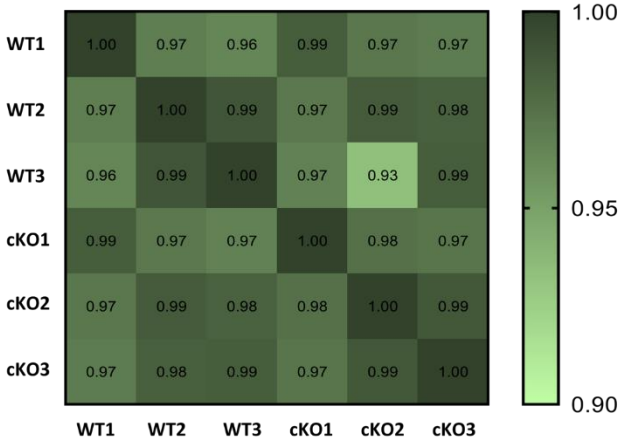

Figure 2. 36 Pearson correlation of the WT and cKO cortex proteomes

Based on the statistical analysis, only 170 proteins (2.4% of the quantified proteome) were found as statistically differentially expressed between *Eml1* cKO and control cortices ($p < 0.05$), 118 significantly upregulated proteins (log2 fold change > 0.2) and 52 significantly downregulated proteins (log2 fold change < -0.2) (Figure 2.37).

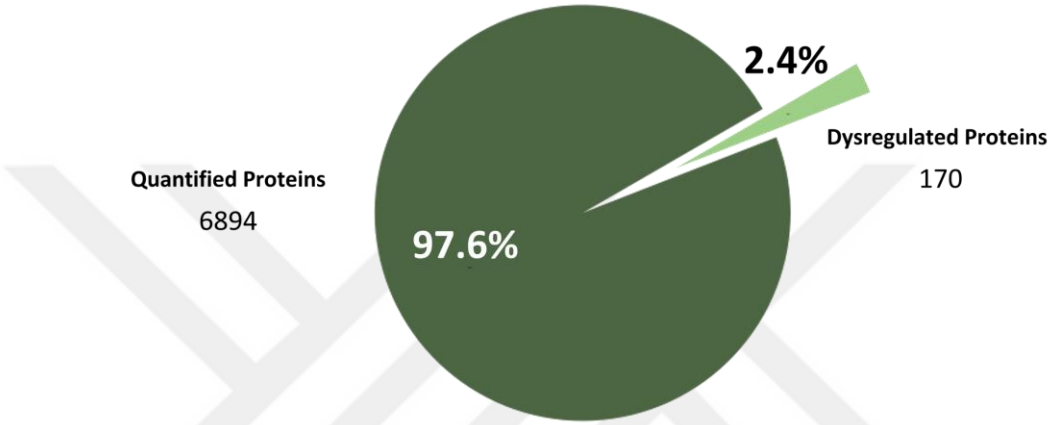

Figure 2. 37 %2.4 of the 6894 quantified proteins were significantly altered in the cortex of *Eml1* cKO mice

Among the identified proteins, CACNA2D3 exhibited the most prominent upregulation, with a log2(fold change) of 5.27, followed by R3HDM4 (3.54) and EPB41L4A (3.20). CACNA2D3 functions as a voltage-gated calcium channel subunit, R3HDM4 belongs to the RNA-binding protein family, and EPB41L4A is involved in cytoskeletal organization, cell polarity, and cell signaling. Conversely, PLEKHA8, a member of the pleckstrin homology domain-containing family, plays roles in cell-cell adhesion and signaling processes, demonstrating the most significant downregulation, with a fold change of -4.01. Importantly, these upregulated and downregulated proteins belong to various cellular functions. Furthermore, except these protein deregulations, there are minimal fold change differences between *Eml1* heterotopic cKOs and controls, indicating subtle yet meaningful alterations in molecular expression profiles associated with *Eml1* depletion at the cortex level.

Using the statistically differentially expressed 170 proteins, we first assessed the cellular component enrichment of these differentially expressed proteins using the Gene Ontology (GO) database (Figure 2.38). The upregulated proteins in *Eml1* cKO heterotopic cortices were mainly associated with synaptic proteins (e.g. NRXN8, PTPRD, ARHGAP44, ABR, RPH3A, EFNB3) (Figure 2.39).

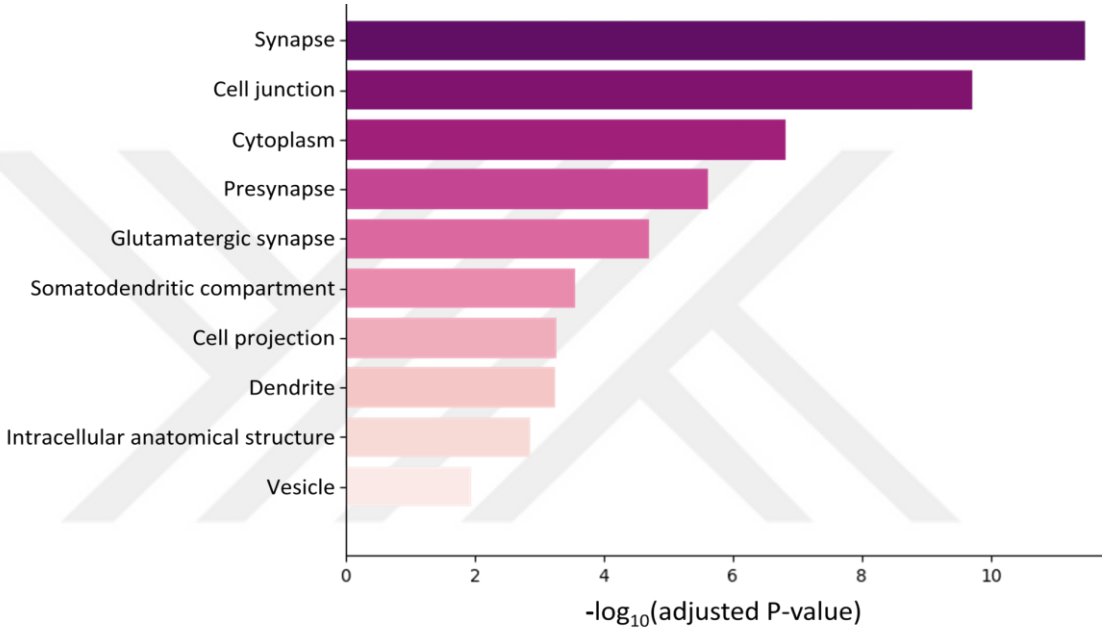

Figure 2. 38 Gene ontology (GO) cellular component annotation of 170 deregulated proteins in the cortex Eml1 cKO mice

Although the role of EMAP proteins during development and in post-mitotic neurons is not well characterized, there are some results suggesting that EMAP proteins can be involved in synaptic plasticity which is the ability to respond of the nervous system to intrinsic or extrinsic inputs, which is the obvious requirement of development of neural circuits. Interestingly, EML4 expression is downregulated following nicotine stimulation and Eml2 can bind to the delta-2 glutamate receptor (Dunckley & Lukas, 2003; Noctor et al., 2001). Although there is no data reporting EML1 association with neuronal plasticity, I observed high

synaptic protein dysregulations in the cortices with EML1 depletion, suggesting the possible role of EML1 in synaptic plasticity regulation at the tissue level. Except for these big synaptic proteins cluster, I have also found actin-related proteins, e.g. Cdc42ep2, Coro1a, Svil, Dmtn e.g.), adhesion (e.g. Ptprd, Nectin1, Fat3 e.g.). and previously malformation-associated proteins (Cenpe, Pnkp, Dnnaf5) in our proteomic results.

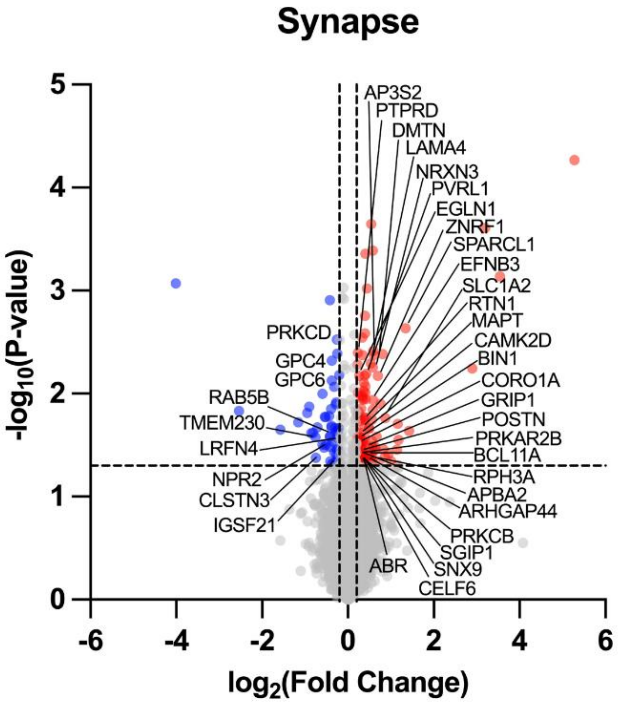

Figure 2. 39 Volcano plot showing all quantified proteins in cortex proteome and the proteins within the CC GO 'Synapse' term highlighted (blue: downregulated, red: upregulated)

After the whole proteome analysis, I defined the phosphoproteome profile of the cortices using 700µg of the same biological samples for identification of the phosphorylation dysregulations which may contribute to the pathogenesis of cortical abnormalities associated with Eml1 depletion. For this, label-free quantitative proteomics with phosphopeptide enrichment was performed and this analysis identified 3945 phosphosites, using two phosphosites in each of three replicates of cortices and applying a probability score of 0.75,

resulting in 1369 quantified phosphosites (Figure 2.40). The distribution of phosphoserine (pS), phosphothreonine (pT), and phosphotyrosine (pY) sites was found to be 91.2%, 8.4%, and 0.4%, respectively (Figure 2. 41).

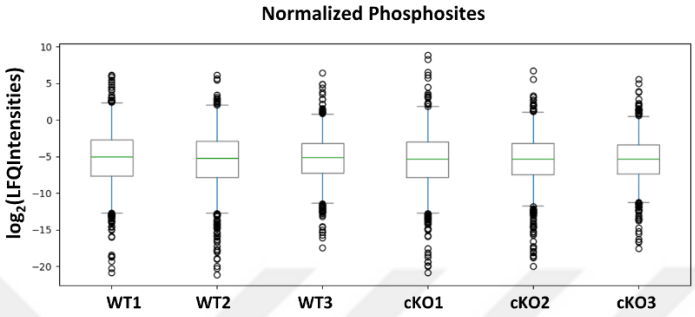

Figure 2. 40 Boxplot distribution of the log2 LFQ Phosphosite Intensities of the three replicates of WT and cKO cortices Values outside this range are plotted as dots and represent outliers. Median values are indicated in the boxplot through the horizontal lines in the center of the distributions.

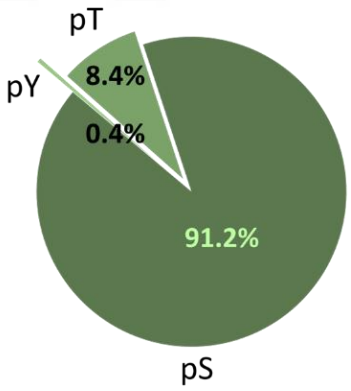

Figure 2. 41 Phosphorylation site distribution of phosphoserine (pS), phosphothreonine (pT), and phosphotyrosine (pY)

Applying a cutoff of the p-value of 0.05 to the quantified phosphosites, there were significant changes only in 39 sites within 1369 quantified phosphosites (Figure 2.42).

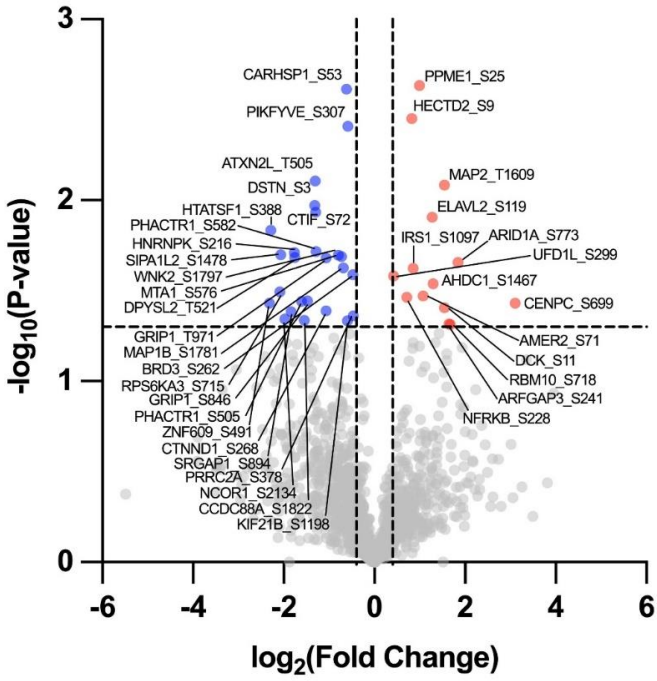

Figure 2. 42 Phosphorylation site deregulations in Eml1 cKO cortices (blue: downregulated, red: upregulated)

Overall, this cortex data suggests dysregulations in the tissue showing potential involvement of synaptic and cell junctional dysregulation in the pathogenesis of cortical abnormalities associated with Eml1 depletion. Despite successfully quantified proteins and phosphosites, the dysregulations were found in relatively low numbers and diverse cellular annotation groups, making their integration challenging.

The cortex region of the E15.5 embryonic brain contains a relatively large number of cell types and complexity (progenitor cells, corticothalamic projection neurons, subcerebral projection neurons, callosal projection neurons, interneurons, cajal-retzius cells) (Di Bella et al., 2021). Thus, the Eml1-dependent proteome and the phosphoproteome changes in the cortices may cause low abundance problems which are outcompeted by the complexity of the tissue region and possibly result in a faint phenotype in the tissue level.

2.3.3 Primary progenitor cells lacking EML1 exhibit dysregulation of microtubule cytoskeleton organization and protein metabolism mechanisms

As heterotopia formation is closely linked to phenotypes in radial glial progenitor cells (RG), we aimed to analyze the proteome of neuronal progenitor primary cells in *Eml1* cKO mice. To this end, we prepared highly enriched populations of Pax6+ neuronal progenitor primary cell cultures from control and *Eml1* cKO mice at E14.5. This minimized the complexity arising from cortex tissue cell composition and allowed for targeted analysis of the progenitor cells.

Unlike the cortex tissue, obtaining a sufficient protein concentration for comprehensive proteome analysis for the primary cells resulted significant challenge. To overcome this, I performed a dimethyl isotopic labeling-based quantitative proteomics method coupled with high-pH fractionation to analyse two biological replicated of only 20µg of control and Eml1-depleted cells. This approach provided nearly 4000 different proteins that had consistent intensity distribution at the biological replicates (Figure 2. 43).

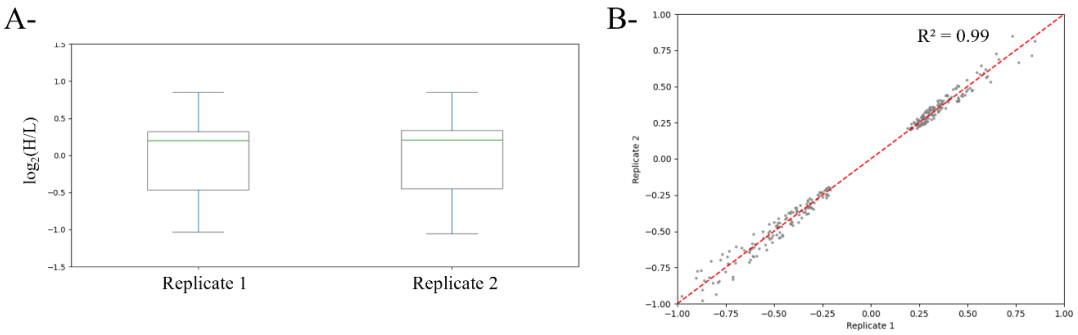

Figure 2. 43 Boxplot of Log2 (dimethyl heavy / dimethyl light) ratios of two biological replicates of neuronal progenitor primary cells (A) and correlation of deregulated proteins in Eml1 cKO neuronal progenitor primary cells (B)

Within these quantified proteins, I identified 266 dysregulated proteins (Figure 2.44). To understand the biological processes affected by Eml1 depletion in primary cortical cultures,

I performed the biological process cluster analysis with all the detected dysregulated proteins. This analysis revealed that Eml1 depletion disrupted many networks of biological processes including cytoplasmic microtubule organization, regulation of response to endoplasmic reticulum stress, translation, and protein localization to the vacuole (Figure 2. 45).

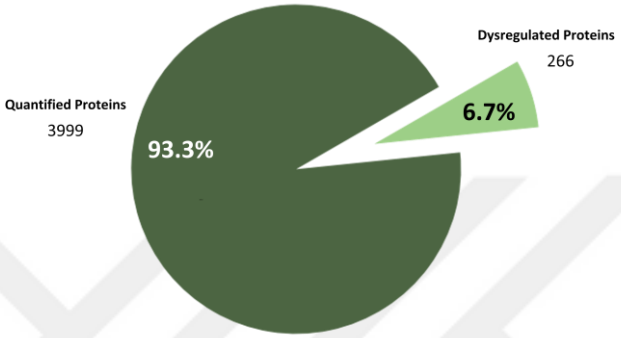

Figure 2. 44 Proteome analysis of *Eml1*-cKO neuronal progenitor cells revealed %6.7 deregulated proteins within 3999 quantified proteins

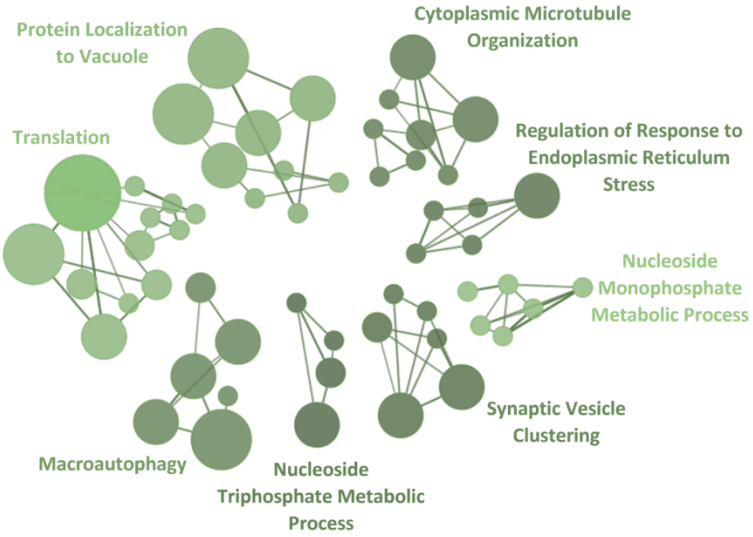

Figure 2. 45 Deregulated biological processes network analysis for Eml1 depleted neuronal progenitor primary cells

Furthermore, the clustering analysis of all detected dysregulated proteins revealed that *Eml1* depletion disrupted many networks of biological processes, including cytoplasmic microtubule organization, regulation of response to endoplasmic reticulum stress, translation, protein localization to the vacuole (Figure 2.45). Out of the dysregulated proteins, 131 were found to be downregulated, while 135 were upregulated. The Gene Ontology (GO) analysis revealed an enrichment of downregulated proteins with the regulation of microtubule cytoskeleton organization, microtubule, and structural constituent of the cytoskeleton, aligning with the known microtubule binding role of EML1 and suggesting its involvement in regulating microtubule organization in neuronal progenitor cells (Figure 2.46 and Figure 27). In contrast, upregulated proteins have enrichment in processes associated with regulation of translation, ribosome biogenesis, and RNA binding components, showing a potential role for EML1 in modulating protein metabolism processes (Figure 2.46 and Figure 27).

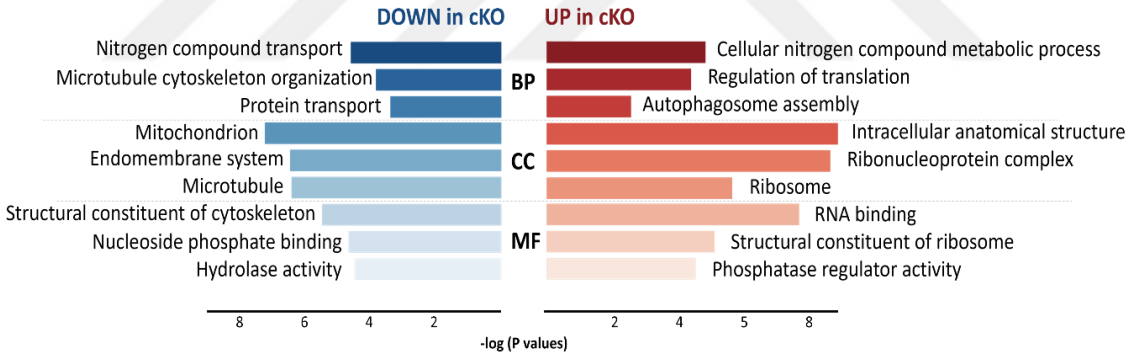

Figure 2. 46 GO enrichment analysis of 131 downregulated and 135 upregulated proteins in *Eml1* cKO neuronal progenitor primary cells (biological process (BP cellular component (CC); molecular function (MF))

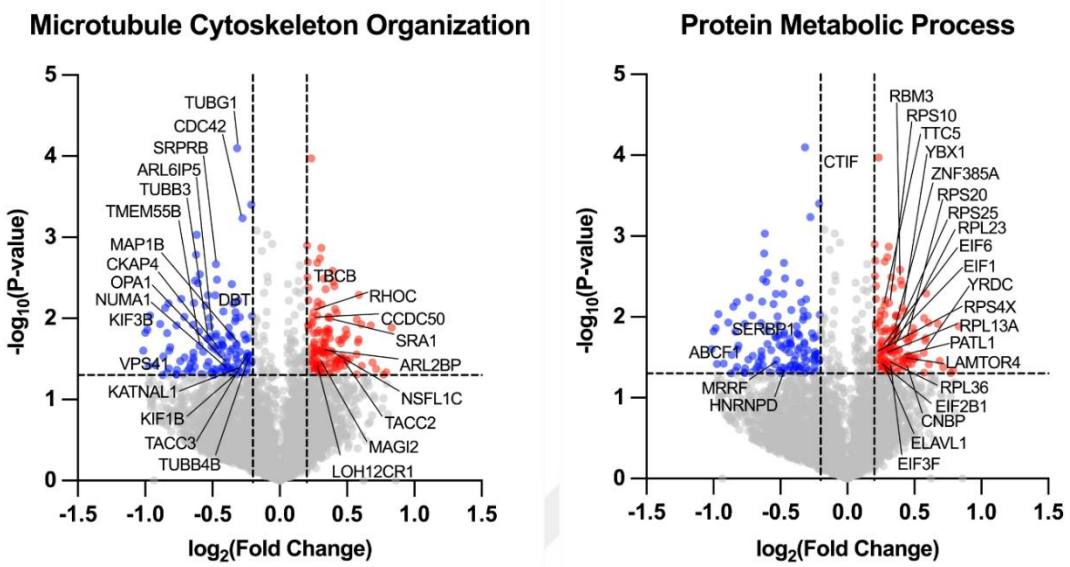

Figure 2. 47 Volcano plots showing BP GO terms of microtubule cytoskeleton organization and protein metabolic process deregulated proteins in *Eml1* cKO neuronal progenitor primary cells

Next, I focused deeper on dysregulated proteins involved in microtubule cytoskeleton organization and protein metabolic process because of their pronounced deregulation upon EML1 depletion (Figure 2.48). Upon further investigation into the dysregulations in microtubule cytoskeleton organization, our analysis revealed distinct clusters of proteins involved in spindle organization, organelle organization, and organelle transport along microtubules. Notably, For the spindle organization, NUMA1, KIF3B, TACC3, TACC4, and TUBG1 are among the down-regulated spindle organization proteins in EML1 depleted progenitor cells, suggesting a role for EML1 in spindle organization. This observation aligns with a previous study showing that perturbations in EML1 lead to decreased spindle length (Bizzotto, Uzquiano et al. 2017). Moreover, similar spindle organization defects have been reported in the context of EML4 and EML6 depletion, further underscoring the importance of EMAP proteins in maintaining spindle integrity (Chen, Ito et al., 2015; Yin, Hou et al., 2020).

Additionally, we observed dysregulations in proteins associated with the microtubule organizing center (MTOC). MTOC is a critical site involved in the microtubule nucleation and organization. TUBG1 is a major component of the MTOC. We observed significant downregulation in this protein for Eml1 cKO progenitor cells. Our recent publication validated the downregulation of TUBG1 in *Eml1* cKO progenitor cells at embryonic stages of *Eml1* cKO E12.5 and E15.5 cortices (Donia et al.2024).

Furthermore, my analysis revealed dysregulations in organelle organization and organelle transport proteins associated with mitochondria, the endoplasmic reticulum (ER), lysosomes, and the Golgi apparatus (e.g., CKAP4, NSL, VSP41, KIF1B, and TEMEM55B). a previous study showed that EMAP proteins involve in the attachment of ribosomes to microtubules, this result is highlighting the possible role for EMAP proteins interplay not only ribosomes but also for other cellular organelles (Suprenant, Dean et al. 1993).

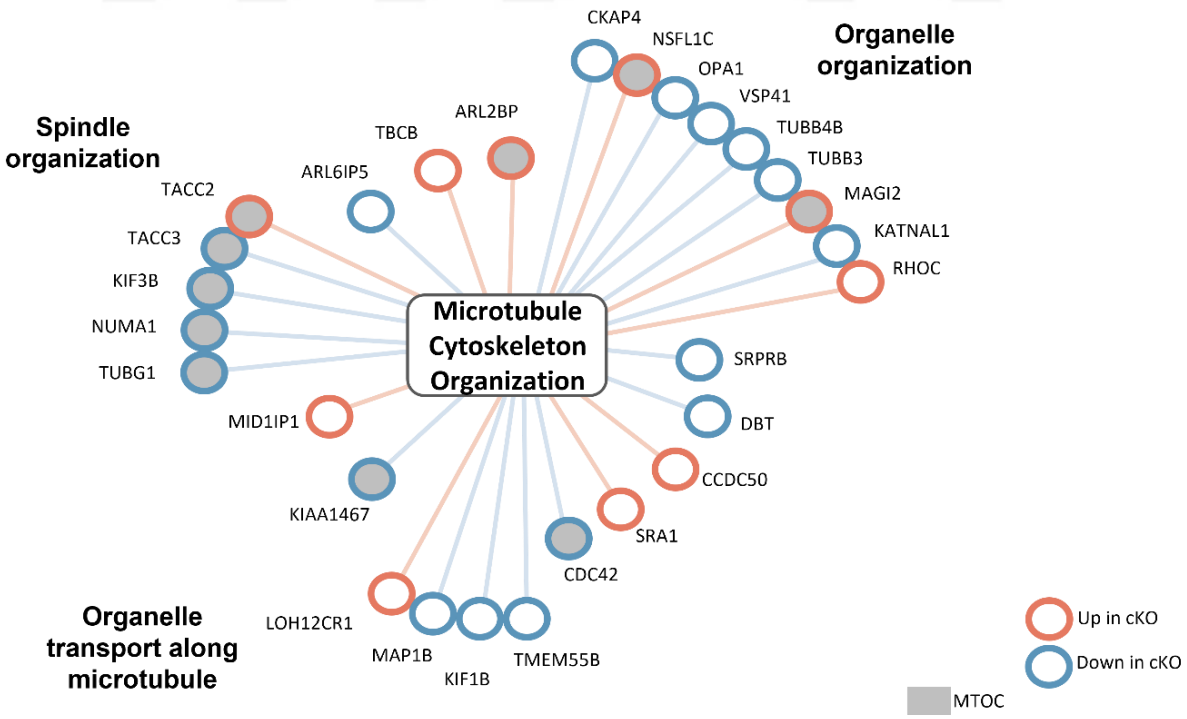

Figure 2. 48 Deregulated microtubule cytoskeleton organization proteins in progenitor proteome

Next, I investigated the protein metabolic process clustered proteins, which can be further clustered in positive regulation of translation and macromolecule biosynthesis process. Strikingly, in this clustering, I have found that ribosomal proteins were strongly upregulated (e.g. RPS20, RPS10, RPL36, RPS25) indicating increased translation activity in the Eml1-depleted progenitor cells. Interestingly I have also found upregulation of TTC5 protein which is a tubulin-specific ribosome-associating factor that triggers cotranslational degradation of tubulin mRNAs in response to excess soluble tubulin (Lin et al., 2020).

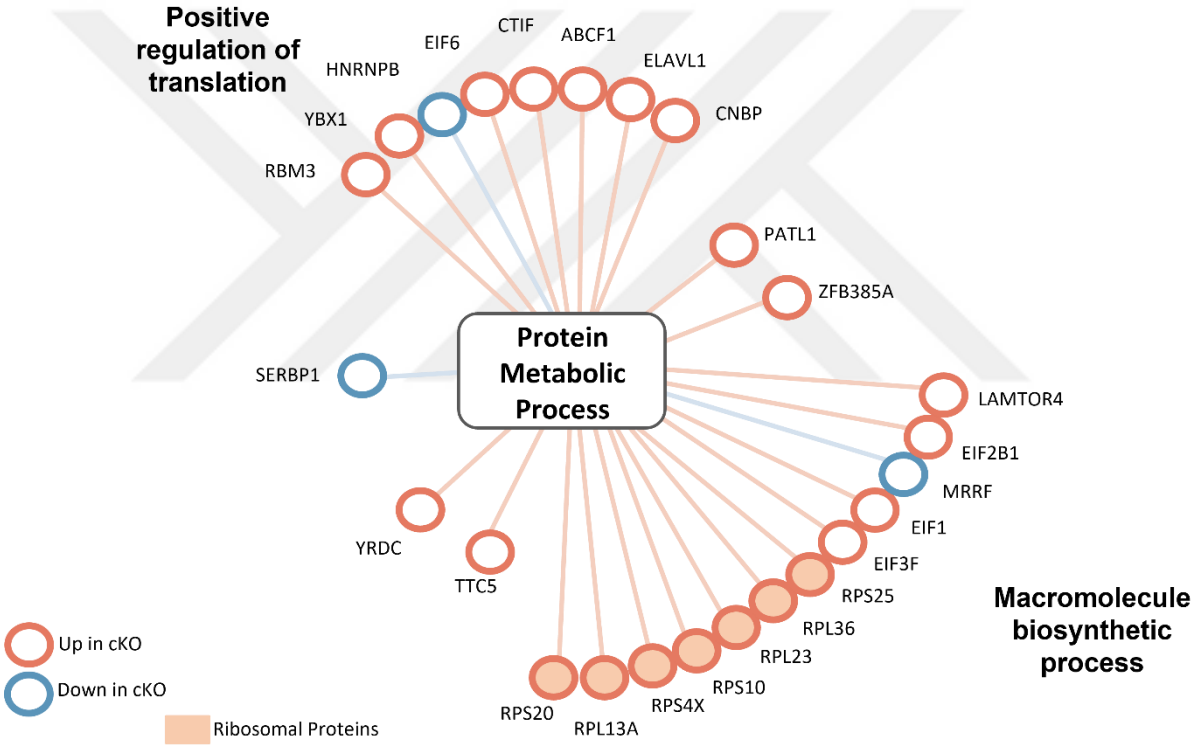

Figure 2. 49 Deregulated protein metabolic process proteins in progenitor proteome

Another interesting protein I found in this clustering is LAMTOR4 upregulation. LAMTOR4 is a component of the Ragulator complex, which functions as a guanine nucleotide exchange factor for the Rag GTPases that signal amino acid levels to mTORC1. Lamtor4 is required for mTORC1 activation by amino acids (Bar-Peled et al., 2012). The mTOR Complex

1 (mTORC1) pathway regulates cell growth in response to numerous cues. Upregulation in this protein might be a key to explaining the increased cell areas and abnormal proliferation in the heterotopic progenitor cells (Bizzotto et al., 2017). Overall, our findings provide a comprehensive understanding of the molecular alterations induced by Eml1 depletion for microtubule dynamics, and protein metabolism.

2.3.4. Eml1 depletion causes severe disruptions in microtubule associated network

Microtubules are structures in eukaryotic cells with a dynamic network by the tubulin heterodimers to perform several crucial cellular processes such as cell division, intracellular structural organization, and transportation of intracellular RNAs, proteins, and organelles, as well as flagellar and ciliary motility. This critical cytoskeleton component and its regulations through polymerization and depolymerization are tightly regulated by microtubule-associated proteins (MAPs). The microtubules and microtubule-associated proteins (MAPs) are some of the main regulators of neurogenesis, including cell proliferation, neuronal migration, and axonal guidance as brain development relies heavily on microtubule function.

To investigate the impact of EML1 depletion on microtubule organization, we focused on microtubules and microtubule-associated proteins (MAPs) in Eml1 cKO neuronal progenitor primary cells. Initially, I polymerized endogenous tubulin with Taxol, sedimented the microtubules and associated MAPs, and subsequently analyzed the microtubules and microtubule bound proteins following gel fractionation using orbitrap mass spectrometry. During gel confirmation, I observed striking differences in protein abundance between control and cKO samples. Even though I started the experiment with equivalent cell numbers in control and cKO samples, both biological replicates of cKO samples exhibited decreased levels of microtubules and associated MAPs on SDS-PAGE gels (Figure 2. 50.).

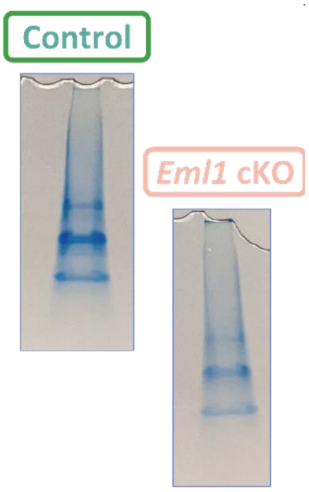

Figure 2. 50 SDS-Page of neuronal progenitor primary cells' microtubule-MAPs pellet

In analyzing the proteomic results, I normalized the protein levels in *Eml1* cKO samples to control samples based on the average tubulin protein intensities, which provided the favoring of the cKO cells. This normalization process revealed 2805 quantified proteins, of which 347 were dysregulated (Figure 2.51). Within these dysregulated proteins, despite the normalization favoring cKO progenitors, 320 proteins were still significantly downregulated (log2 fold change < -0.5), while only 37 proteins were upregulated (log2 fold change > 0.5), which indicates severe disruptions in microtubule associated network upon EML1 depletion.

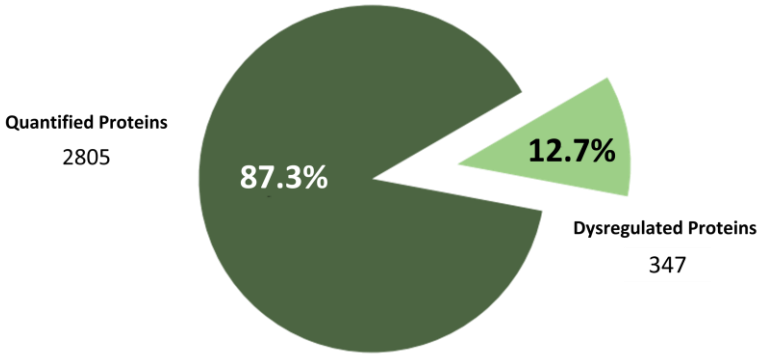

Figure 2. 51 %12.7 deregulated proteins in quantified microtubule-MAPs proteome

In the downregulated prroteins I found EML1's ortholog EML4 protein (Figure 2.52). Although the depletion of EML1 in progenitor cells does not result significant effect on the abundance of EML4 (-logp value=0.67 and log2 foldchange -0.39)., it causes significant downregulation of these proteins on microtubules (-logp value=2.12 and log2 foldchange -4.64). Similarly, we observed a significant effect of EML1 depletion on multiple septin proteins. Septins are GTP-binding proteins that can form a distinct filamentous network alongside microtubules, actin, and intermediate filaments. However, this protein family also has an association with microtubules. Septins can colocalize with perinuclear, golginucleated, subcortical, and axonemal microtubules to regulate microtubule stability and microtubule organization through interaction with microtubule-binding proteins. There are 13 septin genes in mice (Hall, Jung et al. 2005). In our analysis, we identified 9 Septins, with 7 significantly downregulated (SEPT2, SEPT3, SEPT5, SEPT6, SEPT8, SEPT9, and SEPT11), and 2 septin proteins were still downregulated but below the significance threshold (SEPT7 and SEPT10) in Eml1 cKO progenitor cells.

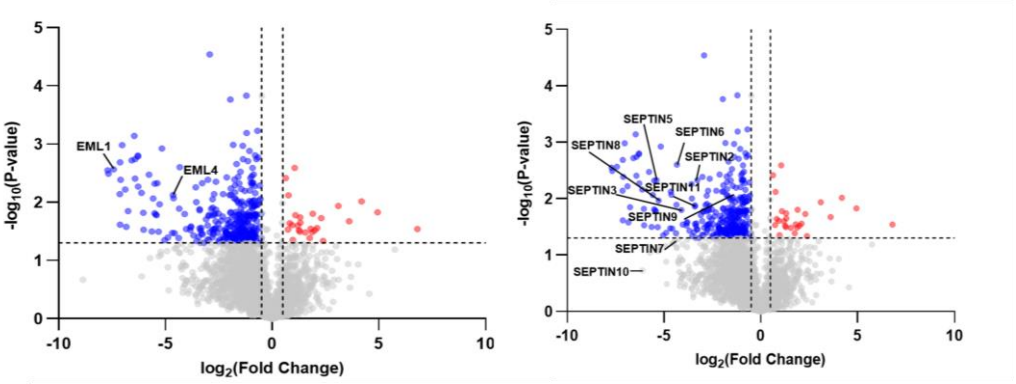

Figure 2. 52 Volcano plot showing deregulated proteins in microtubule-MAPs proteome of *Eml1* depletion primary neuronal progenitor primary cells (EML4 and Septins are highlighted, blue: downregulated, red: upregulated).

While there is no direct known protein-protein interaction between Septins and EMAP proteins, our findings suggest there can be a functional link in microtubule organization processes. EML4 and SEPT2 have common interactors as CKAP5 and DYNC1H1. CKAP5

is cytoskeleton-associated protein 5, which plays a role in microtubule organization and stability as a linker between microtubules and the cell cortex. DYNC1H1, on the other hand, is a component of the dynein motor complex involved in the intracellular transport of organelles and vesicles along microtubules. The downregulation of these two proteins also highlights the perturbations in microtubule organization and trafficking.

Overall, our microtubule and microtubule associated network proteome show that EML1 depletion causes severe disruption of this network, therefore suggesting a role for EML1 in crucial cellular function by microtubule organization. Furthermore, the deregulated proteins comprehensively characterize EML1-dependent microtubule-binding protein differentiation and will set the basis for future work on the EMAP family and heterotopia.

2.4 DISCUSSION

In this study, I chaptalized the heterotopia-associated EML1 mutant protein and dysregulations of *Eml1* conditional knockout (cKO) mice with a forebrain-specific inactivation of *Eml1* at the protein level. Through a combination of imaging, BioID proximity labeling, cortices label-free proteomics, phosphoproteomics, dimethyl labeling, and microtubule proteome, I aim to link the heterotopia formation to the EML1 protein.

The Echinoderm Microtubule-Associated Protein (EMAP) family (EML proteins) is a novel class of MAPs that bind to the microtubule network and function in mitotic spindle formation (Richards et al., 2014; Suprenant et al., 1993). Mammals have six EML proteins, based on their protein structures they can be classified into two subgroups EML1-2-3-4 and EML5-6. EML1-2-3-4 proteins having a molecular weight ranging from 70kDa to 120kDa contain a coiled-coil domain and hydrophobic HELP motif at the N-terminal, and the C-terminal domain has approximately 650 residues of multiple tryptophan-aspartic acid (WD) repeats. Whereas EML5-6 has a molecular weight larger than 200kDa and three hydrophobic HELP motifs and WD repeats (Sabir et al., 2017).

Among the identified EML1 mutations associated with heterotopia formation, the Thr243Ala missense mutation is linked to the formation of severe heterotopia. Thr243 position within the HELP motif and acting as a critical site within a bridge linking β-propeller structures in the EML1 protein (Richards et al., 2014). Using imaging techniques first, I visualized EML1 and EML1Thr243Ala proteins in two different cell lines over their endogenous level of EML1 expression. In literature, it is shown that the HELP motif within the N-terminal is one of the crucial sides for the microtubule binding. It is shown that the

isolated TAPE domain of EML1 and the N-terminal of EML4 tight association with soluble α/β-tubulin heterodimers (Richards et al., 2014; Sabir et al., 2017). Further studies revealed that binding to the microtubules requires also the trimerization domain (Richards et al., 2015). The trimerization domain is composed of the specific amino acid motif and it is essential to maintain the coiled-coil structure. This domain strongly associates with the microtubules and deletion of the trimerization domain from the structure, reducing the interaction of protein-microtubule binding but the trimerization domain alone is not sufficient for the MT binding (Richards et al., 2015).

With the mutation in the HELP motif in the Thr243 position, I have found that there is a severe disruption of microtubule-protein binding in N2A and as well as in HeLa Kyoto cells. Normal EML1 enriches at different locations during cell division. It localizes to the microtubules during interphase, enriches on spindle microtubules during metaphase, and localizes at the midzone during cytokinesis. However, for the mutant protein, these enrichments along microtubules notably decreased across all phases of the cell cycle. This finding is in line with the literature showing that the HELP motif is important for the proper microtubule binding and severe disruption in microtubule-protein binding with the mutation showing the functional significance of this motif in maintaining the integrity for the normal protein to function. There are three known mutations in the HELP motif that are associated with the heterotopia formation Trp225Arg, Gly231Asp, and Val254Met mutations, it is probable that visualizing these proteins might give rise to comparable results with the Thr243 mutation site.

EML1 is associated with heterotopia formation, I have found that the EML1 protein is more enriched on the microtubules in N2A cells than in HeLa Kyoto cells and in HeLa Kyoto cells the protein is more cytosolic. N2A cells originate from mouse neuroblastoma and HeLa Kyoto cells originate from human cervical cancer, which resulting differences in cellular characteristics. These variances include distinct tissue origins and cellular functionalities, such

as neuronal cells' reliance on highly dynamic microtubules for providing a structural backbone for axons and dendrites. Such variances can significantly influence the expression and localization patterns of EML1 protein, as evidenced by the observation of more cytosolic localization in HeLa Kyoto cells compared to N2A cell lines.

After the finding of the microtubule-binding deficiency in the mutant protein, the interactome of the normal and mutant EML1 proteins was also defined using the N2A cell line. N-terminal proximity labeling revealed the resulting 49 and 30 proximal interactor proteins for N-terminal interactors of EML1 and EML1Thr243Ala respectively. Among this, it has been found that only 26 proteins are overlapping between these interactomes resulting in 26 unique close proximity interactors for EML1 and 4 for EML1Thr243Ala. EML1 interacts with proteins in different roles within the cell (e.g. microtubule organization, ciliogenesis, chromosome organization, macromolecular structure, ribosomal proteins, adhesion and migration proteins, etc.) and the interactions of many proteins related to cell division and microtubule skeleton are specific to wild EML1.

The investigation into the molecular mechanism underlying EML1-associated heterotopia has revealed its effect on the destabilization of the primary cilium, which is a signalling hub containing various receptors and signalling molecules involved in developmental pathways regulating crucial processes during cortical development including cell proliferation, differentiation, and neuronal migration. In the HeCo cortices at embryonic day E12.5 and E13.5, there is a reduction of gamma-tubulin and Arl13b indicating that centrosome and primary cilia defects. HeCo progenitors, fibroblasts of heterotopia patients, and cortical progenitors produced from iPSC; It has been shown that there are defects in primary cilia structure (the microtubule-based organelle that is critical for regulating progenitor behaviour) and Golgi functions (Uzquiano et al., 2019). Progenitor cells receive environmental signals by connecting to the ventricular surface with primary cilia structures.

EML1 protein has been found to interact with many microtubules, proteins responsible for cytoskeleton organization, and MAPs such as EML2, EML4, MAP2, MAP4, MAPT, and CEP170). Among these proteins, CEP170 is a centrosomal protein that plays a crucial role in centrosome maturation. The interaction between CEP170 and EML1 was identified as WT specific interactome which means that in the heterotopic mutant interactomes, this interaction is lost, which is further validated in *Eml1* cKO progenitor cells (Donia, 2024). Francis lab. checked the intensity of Cep170 at the centrosomes at the ventricular surface in embryonic brains at E12.5 and E15.5, comparing wild-type and conditional knockout (cKO) *Eml1* embryos and they found a very significant decrease in Cep170 intensity in in Eml1 cKO embryos at both stages, even after normalization to γ-tubulin levels. The centrosomal defect here and catching this interaction also raised a question regarding the stability of the centrosome integrities in the N2A cell lines in normal conditions and as well as the BioID transfected conditions. With immunofluorescent staining, I showed that N2A cells show the normal centrosomal characteristics in the background cells as well as BioID transfected cells and proved that this dysregulation depends on the distribution of EML1.

The Heterotopic Cortex (HeCo) mouse model with spontaneous *Eml1* mutations, shows heterotopic abnormal neuronal cell accumulation in the rostro-medial region of the cortex, and it is found that there are early-born neurons and late-born neurons clustered in this heterotopic region. HeCo mice provided great insight into the disturbed molecular mechanisms involved in heterotopia formation. It is shown that the heterotopia formation in this mouse model is not dependent on the neuronal migration defect, but rather it is caused by disrupted microtubule dynamics in these cells. HeCo neuronal progenitor cells have abnormal microtubule dynamics with specifically slower microtubule plus-end growth rates compared to the wild-type cells (Bizzotto et al., 2017). Additionally, the shape and size of the cell bodies in HeCo cells are quite different from the normal cells, particularly because these cells have increased horizontal area. The primary cilia defects were also absent in the mutant human progenitor cells (Jabali et al., 2022; Markus et al., 2021). *Eml1* full knockout in mice showing

heterotopia formation, along with radial glia (RG) detachment and PC defects, with some observed lethality (Collins et al., 2019). There is also a new mouse model, *Eml1* conditional knockout (cKO) mice with forebrain-specific inactivation of *Eml1*, revealing severe heterotopia but without hydrocephalus (Donia, 2024).

In this thesis, I analysed this cKO mouse model using many proteomics label-free proteomics, phosphoproteomics, dimethyl labelling, and microtubule-MAPs proteome which provide insight into the regulation in many aspects of cortices and primary neuronal cells. The findings demonstrate the broad spectrum of deregulation dependent on EML1 depletion across cortices, primary neuronal progenitor cells, and MTs-MAPs. Our investigation initially unveils that the depletion of EML1 causes dysregulations within cortex proteomes associated with synapse and cell projection. Given that cortical malformations in human patients commonly have epileptic seizures, the observed deregulation within the synapse cluster may serve as a conduit between this pathological condition and its impact at the cortex level. While existing literature has hinted at the potential regulatory roles of EML4 and EML2 in synaptic plasticity, our study states the first exploration into the association between EML1 depletion and synaptic protein dysregulation (Noctor, Flint et al. 2001, Dunckley and Lukas 2003). EML1 and synaptic protein dysregulation at the cortex level can also be linked to abnormal microtubule cytoskeleton organization. Microtubules (MTs) are essential components of all cells, and also in neurons, they facilitate branching structures and provide intracellular transport (Kapitein and Hoogenraad 2015).

Another important finding in our results is that EML1 depletion in neuronal progenitor primary cells affects the cytoplasmic microtubule organization and the regulation of translation. Specifically, we observed downregulated proteins clustered in cytoplasmic microtubule organization and upregulated proteins clustered in protein metabolism. Although we did analyze the dysregulation of protein metabolism mechanisms in Eml1 cKOs more deeply, there appears to be a connection between EMAP proteins and ribosomes. EMAP proteins attach ribosomes to microtubules (Suprenant, Dean et al. 1993), and the increase in

various ribosomal protein abundances in these cells might be attributed to the improper binding of ribosomes to microtubules causing increased abundancy. Additionally, we saw the upregulation of LAMTOR4. LAMTOR4 is a component of the Ragulator complex, which serves as a guanine nucleotide exchange factor for Rag GTPases signaling amino acid levels to mTORC1. In EML1-deficient progenitor cells, early detachment from the ventricular zone disrupts connection with cerebrospinal fluid (CSF), which serves as a proliferative niche and nutrient source for neuronal progenitor cells (Lehtinen, Zappaterra et al. 2011). While we did not investigate this aspect, the link between protein metabolism and disconnection from CSF may offer aspects to the heterotopic cells in nutrient sensing and perturbed primary cilia in the *Eml1* heterotopic cells can solely influence the nutrient sensing (Boehlke, Kotsis et al. 2010, Uzquiano, Cifuentes-Diaz et al. 2019). TTC5 protein is a tubulin-specific ribosome-associating factor that triggers cotranslational degradation of tubulin mRNAs in response to excess soluble tubulin (Lin et al., 2020). Interestingly, EML4 has been identified as an interaction partner of TTC5 protein in HEK cells. With the Eml1 depletion, TTC5 is upregulated in progenitor cells, which is also important to link the increased translation activities and affected microtubule dynamics.

For the microtubule organization deregulations in neuronal progenitor primary cells, we observed several protein deregulations, predominantly downregulation, in spindle organization, organelle transport, and organelle organization. Regarding spindle organization, it is known that the disruption of EML1 results in longer spindles (Bizzotto, Uzquiano et al. 2017). Spindle organization defects have been reported in the context of EML4 and EML6 depletion, further emphasizing the significance of EMAP proteins in maintaining spindle integrity (Chen, Ito et al. 2015, Yin, Hou et al. 2020).

Furthermore, we saw dysregulations in proteins associated with the microtubule organizing center (MTOC), a microtubule nucleation and organization site. Several members of the EMAP family affect the microtubule dynamics. Eml2 stabilizes the microtubule cytoskeleton by slowing MT shortening and increasing rescues, while also recognizing and

regulating tyrosinated microtubules (Hotta et al., 2022). Similarly, Eml4 also increases microtubule stability, leading to a reduction in the amount of free tubulin and microtubule growth rate (Houtman et al., 2007; O'Regan et al., 2020). Notably, TUBG1, a vital component of the MTOC, displayed significant downregulation in Eml1 cKO progenitor cells. Our recent publication provided further evidence by confirming the downregulation of TUBG1 in Eml1 cKO progenitor cells (Donia 2024). Moreover, we emphasize the importance of validating other MTOC protein deregulations alongside TUBG1 downregulation to gain deeper insights into the microtubule nucleation problems associated with Eml1 depletion. (Donia, 2024). for other cellular organelles.

Our investigation into MAP microtubule binding revealed that EML1 depletion causes severe disruptions in MAPs and microtubules. When EML1 is depleted on the microtubules, this causes a reduction of EML4 on microtubules. EML1 and EML4 proteins have trimerization domains in their N-terminal regions, suggesting functional cooperation between these proteins. While literature highlights EML4 homotrimerization (Papageorgiou, Pashley et al. 2022), there is potential for other EMAP proteins to engage in similar interactions.

There is no direct link between EMAP and Septin protein families. However, with the depletion of EML1, Septin protein family dramatically downregulated. In our MPs-MAPs proteome we identified nine septins, with seven significantly downregulated (SEPT2, SEPT3, SEPT5, SEPT6, SEPT8, SEPT9, and SEPT11), and two septin proteins were still downregulated but below the significance threshold (SEPT7 and SEPT10) in Eml1 cKO progenitor cells. Depletion of Septin proteins also linked increase acetylated tubulin, loss or shortening of cilia and synaptic vesicle recycling which in all aspect can be linked to EML1 cKOs.

Overall, in this thesis, I investigate the dysregulations of *Eml1* depletion on cortical development with analysis of imaging and interactome network analysis of heterotopia-associated mutant EML1 protein and the proteome change of *Eml1* conditional knockout (cKO) mice with a forebrain-specific inactivation of *Eml1*. These comprehensive proteomic analyses serve as a valuable resource for further investigating the underlying mechanisms involved in the EMAP protein family, brain development and heterotopia formation.

Chapter 3

FUNCTIONAL ANALYSIS OF EML1 IN CORTICAL MALFORMATION

3.1 LITERATURE REVIEW

3.1.1 Regulation of plasma membrane during the cell cycle

The cell cycle is a fundamental process of cells to replication and separation of DNA and cellular contents into two daughter cells. The cell cycle of eukaryotic cells consists of four stages, G1 (cell growth), S (DNA synthesis), G2 (preparation for the division), and M (mitosis) to result in two daughter cells. These stages are highly complex and tightly regulated events with the cell cycle checkpoints to ensure proper DNA duplication segregation. Any abnormalities in these stages cause failure in cell cycle checkpoints and initiate the apoptosis process which is one of the processes cancer cells find an escape without the proper control mechanism.

To achieve a successful cell cycle, eukaryotic cells undergo a remarkable series of structural changes in combination with cellular organelle regulations (Ramkumar & Baum, 2016). uring the mitosis stage, cells undergo rapid changes in cell volume and plasma membrane surface (Figure 3. 1). Since the cells have limitations for membrane synthesis, they rely on membrane sharing and remodeling processes such as exocytosis or endocytic recycling of protein tracking and membrane blebbing (Boucrot & Kirchhausen, 2007).

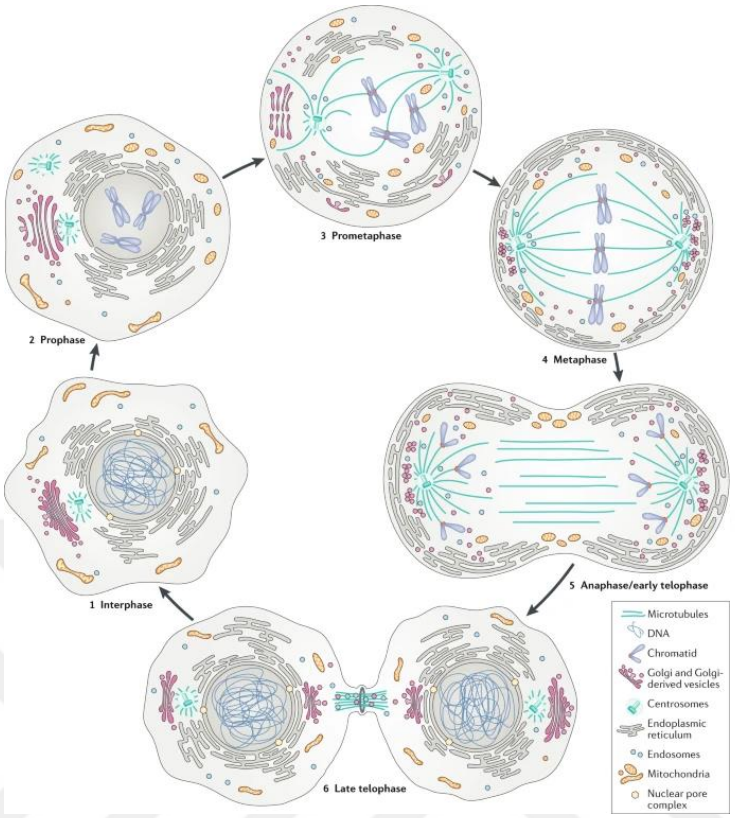

Figure 3. 1 Cellular organelle and plasma membrane regulations during division (Adapted from (Carlton et al., 2020))

The adherent cells transiently round-up as they enter the mitosis. Then, the expansion of the cell membrane during anaphase has a crucial role in positioning the spindle correctly to ensure the successful symmetric division which resulting the reciprocal relationship between the plasma membrane and spindle positioning (Sedzinski et al., 2011). The adherent cells transiently round-up as they enter the mitosis. Then, the expansion of the cell membrane during anaphase has a crucial role in positioning the spindle correctly to ensure the successful symmetric division which resulting the reciprocal relationship between the plasma membrane and spindle positioning (Kunda et al., 2008; Piekny & Glotzer, 2008). Other protein regulators

of the actin structures are the capping protein, cofilin, myosin II, and profilin (Carlton et al., 2020). Understanding the mechanism of controlling and remodelling of the plasma membrane and its link to the cortex is one of the challenges in the literature.

3.1.2 Protocadherin protein family

Protocadherins (Pcdhs) are cell adhesion proteins and with more than 70 identified genes, Pcdhs represents the largest subgroup of the cadherin family and predominantly expressed in the nervous system (Hirano et al., 2012; Hirayama & Yagi, 2006). Based on their structural and genomic organization, Pcdhs are classified in two groups clustered and nonclustered protocadherins (Figure 3. 2).

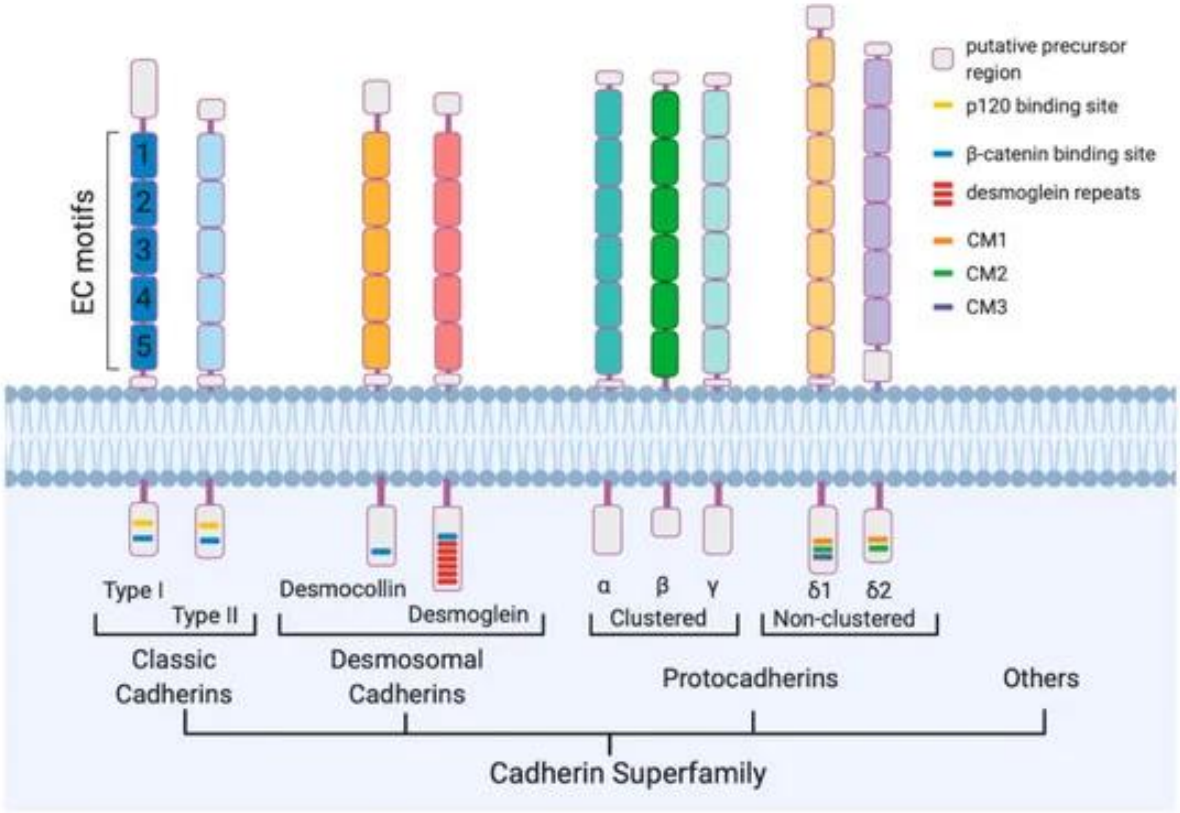

Figure 3. 2 Cadherin superfamily showing the protocadherins and classification as clustered and nonclustered protocadherins (Adapted from (Mancini et al., 2020))

In clustered PCDHs, there are three groups PCDHα, PCDHβ, and PCDHγ. These gene clusters are arranged in in a small genome locus on a single chromosome (human chromosome 5q31; mouse chromosome 18) and in the non-clustered ones they do not locate on a clustered genome locus, but these are dispersed on different sites of the chromosomes. Non-clustered PCDHs are divided into two sub-groups PCDHδ and solitary PCDHs (Figure 3. 3).

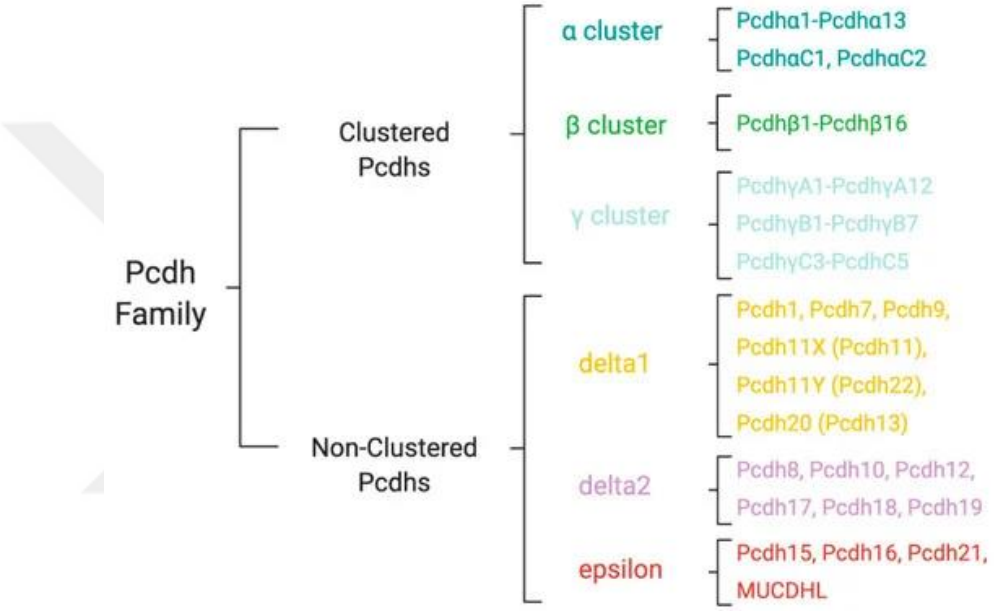

Figure 3. 3 Subgroups of PCDHs (Adapted from (Mancini et al., 2020))

PCDH7 belongs to the δ1-Pcdh family of the non-clustered PCDHs and it has an extracellular domain containing 7 cadherin repeats (Zhang & Fu, 2021). PCDH7 play important roles in cell adhesion, cell recognition and there are several studies showing that in various cancer types PCDH7 is dysregulated. It is found that PCDH7 upregulated in human non-small cell lung cancer and downregulated in non-muscle invasive bladder cancer (Zhou et al., 2017) (Lin et al., 2016).

In our laboratory's previous study, the interphase and mitotic cell surfaces of HeLa cells were analyzed using the SILAC quantitative proteomic approach. This analysis revealed that 15 statistically significant mitosis-selective proteins had a median ratio above 2.5-fold. PCDH7 is one of these proteins showing the median SILAC ratio of 5.15 (Özlü et al., 2015). This indicates that PCDH7 is a specific mitotic surface marker. Additionally, It is also shown that as the cell progressed into prometaphase, became rounded and less adhesive, PCDH7 localized to the retraction fibers around the cortex and during metaphase, PCDH7 localized to the plasma membrane (Özlü et al., 2015).

To understand the further mechanisms of PCDH7 localization to the plasma membrane, we published a new article, which include this thesis results (Özkan et al., 2023). In this its proximal interactors of PCDH7 during the interphase and mitosis are identified (Figure 3. 4). The analysis identified 78 proteins specific to mitosis, 129 specific to interphase, with 47 proteins common to both phases. The identified proteins were further analysed using the STRING database and clustered based on Gene Ontology (GO) and KEGG pathway enrichments included proteins related to the actomyosin network, cell adhesion, cadherin-binding, vesicular transport, and ERM family proteins, provides on the potential roles PCDH7 function during different cell cycle phases.

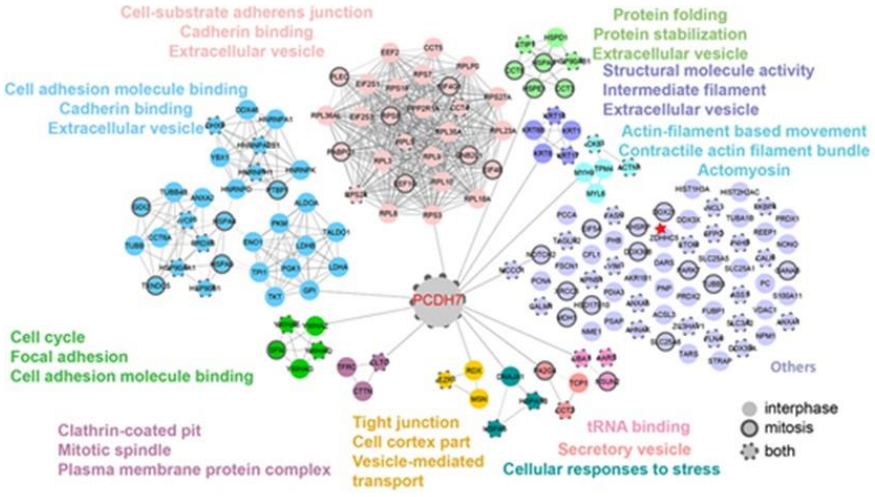

Figure 3. 4 Proximal interactors of PCDH7 during interphase and mitosis (Özkan et al., 2023)

3.2. MATERIAL AND METHODS

3.2.1 Cell lines and cell cycle syhronizations

HeLa S3 cells stably expressing PCDH7-GFP were generated by transduction of pLenti-PCDH7-GFP viral backbone. For viral transduction, lentivirus was packaged in HEK293T cells using packaging vector (psPAX2, Addgene #12260) and envelope vector (pCMV-VSV-G, Addgene #8454) and transfected with PEI transfection. The viruses were collected at 48- and 72-hours post-transfection and filtered. These prepared viruses were then added to HeLaS3 cells in the presence of 2 micrograms/ml protamine sulfate. From the pool population, single cell colonies were performed, and imaging were performed with A3 colony of HeLaS3-PCDH7-GFP. These cell lines were cultured in DMEM supplemented with 1% P/S, 10% FBS.

The PCDH7-GFP-BAC transgenic cell line was provided by Dr. Ina Poser (Max Planck Institute of Molecular Cell Biology and Genetics, Germany) and was cultured in DMEM supplemented with 1% P/S, 10% FBS, and 400µg/ml G418 (Santa Cruz Biotechnology, sc-29065A).

Cells were synchronized to interphase using a double thymidine block with 2.5 mM thymidine (Santa Cruz Biotechnology, sc-296542). To induce monopolar mitosis, cells were treated with 10 µM S-trityl-L-cysteine (STC) (Sigma-Aldrich, 164739). To synchronize bipolar, cells were incubated with 10 ng/ml of nocodazole (Calbiochem, 487928) for 5 h for mitosis and then released from nocodazole for 1 h for cytokinesis.

3.3.2 Inhibition of palmitoylation mechanisms through chemical inhibitor and knockdown using siRNA and shRNA systems

Palmitoylation experiments were performed with PCDH7-GFP-BAC transgenic cell line. To inhibit palmitoylation with chemical inhibitor, cells were treated with 100 μM 2BP (Sigma-Aldrich, 21604) overnight.

For the specific knockdown of ZDHHC5 shRNA and siRNA approaches were used. The shZDHHC5 construct was provided by Dr.Ekin Atilla-Gökcümen (Department of Chemistry, University at Buffalo, The State University of New York, Buffalo, USA) The sequence of shZDHHC5: 5′CCCAGTTACTAACTACGGAAA-3′ in pLKO.1 vector. This vector transduced to the PCDH7-GFP-BAC cells.

For siRNA approach, siGENOME siRNA pools (Dharmacon, D-026577-01-0020, target sequence: 5′-GGACUAAGCCUGUAUGUGU-3’) and non-targeting siRNA (Dharmacon, D-001210-01-05) were used using Lipofectamine RNAiMAX transfection reagent (Thermo Fisher Scientific). For this, PCDH7-GFP-BAC were seeded into 12-well plate and transfected with 15pmol of siRNA twice, at 24 h and 48 h. After 72 h post-seeding, cells were either pelleted for western blotting analysis or fixed for immunofluorescence analysis.

3.3.3 Western blotting analysis, immunofluorescence analysis, live cell imaging

For western blotting, the samples were lysed in the PBS supplemented with %0.1 Tween and protease inhibitor. Then lysed samples were run into 10% Sds-Page gels and transferred to a nitrocellulose membrane. The membrane was blocked with 4% non-fat dry milk in TBS containing 0.1% Tween-20 and probed with the primary antibody diluted in 2% BSA in TBS containing 0.1% Tween-20. The used antibodies: anti-PCDH7 (Abcam, ab139274, 1:400), anti-phospho-histone H3 (Upstate, 06-570, 1:500), GFP (custom antibody, 1:5000), anti-

ZDHHC5 (Atlas Antibodies, HPA014670, 1:2000) and HRP-conjugated secondary antibodies (Cell Signaling Technology, 7074S and 70765; 1:2000).

For immunofluorescence analysis, the cells in 12-well plates were fixed with 3% paraformaldehyde, blocked, and incubated with primary and secondary antibodies in 2% BSA in PBST. The used antibodies: anti-β-tubulin (Cell Signaling Technology, CS2128S, 1:500), anti-α-tubulin (Cell Signaling Technology, 3873S, 1:1000), anti-tubulin (Abcam, ab6160, 1:500), anti-ZDHHC5 (Atlas Antibodies, HPA014670, 1:500), anti-GFP (Invitrogen, A11120, 1:1000). The images of siRNA and shRNA were taken by Nazlı Ezgi Özkan, using Leica DMi8/SP8 TCS-DLS confocal microscopy. The quantification of these images was also performed by Nazlı Ezgi Özkan.

For live cell imaging, HeLaS3-PCDH7-GFP were seeded into ibiTreat μ-Slide 4-well plates. The cells were visualized using Leica DMi8 widefield fluorescence microscope equipped with 37°C and 5% CO_2 chamber taking three z-stacks every 3 min.

3.3 RESULTS

3.3.1 PCDH7 localizes to the mitotic cell surface and cleavage furrow during cell division

In our previous study the localization of PCDH7 was found as enrichment at the cell surface as the cell progresses into mitosis (Özlü et al., 2015). In this thesis I further investigated the spatiotemporal regulation of PCDH7. Although not a novel finding, I generated a new stable cell line colony and improved imaging techniques to obtain higher-quality images of this protein translocation during cell division.

To understand the translocation of PCDH7 during cell division, I initially conducted immunofluorescence experiments using the PCDH7-GFP-BAC cell line. This revealed that PCDH7 localized to the cell–cell contacts during interphase, then to the mitotic cell surface during mitosis, and finally to the cleavage furrow during cytokinesis (Figure 3. 5).

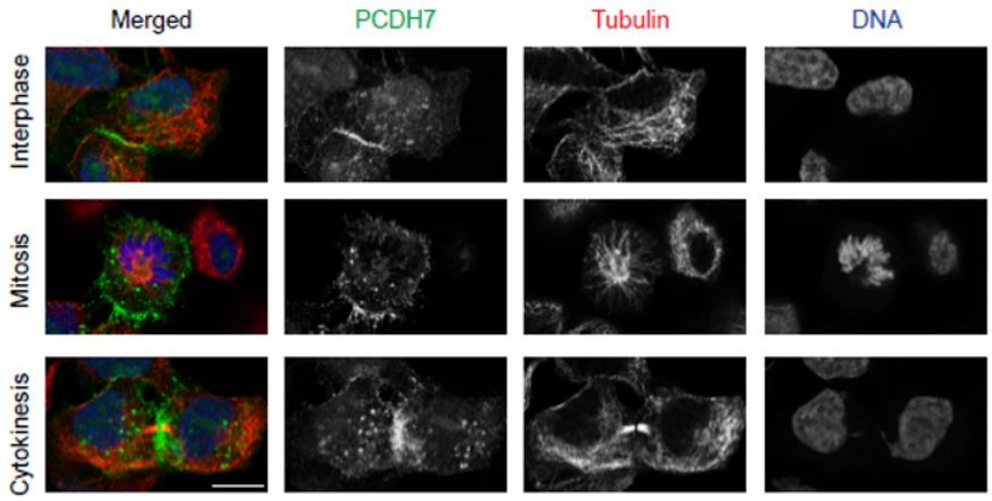

Figure 3. 5 Subcellular localization of PCDH7 in PCDH7-GFP-BAC cells in interphase, mitosis, and cytokinesis

After these initial findings, I performed similar experiments using live cell imaging with the HeLa S3-PCDH7-GFP A3 colony. Once again, I observed localization of PCDH7 at the mitotic cell surface and cleavage furrow during the cell cycle (Figure 3. 6).

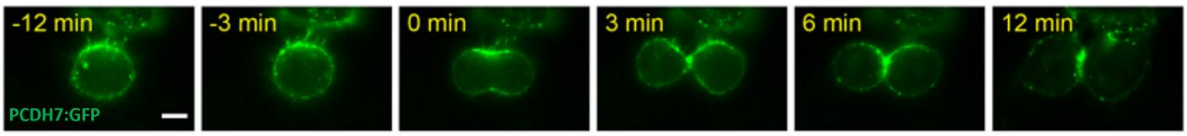

Figure 3. 6 Live imaging HeLa S3-PCDH7-GFP A3 cells during cell division

3.3.2. Palmitoylation of PCDH7 is required for its localization to the mitotic cell surface

In the article, Nazlı Ezgi Özkan performed BioID proximity labeling proximal interactors of PCDH7 during the interphase and mitosis are identified (Figure 4). The analysis identified 78 proteins specific to mitosis, 129 specific to interphase, with 47 proteins common to both phases. In these proximal interactors, Nazlı found that PCDH7 interacts with one of palmitoyltransferase ZDHHC5. Palmitoylation is one of the reversible post-translational modifications that are important for controlling protein trafficking to the membrane.

To further investigate the possible palmitoylation mechanism of PCDH7, I used one of the global palmitoylation inhibitors, 2-bromopalmitate (2BP). With the inhibition of the palmitoylation mechanism, it has been found although 2BP treatment did not affect the interphase localization of PCDH7, it notably reduced the enrichment of PCDH7 in the mitotic membrane compared to the DMSO control (Figure 3. 7). This result showed that PCDH7 localization to the cell surface during mitosis is dependent on the palmitoylation mechanism.

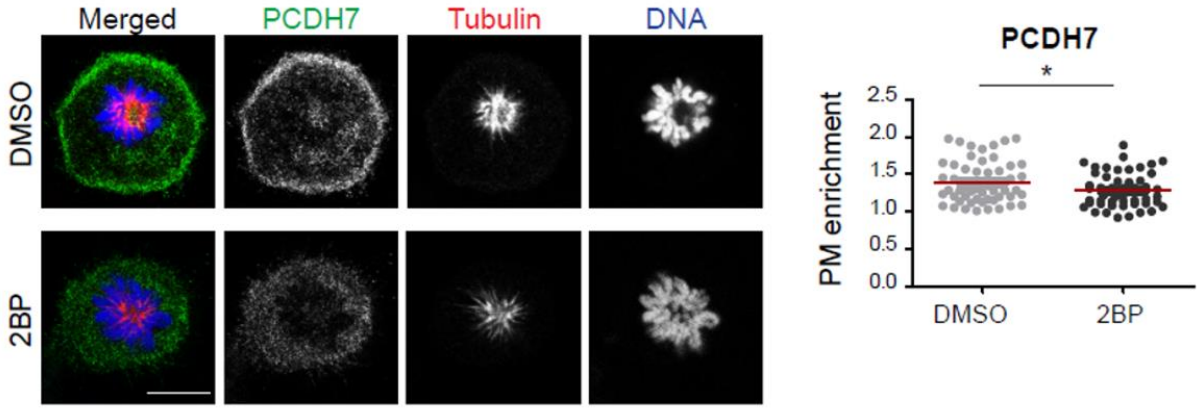

Figure 3. 7 Inhibition of palmitoylation mechanism with 2 BP causes perturbation of mitotic cell surface localization of PCDH7

To expand the palmitoylation mechanism further, I started to analyze the interaction partner of PCDH7 which is the ZDHH5. For that, I first suppressed the ZDHHC5 using the siRNA and confirmed the knockdown efficiency. According to this, using double treatment of siRNA results in very high efficiency in the ZDHHC5 blot and the knockdown of this protein does not change the abundance of PCDH7 protein (Figure 8). Then I performed an immunofluorescent experiment to check the localization of PCDH7 upon ZDHHC5 siRNA. For this, I again performed double siRNA treatment Coupled with coupled cell synorization to the cells to the mitosis phase. This experiment revealed that consistent with our previous 2BP observations, the knockdown of ZDHCC5 led to a significant reduction in the PCDH7 signal at the mitotic cell surface (Figure 3. 8). In this experiment, I performed the western blotting and immunofluorescent experiments, and Nazlı did the imaging and quantification of images.

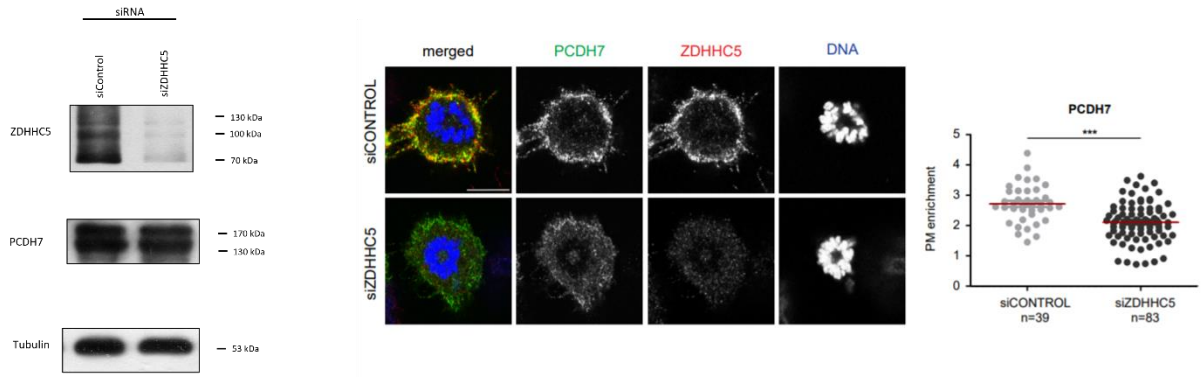

Figure 3. 8 ZDHH5 targets PCDH7 to the plasma membrane during mitosis

3.3.3 Palmitoylation mechanism directs PCDH7 to the cleavage furrow

After the clarification of mitotic enrichment of PCDH7 localization, I conducted similar experiments on cells synchronized during cytokinesis to investigate whether the palmitoylation mechanism also controls the cytokinesis localization of the protein. Initially, I again used 2BP to inhibit the global palmitoylation mechanism, revealing that inhibition of palmitoylation significantly disrupted the localization of PCDH7 at the cleavage furrow and equatorial region during cytokinesis (Figure 3. 9) and resulted in a reduction in the levels of PCDH7 at the cleavage furrow. Together with the mitosis experiment, it is shown that palmitoylation is not necessary at cell–cell contacts during interphase but is essential for its cortical and cleavage furrow localization during mitosis and cytokinesis.

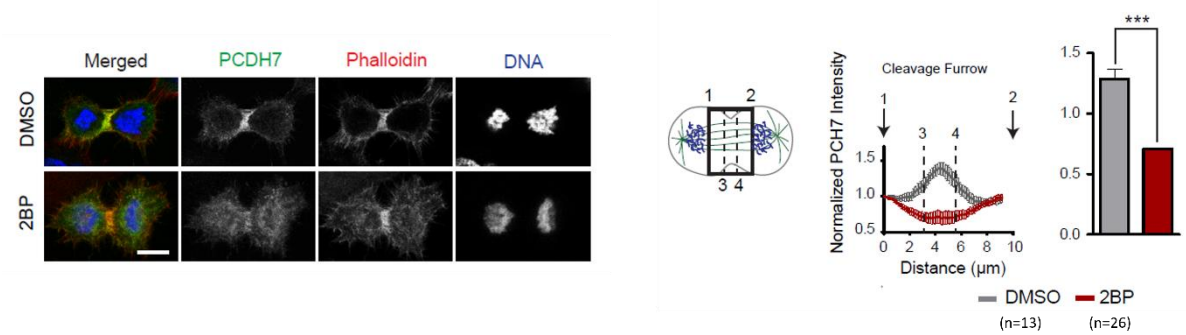

Figure 3. 9 Inhibition of palmitoylation perturbs cleavage furrow localization of PCDH7

Next, I investigated the role of ZDHHC5 in targeting PCDH7 to the cleavage furrow during the cytokinesis. When the ZDHHC5 was knockdown, the localization of PCDH7 at the cleavage furrow was disrupted (Figure 3. 10). Specifically, PCDH7 was no longer concentrated at the cleavage furrow or the equatorial zone during late cytokinesis in ZDHHC5. In this experiment, I performed the western blotting and immunofluorescent experiments, and Nazlı did the imaging and quantification of images.

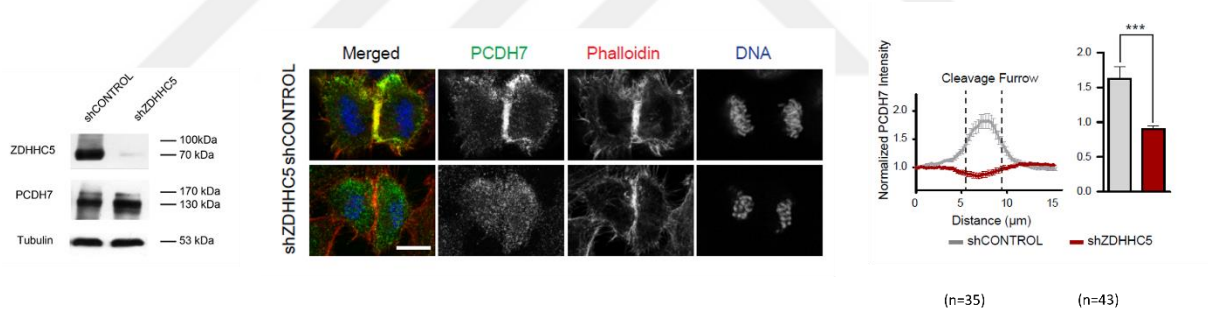

Figure 3. 10 ZDHHC5 directs PCDH7 to the cleavage furrow

3.4 DISCUSSION

This thesis section aims to understand the underlying mechanism of cell cycle-dependent localization of PCDH7. This analysis revealed the role of palmitoylation in the translocation of PCDH7 to the mitotic cell surface and cleavage furrow. With using several imaging and knockdown approaches I showed that palmitoylation mechanisms control PCDH7 localization to the mitotic membrane and cleavage furrow specifically, via a specific palmitoyltransferase, ZDDHC5. This study revealed the spatiotemporal regulation of PCDH7 and its dependence on palmitoylation mechanisms during cell division and PCDH7 became one of the first examples of the role of palmitoylation in the cell cycle-dependent localization of a protein.

Protein palmitoylation is a lipid modification process where one or more cysteine thiols on a substrate protein are modified with a palmitoyl group. This lipid modification is reversible, enabling regulation of the function of numerous cellular proteins including protein trafficking, stability, and degradation (Guan & Fierke, 2011). Although this known concept of protein palmitoylation, with catching the regulation of PCDH7 cell cycle localization mechanism targeted by ZDHHC5, we showed the the importance of palmitoylation in the context of cell division which is a newly emerging topic.

Future studies will expand upon the palmitoylation-dependent regulatory mechanisms during cell division by investigating palmitoyltransferases and their target molecules that function in mitosis and cytokinesis.

BIBLIOGRAPHY

Anton, E., Marchionni, M., Lee, K., & Rakic, P. (1997). Role of GGF/neuregulin signaling in interactions between migrating neurons and radial glia in the developing cerebral cortex. *Development*, *124*(18), 3501-3510.

Arata, Y., Lee, J.-Y., Goldstein, B., & Sawa, H. (2010). Extracellular control of PAR protein localization during asymmetric cell division in the C. elegans embryo. *Development*, *137*(19), 3337-3345.

Azevedo, F. A., Carvalho, L. R., Grinberg, L. T., Farfel, J. M., Ferretti, R. E., Leite, R. E., Filho, W. J., Lent, R., & Herculano-Houzel, S. (2009). Equal numbers of neuronal and nonneuronal cells make the human brain an isometrically scaled-up primate brain. *Journal of Comparative Neurology*, *513*(5), 532-541.

Beattie, R., Postiglione, M. P., Burnett, L. E., Laukoter, S., Streicher, C., Pauler, F. M., Xiao, G., Klezovitch, O., Vasioukhin, V., & Ghashghaei, T. H. (2017). Mosaic analysis with double markers reveals distinct sequential functions of Lgl1 in neural stem cells. *Neuron*, *94*(3), 517-533. e513.

Bizzotto, S., Uzquiano, A., Dingli, F., Ershov, D., Houllier, A., Arras, G., Richards, M., Loew, D., Minc, N., & Croquelois, A. (2017). Eml1 loss impairs apical progenitor spindle length and soma shape in the developing cerebral cortex. *Scientific reports*, *7*(1), 17308.

Boersema, P. J., Raijmakers, R., Lemeer, S., Mohammed, S., & Heck, A. J. (2009). Multiplex peptide stable isotope dimethyl labeling for quantitative proteomics. *Nature protocols*, *4*(4), 484-494.

Boucrot, E., & Kirchhausen, T. (2007). Endosomal recycling controls plasma membrane area during mitosis. *Proceedings of the National Academy of Sciences*, *104*(19), 7939-7944.

Campbell, K., & Götz, M. (2002). Radial glia: multi-purpose cells for vertebrate brain development. *Trends in neurosciences*, *25*(5), 235-238.

Cappello, S., Böhringer, C. R., Bergami, M., Conzelmann, K.-K., Ghanem, A., Tomassy, G. S., Arlotta, P., Mainardi, M., Allegra, M., & Caleo, M. (2012). A radial glia-specific role of RhoA in double cortex formation. *Neuron*, *73*(5), 911-924.

Carlton, J. G., Jones, H., & Eggert, U. S. (2020). Membrane and organelle dynamics during cell division. *Nature reviews Molecular cell biology*, *21*(3), 151-166.

Chen, D., Ito, S., Yuan, H., Hyodo, T., Kadomatsu, K., Hamaguchi, M., & Senga, T. (2015). EML4 promotes the loading of NUDC to the spindle for mitotic progression. *Cell Cycle*, *14*(10), 1529-1539.

Chenn, A., & McConnell, S. K. (1995). Cleavage orientation and the asymmetric inheritance of notchl immunoreactivity in mammalian neurogenesis. *Cell*, *82*(4), 631-641.

Collins, S. C., Uzquiano, A., Selloum, M., Wendling, O., Gaborit, M., Osipenko, M., Birling, M. C., Yalcin, B., & Francis, F. (2019). The neuroanatomy of Eml1 knockout mice, a model of subcortical heterotopia. *Journal of Anatomy*, *235*(3), 637-650.

Corbit, K. C., Aanstad, P., Singla, V., Norman, A. R., Stainier, D. Y., & Reiter, J. F. (2005). Vertebrate Smoothened functions at the primary cilium. *Nature*, *437*(7061), 1018-1021.

Cox, J., & Mann, M. (2008). MaxQuant enables high peptide identification rates, individualized ppb-range mass accuracies and proteome-wide protein quantification. *Nature biotechnology*, *26*(12), 1367-1372.

Di Bella, D. J., Habibi, E., Stickels, R. R., Scalia, G., Brown, J., Yadollahpour, P., Yang, S. M., Abbate, C., Biancalani, T., & Macosko, E. Z. (2021). Molecular logic of cellular diversification in the mouse cerebral cortex. *Nature*, *595*(7868), 554-559.

Di Donato, N., Timms, A. E., Aldinger, K. A., Mirzaa, G. M., Bennett, J. T., Collins, S., Olds, C., Mei, D., Chiari, S., & Carvill, G. (2018). Analysis of 17 genes detects mutations in 81% of 811 patients with lissencephaly. *Genetics in Medicine*, *20*(11), 1354-1364.

Donia, Z. K., Chinnappa; Berfu Nur, Yigit; Valeria, Viola; Carmen, Cifuentes-Dias; Ammar, Jabali; Ana, Uzquiano; Emilie, Lemesre; Franck, Perez; Julia, Ladewig; Julien, Ferent; Nurhan, Ozlu; Fiona, Francis. (2024). *Eml1 cortical-specific depletion leads to apical progenitor cell cycle and centrosomal dysfunction during subcortical heterotopia formation*.

Dunckley, T., & Lukas, R. J. (2003). Nicotine modulates the expression of a diverse set of genes in the neuronal SH-SY5Y cell line. *Journal of Biological Chemistry*, *278*(18), 15633-15640.

Eggenschwiler, J. T., & Anderson, K. V. (2007). Cilia and developmental signaling. *Annu. Rev. Cell Dev. Biol.*, *23*, 345-373.

Fietz, S. A., Kelava, I., Vogt, J., Wilsch-Bräuninger, M., Stenzel, D., Fish, J. L., Corbeil, D., Riehn, A., Distler, W., & Nitsch, R. (2010). OSVZ progenitors of human and ferret neocortex are epithelial-like and expand by integrin signaling. *Nature neuroscience*, *13*(6), 690-699.

Florio, M., & Huttner, W. B. (2014). Neural progenitors, neurogenesis and the evolution of the neocortex. *Development*, *141*(11), 2182-2194.

Fry, A. M., O'Regan, L., Montgomery, J., Adib, R., & Bayliss, R. (2016). EML proteins in microtubule regulation and human disease. *Biochemical Society Transactions*, *44*(5), 1281-1288.

Gibson, D. G., Young, L., Chuang, R.-Y., Venter, J. C., Hutchison, C. A., & Smith, H. O. (2009). Enzymatic assembly of DNA molecules up to several hundred kilobases. *Nature methods*, *6*(5), 343-345.

Götz, M., & Huttner, W. B. (2005). The cell biology of neurogenesis. *Nature reviews Molecular cell biology*, *6*(10), 777-788.

Greig, L. C., Woodworth, M. B., Galazo, M. J., Padmanabhan, H., & Macklis, J. D. (2013). Molecular logic of neocortical projection neuron specification, development and diversity. *Nature Reviews Neuroscience*, *14*(11), 755-769.

Hansen, D. V., Lui, J. H., Parker, P. R., & Kriegstein, A. R. (2010). Neurogenic radial glia in the outer subventricular zone of human neocortex. *Nature*, *464*(7288), 554-561.

Haubensak, W., Attardo, A., Denk, W., & Huttner, W. B. (2004). Neurons arise in the basal neuroepithelium of the early mammalian telencephalon: a major site of neurogenesis. *Proceedings of the National Academy of Sciences*, *101*(9), 3196-3201.

Haydar, T. F., Ang Jr, E., & Rakic, P. (2003). Mitotic spindle rotation and mode of cell division in the developing telencephalon. *Proceedings of the National Academy of Sciences*, *100*(5), 2890-2895.

Hevner, R. F. (2006). From radial glia to pyramidal-projection neuron: transcription factor cascades in cerebral cortex development. *Molecular neurobiology*, *33*, 33-50.

Hevner, R. F., & Haydar, T. F. (2012). The (not necessarily) convoluted role of basal radial glia in cortical neurogenesis. *Cerebral cortex*, *22*(2), 465-468.

Hirano, K., Kaneko, R., Izawa, T., Kawaguchi, M., Kitsukawa, T., & Yagi, T. (2012). Single-neuron diversity generated by Protocadherin-β cluster in mouse central and peripheral nervous systems. *Frontiers in molecular neuroscience*, *5*, 90.

Hirayama, T., & Yagi, T. (2006). The role and expression of the protocadherin-alpha clusters in the CNS. *Current opinion in neurobiology*, *16*(3), 336-342.

Hirokawa, N., Noda, Y., Tanaka, Y., & Niwa, S. (2009). Kinesin superfamily motor proteins and intracellular transport. *Nature reviews Molecular cell biology*, *10*(10), 682-696.

Hotta, T., McAlear, T. S., Yue, Y., Higaki, T., Haynes, S. E., Nesvizhskii, A. I., Sept, D., Verhey, K. J., Bechstedt, S., & Ohi, R. (2022). EML2-S constitutes a new class of proteins that recognizes and regulates the dynamics of tyrosinated microtubules. *Current Biology*, *32*(18), 3898-3910. e3814.

Houtman, S., Rutteman, M., De Zeeuw, C., & French, P. (2007). Echinoderm microtubule-associated protein like protein 4, a member of the echinoderm microtubule-associated protein family, stabilizes microtubules. *Neuroscience*, *144*(4), 1373-1382.

Huttner, W. B., & Brand, M. (1997). Asymmetric division and polarity of neuroepithelial cells. *Current opinion in neurobiology*, *7*(1), 29-39.

Jabali, A., Hoffrichter, A., Uzquiano, A., Marsoner, F., Wilkens, R., Siekmann, M., Bohl, B., Rossetti, A. C., Horschitz, S., & Koch, P. (2022). Human cerebral organoids reveal progenitor pathology in EML1-linked cortical malformation. *EMBO reports*, *23*(5), e54027.

Kaverina, I., & Straube, A. (2011). Regulation of cell migration by dynamic microtubules. Seminars in cell & developmental biology,

Kelava, I., Lewitus, E., & Huttner, W. B. (2013). The secondary loss of gyrencephaly as an example of evolutionary phenotypical reversal. *Frontiers in neuroanatomy*, *7*, 16.

Kielar, M., Tuy, F. P. D., Bizzotto, S., Lebrand, C., de Juan Romero, C., Poirier, K., Oegema, R., Mancini, G. M., Bahi-Buisson, N., & Olaso, R. (2014). Mutations in Eml1 lead to ectopic progenitors and neuronal heterotopia in mouse and

human. *Nature neuroscience*, *17*(7), 923-933.

Kirkcaldie, M. T., & Dwyer, S. T. (2017). The third wave: Intermediate filaments in the maturing nervous system. *Molecular and Cellular Neuroscience*, *84*, 68-76.

Knoblich, J. A. (2008). Mechanisms of asymmetric stem cell division. *Cell*, *132*(4), 583-597.

Kosodo, Y., Röper, K., Haubensak, W., Marzesco, A. M., Corbeil, D., & Huttner, W. B. (2004). Asymmetric distribution of the apical plasma membrane during neurogenic divisions of mammalian neuroepithelial cells. *The EMBO journal*, *23*(11), 2314-2324.

Kosodo, Y., Toida, K., Dubreuil, V., Alexandre, P., Schenk, J., Kiyokage, E., Attardo, A., Mora-Bermúdez, F., Arii, T., & Clarke, J. D. (2008). Cytokinesis of neuroepithelial cells can divide their basal process before anaphase. *The EMBO journal*, *27*(23), 3151-3163.

Kowalczyk, T., Pontious, A., Englund, C., Daza, R. A., Bedogni, F., Hodge, R., Attardo, A., Bell, C., Huttner, W. B., & Hevner, R. F. (2009). Intermediate neuronal progenitors (basal progenitors) produce pyramidal–projection neurons for all layers of cerebral cortex. *Cerebral cortex*, *19*(10), 2439-2450.

Kunda, P., Pelling, A. E., Liu, T., & Baum, B. (2008). Moesin controls cortical rigidity, cell rounding, and spindle morphogenesis during mitosis. *Current Biology*, *18*(2), 91-101.

Lasser, M., Tiber, J., & Lowery, L. A. (2018). The role of the microtubule cytoskeleton in neurodevelopmental disorders. *Frontiers in cellular neuroscience*, *12*, 165.

Lehtinen, M. K., Zappaterra, M. W., Chen, X., Yang, Y. J., Hill, A. D., Lun, M., Maynard, T., Gonzalez, D., Kim, S., & Ye, P. (2011). The cerebrospinal fluid provides a proliferative niche for neural progenitor cells. *Neuron*, *69*(5), 893-905.

Lin, Y.-L., Wang, Y.-L., Fu, X.-L., Li, W.-P., Wang, Y.-H., & Ma, J.-G. (2016). Low expression of protocadherin7 (PCDH7) is a potential prognostic biomarker for primary non-muscle invasive bladder cancer. *Oncotarget*, *7*(19), 28384.

Lin, Z., Gasic, I., Chandrasekaran, V., Peters, N., Shao, S., Mitchison, T. J., & Hegde, R. S. (2020). TTC5 mediates autoregulation of tubulin via mRNA degradation. *Science*, *367*(6473), 100-104.

Liu, X., Salokas, K., Weldatsadik, R. G., Gawriyski, L., & Varjosalo, M. (2020). Combined proximity labeling and affinity purification− mass spectrometry workflow for mapping and visualizing protein interaction networks. *Nature protocols*, *15*(10), 3182-3211.

Mancini, M., Bassani, S., & Passafaro, M. (2020). Right place at the right time: how changes in protocadherins affect synaptic connections contributing to the etiology of neurodevelopmental disorders. *Cells*, *9*(12), 2711.

Markus, F., Kannengießer, A., Näder, P., Atigbire, P., Scholten, A., Vössing, C., Bültmann, E., Korenke, G. C., Owczarek-Lipska, M., & Neidhardt, J. (2021). A novel missense variant in the EML1 gene associated with bilateral ribbon-like

subcortical heterotopia leads to ciliary defects. *Journal of Human Genetics*, *66*(12), 1159-1167.

Matsuzaki, F., & Shitamukai, A. (2015). Cell division modes and cleavage planes of neural progenitors during mammalian cortical development. *Cold Spring Harbor perspectives in biology*, *7*(9), a015719.

Menon, S., & Gupton, S. L. (2016). Building blocks of functioning brain: cytoskeletal dynamics in neuronal development. *International review of cell and molecular biology*, *322*, 183-245.

Mora-Bermúdez, F., Matsuzaki, F., & Huttner, W. B. (2014). Specific polar subpopulations of astral microtubules control spindle orientation and symmetric neural stem cell division. *Elife*, *3*, e02875.

Mori, N., Kuwamura, M., Tanaka, N., Hirano, R., Nabe, M., Ibuki, M., & Yamate, J. (2012). Ccdc85c encoding a protein at apical junctions of radial glia is disrupted in hemorrhagic hydrocephalus (hhy) mice. *The American journal of pathology*, *180*(1), 314-327.

Mostowy, S., & Cossart, P. (2012). Septins: the fourth component of the cytoskeleton. *Nature reviews Molecular cell biology*, *13*(3), 183-194.

Noctor, S. C., Flint, A. C., Weissman, T. A., Dammerman, R. S., & Kriegstein, A. R. (2001). Neurons derived from radial glial cells establish radial units in neocortex. *Nature*, *409*(6821), 714-720.

O'Connor, V., Houtman, S., De Zeeuw, C., Bliss, T., & French, P. (2004). Eml5, a novel WD40 domain protein expressed in rat brain. *Gene*, *336*(1), 127-137.

O'Regan, L., Barone, G., Adib, R., Woo, C. G., Jeong, H. J., Richardson, E. L., Richards, M. W., Muller, P. A., Collis, S. J., & Fennell, D. A. (2020). EML4–ALK V3 oncogenic fusion proteins promote microtubule stabilization and accelerated migration through NEK9 and NEK7. *Journal of cell science*, *133*(9), jcs241505.

Oegema, R., Barkovich, A. J., Mancini, G. M., Guerrini, R., & Dobyns, W. B. (2019). Subcortical heterotopic gray matter brain malformations: classification study of 107 individuals. *Neurology*, *93*(14), e1360-e1373.

Özkan, N. E., Yigit, B. N., Degirmenci, B. S., Qureshi, M. H., Yapici, G. N., Kamacıoglu, A., Bavili, N., Kiraz, A., & Ozlu, N. (2023). Cell cycle-dependent palmitoylation of protocadherin 7 by ZDHHC5 promotes successful cytokinesis. *Journal of cell science*, *136*(6), jcs260266.

Özlü, N., Qureshi, M. H., Toyoda, Y., Renard, B. Y., Mollaoglu, G., Özkan, N. E., Bulbul, S., Poser, I., Timm, W., & Hyman, A. A. (2015). Quantitative comparison of a human cancer cell surface proteome between interphase and mitosis. *The EMBO journal*, *34*(2), 251-265.

Pacheco, A., & Gallo, G. (2016). Actin filament-microtubule interactions in axon initiation and branching. *Brain research bulletin*, *126*, 300-310.

Piekny, A. J., & Glotzer, M. (2008). Anillin is a scaffold protein that links RhoA, actin, and myosin during cytokinesis. *Current Biology*, *18*(1), 30-36.

Poirier, K., Lebrun, N., Broix, L., Tian, G., Saillour, Y., Boscheron, C., Parrini, E., Valence, S., Pierre, B. S., & Oger, M. (2013). Mutations in TUBG1, DYNC1H1, KIF5C and KIF2A cause malformations of cortical development and microcephaly. *Nature genetics*, *45*(6), 639-647.

Rakic, P. (1988). Specification of cerebral cortical areas. *Science*, *241*(4862), 170-176.

Rakic, P. (2007). The radial edifice of cortical architecture: from neuronal silhouettes to genetic engineering. *Brain research reviews*, *55*(2), 204-219.

Ramkumar, N., & Baum, B. (2016). Coupling changes in cell shape to chromosome segregation. *Nature reviews Molecular cell biology*, *17*(8), 511-521.

Raudvere, U., Kolberg, L., Kuzmin, I., Arak, T., Adler, P., Peterson, H., & Vilo, J. (2019). g: Profiler: a web server for functional enrichment analysis and conversions of gene lists (2019 update). *Nucleic acids research*, *47*(W1), W191-W198.

Reillo, I., de Juan Romero, C., García-Cabezas, M. Á., & Borrell, V. (2011). A role for intermediate radial glia in the tangential expansion of the mammalian cerebral cortex. *Cerebral cortex*, *21*(7), 1674-1694.

Richards, M. W., Law, E. W., Rennalls, L. V. P., Busacca, S., O'Regan, L., Fry, A. M., Fennell, D. A., & Bayliss, R. (2014). Crystal structure of EML1 reveals the basis for Hsp90 dependence of oncogenic EML4-ALK by disruption of an atypical β-propeller domain. *Proceedings of the National Academy of Sciences*, *111*(14), 5195-5200.

Richards, M. W., O'Regan, L., Roth, D., Montgomery, J. M., Straube, A., Fry, A. M., & Bayliss, R. (2015). Microtubule association of EML proteins and the EML4-ALK variant 3 oncoprotein require an N-terminal trimerization domain. *Biochemical Journal*, *467*(3), 529-536.

Rieder, C. L., & Khodjakov, A. (2003). Mitosis through the microscope: advances in seeing inside live dividing cells. *Science*, *300*(5616), 91-96.

Romero, D. M., Bahi-Buisson, N., & Francis, F. (2018). Genetics and mechanisms leading to human cortical malformations. Seminars in cell & developmental biology,

Sabir, S. R., Yeoh, S., Jackson, G., & Bayliss, R. (2017). EML4-ALK variants: biological and molecular properties, and the implications for patients. *Cancers*, *9*(9), 118.

Sedzinski, J., Biro, M., Oswald, A., Tinevez, J.-Y., Salbreux, G., & Paluch, E. (2011). Polar actomyosin contractility destabilizes the position of the cytokinetic furrow. *Nature*, *476*(7361), 462-466.

Shaheen, R., Sebai, M. A., Patel, N., Ewida, N., Kurdi, W., Altweijri, I., Sogaty, S., Almardawi, E., Seidahmed, M. Z., & Alnemri, A. (2017). The genetic landscape of familial congenital hydrocephalus. *Annals of neurology*, *81*(6), 890-897.

Shannon, P., Markiel, A., Ozier, O., Baliga, N. S., Wang, J. T., Ramage, D., Amin, N., Schwikowski, B., & Ideker, T. (2003). Cytoscape: a software environment for integrated models of biomolecular interaction networks. *Genome research*, *13*(11), 2498-2504.

Stocker, A. M., & Chenn, A. (2015). The role of adherens junctions in the developing neocortex. *Cell adhesion & migration*, *9*(3), 167-174.

Stouffer, M. A., Golden, J. A., & Francis, F. (2016). Neuronal migration disorders: focus on the cytoskeleton and epilepsy. *Neurobiology of disease*, *92*, 18-45.

Stouffer, M. A., Golden, J. A., & Francis, F. (2016). Neuronal migration disorders: focus on the cytoskeleton and epilepsy. *Neurobiology of disease*, *92*, 18-45.

Sun, T., & Hevner, R. F. (2014). Growth and folding of the mammalian cerebral cortex: from molecules to malformations. *Nature Reviews Neuroscience*, *15*(4), 217-232.

Sun, T., Wang, X.-J., Xie, S.-S., Zhang, D.-L., Wang, X.-P., Li, B.-Q., Ma, W., & Xin, H. (2011). A comparison of proliferative capacity and passaging potential between neural stem and progenitor cells in adherent and neurosphere cultures. *International Journal of Developmental Neuroscience*, *29*(7), 723-731.

Suprenant, K. A., Dean, K., McKee, J., & Hake, S. (1993). EMAP, an echinoderm microtubule-associated protein found in microtubule-ribosome complexes. *Journal of cell science*, *104*(2), 445-450.

Szklarczyk, D., Gable, A. L., Nastou, K. C., Lyon, D., Kirsch, R., Pyysalo, S., Doncheva, N. T., Legeay, M., Fang, T., & Bork, P. (2021). The STRING database in 2021: customizable protein–protein networks, and functional characterization of user-uploaded gene/measurement sets. *Nucleic acids research*, *49*(D1), D605-D612.

Taverna, E., Götz, M., & Huttner, W. B. (2014). The cell biology of neurogenesis: toward an understanding of the development and evolution of the neocortex. *Annual review of cell and developmental biology*, *30*, 465-502.

Teo, G., Liu, G., Zhang, J., Nesvizhskii, A. I., Gingras, A.-C., & Choi, H. (2014). SAINTexpress: improvements and additional features in Significance Analysis of INTeractome software. *Journal of proteomics*, *100*, 37-43.

Tyanova, S., Temu, T., Sinitcyn, P., Carlson, A., Hein, M. Y., Geiger, T., Mann, M., & Cox, J. (2016). The Perseus computational platform for comprehensive analysis of (prote) omics data. *Nature methods*, *13*(9), 731-740.

Uzquiano, A., Cifuentes-Diaz, C., Jabali, A., Romero, D. M., Houllier, A., Dingli, F., Maillard, C., Boland, A., Deleuze, J.-F., & Loew, D. (2019). Mutations in the heterotopia gene Eml1/EML1 severely disrupt the formation of primary cilia. *Cell Reports*, *28*(6), 1596-1611. e1510.

Vanderhaeghen, P., & Polleux, F. (2023). Developmental mechanisms underlying the evolution of human cortical circuits. *Nature Reviews Neuroscience*, *24*(4), 213-232.

Vriend, I., & Oegema, R. (2021). Genetic causes underlying grey matter heterotopia. *European Journal of Paediatric Neurology*, *35*, 82-92.

Weirich, C. S., Erzberger, J. P., & Barral, Y. (2008). The septin family of GTPases: architecture and dynamics. *Nature reviews Molecular cell biology*, *9*(6), 478-489.

Yin, H., Hou, X., Zhang, T., Shi, L., & Su, Y.-Q. (2020). Participation of EML6 in the regulation of oocyte meiotic progression in mice. *Journal of Biomedical Research*, *34*(1), 44.

Yin, H., Zhang, T., Wang, H., Hu, X., Hou, X., Fang, X., Yin, Y., Li, H., Shi, L., & Su, Y.-Q. (2021). Echinoderm microtubule associated protein like 1 is indispensable for oocyte spindle assembly and meiotic progression in mice. *Frontiers in Cell and Developmental Biology*, *9*, 687522.

Zhang, S., & Fu, X. (2021). The clinical significance and biological function of PCDH7 in cervical cancer. *Cancer Management and Research*, 3841-3847.

Yin, H., Zhang, T., Wang, H., Hu, X., Hou, X., Fang, X., Yin, Y., Li, H., Shi, L., & Su, Y.-Q. (2021). Echinoderm microtubule associated protein like 1 is indispensable for oocyte spindle assembly and meiotic progression in mice. *Frontiers in Cell and Developmental Biology*, *9*, 687522.

Zhang, S., & Fu, X. (2021). The clinical significance and biological function of PCDH7 in cervical cancer. *Cancer Management and Research*, 3841-3847.

Zhou, X., Updegraff, B. L., Guo, Y., Peyton, M., Girard, L., Larsen, J. E., Xie, X.-J., Zhou, Y., Hwang, T. H., & Xie, Y. (2017). PROTOCADHERIN 7 Acts through SET and PP2A to Potentiate MAPK Signaling by EGFR and KRAS during Lung Tumorigenesis. *Cancer research*, *77*(1), 187-197.